ISBN 978-82-575-1003-9
ISSN 1503-1667

Norwegian Institute for Agricultural and Environmental Research (Bioforsk)
Soil and Environment Division
Frederik A. Dahls vei 20
NO-1432 Ås
Phone: +47 40 60 41 00
www.bioforsk.no, e-post:jord@bioforsk.no

Norwegian University of Life Sciences
NO–1432 Ås, Norway
Phone +47 64 96 50 00
www.umb.no, e-mail: postmottak@umb.no

Sigrun Hjalmarsdottir Kværnø

Norwegian University of Life Sciences • Universitetet for miljø- og biovitenskap
Department of Plant and Environmental Sciences
Philosophiae Doctor (PhD) Thesis 2011:40

Philosophiae Doctor (PhD) Thesis 2011:40

Variability and uncertainty in soil physical properties: effects of data source on functional criteria

Variabilitet og usikkerhet i jordas fysiske egenskaper: effekter av datakilde på funksjonelle kriterier

Sigrun Hjalmarsdottir Kværnø

Variability and uncertainty in soil physical properties: effects of data source on functional criteria

Variabilitet og usikkerhet i jordas fysiske egenskaper:
effekter av datakilde på funksjonelle kriterier

Philosophiae Doctor (PhD) Thesis

Sigrun Hjalmarsdottir Kværnø

Department of Plant and Environmental Sciences

Norwegian University of Life Sciences

Soil and Environment Division

Norwegian Institute for Agricultural and Environmental Research

Ås 2011

Thesis number 2011: 40
ISSN 1503-1667
ISBN 978-82-575-1003-9

PhD supervisors:

Prof. Trond Børresen
Norwegian University of Life Sciences
Department of Plant and Environmental Sciences
P.O. Box 5003
NO-1432 Ås

Dr. Jannes Stolte
Norwegian Institute for Agricultural and Environmental Research (Bioforsk)
Soil and Environment Division
Frederik A. Dahls vei 20
NO-1432 Ås

Dr. Lars Egil Haugen
The Norwegian Water Resources and Energy Directorate (NVE)
Hydrology Department
P.O. Box 5091 Majorstua
NO-0301 Oslo

Evaluation committee:

Dr. Helen K. French
Norwegian University of Life Sciences
Department of Plant and Environmental Sciences
P.O. Box 5003
NO-1432 Ås

Prof. Nicholas Jarvis
Swedish University of Agricultural Sciences
Department of Soil and Environment
P.O. Box 7014
SE-750 07 Uppsala

Dr. Henk Wösten
Alterra, Wageningen UR
Soil Science Centre
P.O. Box 47
NL-6700AA Wageningen

Preface

The work presented in this thesis focuses on the variability in soil physical properties and uncertainty related to soil physical properties data sources, and effects thereof on simulated responses related to soil workability, runoff and erosion. Originally, this work was part of a Strategic Institute Programme on "Soil Quality and Precision Agriculture" (project no. 143294/I10), funded by the Norwegian Research Council (NFR). The work has also been part of and funded by the NFR projects "Seasonal frozen soils: temporal and spatial variability in hydrological and soil physical properties - WinterSoil" (133494/110), and "ExFlood" (200678/S30).

After a total time span of ten years, with joys and frustrations, successes and failures, I am very happy to finally have concluded my thesis. I thank Nils Vagstad and Arne Grønlund (both at Bioforsk) for including me as a PhD-student in the project "Soil Quality and Precision Agriculture". From the start until 2010, Lars Egil Haugen (then UMB-IPM, now NVE) was my supervisor, and I am grateful to him for several years of supervision, as well as invaluable help with both field and laboratory work, and collaboration on two papers. In 2010 Trond Børresen (UMB-IPM) and Jannes Stolte (Bioforsk) stepped in as main supervisor and local/assisting supervisor respectively. At this stage conclusion of the PhD seemed ever so far away due to big challenges in my life, and I deeply appreciate how they helped me to reach my goal through steady supervision, motivating force and relaxed attitude. Jannes has put a lot of time into discussions, collaboration on the work, help with manuscripts, and strong moral support, and so has Lillian Øygarden (Bioforsk), leader of the WinterSoil project and coauthor on one paper. Their contributions have been of major importance, and I am very grateful for their efforts.

I also thank several other persons who have provided additional data, helped with field and laboratory work, offered technical assistance related to modeling, GIS, statistical analyses and programming, interesting discussions, moral support, and friendship: Csilla Farkas, Johannes Deelstra, Marianne Bechmann, Stine M. Vandsemb, Hege Bergheim, Rut M. Skjevdal, Robert Barneveld, Konrad Bjoner, Tore Sveistrup, Trond Knapp Haraldsen, Hugh Riley, Christian Uhlig, Åge Nyborg, Stein Turtumøygard, Live Semb Vestgarden, Heidi Grønsten, Petter Snilsberg and Per Ivar Hanedalen. Thanks also to the farmers who kindly gave me access to their fields and permission to install equipment and collect soil: Thom Wetlesen, Kristian Hoel Sæther and Ole K. Vandsemb. Finally, I thank my friends and family for help, support and for believing in me until the bitter end.

Ås, 2011

Sigrun H. Kværnø

Contents

List of papers

Paper I:

Kværnø, S.H., Haugen, L.E., Børresen, T., 2007. Variability in topsoil texture and carbon content within soil map units and its implications in predicting soil water content for optimum workability. *Soil & Tillage Research 95*, 332-347.

Paper II:

Kværnø, S.H., Øygarden, L., 2006. The influence of freeze–thaw cycles and soil moisture on aggregate stability of three soils in Norway. *Catena 67*, 175-182.

Paper III:

Kværnø, S.H., Haugen, L.E., 2011. Performance of pedotransfer functions in predicting soil water characteristics of soils in Norway. *Acta Agriculturae Scandinavica Section B – Soil and Plant Science 61*, 264-280.

Paper IV:

Kværnø, S.H. & Stolte, J., 2011. Effects of soil physical data sources on discharge and soil loss simulated by the LISEM model. Submitted to *Catena*.

Sammendrag

Modeller har blitt uunngåelige verktøy for en lang rekke problemstillinger knyttet til landbruk og miljø. Samtidig er modellering forbundet med usikkerhet, noe som kan ha konsekvenser når beslutninger skal fattes. En av hovedkildene til usikkerhet i modellering er inputdata, blant annet for jordas fysiske egenskaper. Jordas fysiske egenskaper kan variere sterkt i tid og rom, og er vanskelig og kostbart å måle. Mangel på måledata av høy kvalitet er derfor ofte et problem, og data må dermed avledes fra alternative kilder og via tilleggsmodeller, for eksempel pedotransferfunksjoner (PTFer). Med bakgrunn i dette var hovedformålet med denne avhandlingen å kvantifisere variasjon i jordas fysiske egenskaper, usikkerheter forbundet med datakilde, og effekter av variasjon og usikkerhet på utvalgte funksjonelle kriterier. Hovedstudieområde var Skuterudbekkens nedbørfelt (450 ha) i Sørøst-Norge, representativt for jordbruksområder med kornproduksjon på marine avsetninger.

Studier av romlig variasjon og usikkerhet knyttet til jordsmonnkart ble utført gjennom statistiske analyser av data for kornfordeling og karboninnhold i matjordlaget, innsamlet i to rutenett: ett rutenett med 100 m prøveavstand, som dekket all dyrka mark i feltet, og et rutenett med 10 m prøveavstand som lå midt på grensen mellom to kartenheter, den ene sandig strandavsetning, den andre leirholdig havavsetning. Romlig variasjon i disse jordegeskapene var betydelig, og romlig korrelert. Parametre for romlig korrelasjon avhang av rutenettskala. Variasjon innen de mest utbredte jordseriene ble kvantifisert – variasjonskoeffisientene var mellom 10 og 69 %, og spennet i variabelverdier var stort for alle jordserier. Sammenlikning av faktisk teksturklasse og teksturklasse basert på jordsmonnkartet viste at det var betydelig feilklassifikasjon i jordsmonnkartet. Lettleire og sandig lettleire var særlig underrepresentert, mens siltig lettleire var overrepresentert. Feilklassifisering var særlig høy i det minste rutenettet, og indikerte glidende grenseovergang mellom kartfigurer og større usikkerhet i jordsmonnkartet i disse områdene.

Et bestemt aspekt av tidsvariasjon ble undersøkt, dvs. effekter av frysing og tining på aggregatstabilitet. Tre jordtyper ble samlet til dette formålet: en mellomleire fra den mest utbredte jordserien i Skuterud, samt en siltjord og en planert siltig mellomleire fra et annet område. Repakkede aggregater (1-4 mm) ble fuktet opp til vanninnhold tilsvarende tre bestemte matrikspotensialer, og deretter frosset og tint ulikt antall ganger. Aggregatstabilitet ble målt med regnsimulator og med våtsikting. Studien viste at aggregatstabilitet ble redusert ved gjentatt frysing og tining. Reduksjonen var større for den i utgangspunktet mer ustabile siltjorda (relativ effekt 55 % reduksjon etter 6 fryse-tinesykluser) enn på de to mer stabile

leirjordstypene (ca 20 % reduksjon). Ulike måleteknikker ga ulik aggregatstabilitet, og forskjellen i aggregatstabilitet mellom de to metodene var større jo mer ustabil jorda var (siltjord, mange fryse-tinesykluser).

Usikkerheten i PTFer for jordas fuktighetskarakteristikk (SWRC) ble evaluert på et datasett bestående av 540 jordprøver fra ulik jord i Norge. Tekstur varierte fra sand til stiv leire. For hver prøve var det målt kornfordeling, organisk materiale, jordtetthet (ρ_b) og vanninnhold ved bestemte matrikspotensialer. To punkt-PTFer utviklet for jord i Norge, og seks parameter-PTFer utviklet for jord i Europa og USA, ble evaluert ved hjelp av flere statistiske indikatorer. Punkt-PTFene ga generelt gode resultater. Parameter-PTFene ga variable resultater. En av parameter-PTFene som ga gode resultater i de fleste tilfeller, var en kontinuerlig PTF utviklet av Wösten et al. (1999). Klasse-PTFene ga dårligere resultater enn de kontinuerlige PTFene, særlig hvis organisk materiale ikke var en input til PTFen.

Konsekvenser av variasjon, usikkerhet og datakilde ble undersøkt for utvalgte funksjonelle kriterier i Skuterudfeltet. Maksimalt vanninnhold for optimal laglighet (W_{opt}) ble beregnet vha. en eksisterende PTF, og antall dager til W_{opt} ble oppnådd etter snøsmelting om våren, ble beregnet vha. en enkel funksjon der vanninnhold ved feltkapasitet og ρ_b, begge beregnet vha. PTFer, og potensiell fordamping og W_{opt} var input. Episodedrevet overflateavrenning og jordtap fra nedbørfeltet ble simulert vha. den prosessbaserte modellen Limburg soil erosion model (LISEM). Tekstur og organisk materiale ble brukt for å avlede modellinput for vannledningsevne, SWRC, aggregatstabilitet og kohesjon. Sistnevnte ble beregnet for hele nedbørfeltet vha. en lokal PTF, utviklet fra målte skjærfasthetsdata. De andre inputene ble beregnet med eksisterende PTFer. For alle de funksjonelle kriterer ble både lokale måledata for tekstur og organisk materiale, og data avleda fra jordsmonnkart, brukt i beregningene. Effekten av variasjon på W_{opt} og Nd så ut til å være viktig, tatt i betraktning små marginer pga. få dager sammenhengende uten nedbør om våren. Effekt av datakilde på simulert overflateavrenning og jordtap var stor, med høyere verdier simulert ved bruk av data avledet fra jordsmonnkart og jordsmonndatabasen enn ved bruk av lokale måledata. I denne studien var det lite forskjell i resultater ved å beholde informasjon om variasjon innen kartenheter ved stokastisk fordeling av måledata sammenliknet med å bruke en middelverdi av måledata for hver kartenhet. Studien viste også at forskjellene relatert til datakilde kan være større enn forskjeller som resultat av forskjellig risiko for avrenning og erosjon (situasjon med plantedekke sammenliknet med ”worst case”-situasjon med redusert stabilitet og uten plantedekke).

Hovedkonklusjonen av dette arbeidet er at inadekvat valg av inputdatakilder kan gi betydelig under- eller overestimering av W_{opt}, antall dager til W_{opt} oppnås, overflateavrenning og jordtap, og dermed også effekter av for eksempel klimaendring og tiltak.

Summary

Models have become inevitable tools for a wide range of applications in agricultural and environmental management. At the same time, modeling is associated with uncertainty, which can have consequences for decision making. One of the main sources of modeling uncertainty is the model input data, among these the soil physical properties. Soil physical properties are often highly variable in time and space and difficult and costly to measure. Lack of high-quality measured soil physical data is therefore often a problem, and data need to be derived from alternative sources and by means of additional models, e.g. pedotransfer functions (PTFs). With this as background, the main objective of this thesis was to quantify variability in soil physical properties on arable land, uncertainties related to data sources, and effects of variability and uncertainty on selected functional criteria. The main study area was the Skuterud catchment (450 ha) in South-east Norway, representative of agricultural areas with cereal production on marine deposits.

Studies of spatial variability and soil map uncertainty were carried out by statistical analyses of data for topsoil particle size distribution and carbon content, collected in two sample grids: one grid with 100 m spacing covering the total area of arable land, and one grid with 10 m spacing located directly on the boundary between a sandy shore deposit map unit and a clayey marine deposit map unit. Spatial variability in these soil properties was considerable, and spatially correlated. Spatial correlation parameters depended on the grid scale. Variability within the major soil series was quantified – coefficients of variation ranged between 10 and 69 %, and the span in variable values was large for all soil series. Comparison of actual and soil map texture class revealed substantial misclassification in the soil map, with underrepresentation of loam and sandy loam soils, and overrepresentation of silt loam soil. Misclassification was particularly high in the small sample grid located on the border between a sandy shore deposit soil and a clayey marine deposit soil, indicating fuzzy boundaries between map units and high uncertainty in these areas.

A specific aspect of temporal variability was investigated, i.e. effects of freezing and thawing on aggregate stability. For this study three soils were collected: a clay loam from the most widespread soil series in Skuterud, and a silt soil and artificially leveled silty clay loam

from another site. Repacked soil aggregates (1-4 mm) were wetted to water contents corresponding to three different matric potentials, and subjected to different number of freeze-thaw cycles (FTCs), including no freezing. Aggregate stability was measured using a rainfall simulator, and a wet-sieving apparatus. The study showed that aggregate stability decreased with repeated freezing and thawing. The decrease was larger for the initially more unstable silt soil (relative effect 55 % reduction after 6 FTCs) than the two more stable clay soils (around 20 % reduction). Different measurement techniques yielded different aggregate stability values, and the difference in aggregate stability measured by the two techniques was greater the more unstable the soil was (silt soil, many FTCs).

Performance of PTFs for the soil water retention curve (SWRC) was evaluated on a dataset of 540 soil samples from different soils in Norway. The texture of the soils ranged from sand to heavy clay. For each sample data on particle size distribution, soil organic matter, bulk density (ρ_b) and soil water content at different matric potential had been measured. Two point PTFs developed for soils in Norway, and six parameter PTFs developed for soils in Europe and USA, were evaluated using multiple statistical indicators. The point PTFs showed overall good performance. The parameter PTFs showed variable performance. One of the PTFs that performed well in most cases was the continuous PTF by Wösten et al. (1999). The class PTFs showed poorer performance than the continuous PTFs, especially if organic matter was not an input to the PTF.

Implications of variability, uncertainty and data source were investigated for selected "functional criteria" in the Skuterud catchment. The maximum water content for optimum workability (W_{opt}) was calculated using an existing PTF, and the number of days until W_{opt} is reached after spring snowmelt (Nd) was calculated by a simple equation in which water content at field capacity and ρ_b, both derived via PTFs, and potential evaporation and W_{opt} were inputs. Storm event driven catchment surface discharge and soil loss were simulated using the process based Limburg soil erosion model (LISEM). Texture and organic matter were used to derive model inputs for hydraulic conductivity, SWRC, aggregate stability, and cohesion. The latter was calculated for the whole catchment using a locally developed PTF based on measured cohesion. The other inputs were calculated using existing PTFs. For all functional criteria, both locally measured data and soil map derived data for soil texture and organic matter were used as input to the models. The effect of variability on W_{opt} and Nd appeared to be important, considering small margins with respect to the usually low number of consecutive dry days in spring. The effect of data source on simulated surface discharge and soil loss was large, with higher values simulated using input data derived from the soil

map and soil survey database than when using locally measured input data. In this particular study, there was no merit in retaining information about variability within map units by stochastic assignment of measured data, as compared to simply using a mean value for each map unit. This study also showed that differences related to choice of data source could be larger than differences as a result of different risk of runoff and erosion (crop covered situation versus "worst case" situation with reduced soil stability and without crop cover).

The major conclusion of this work is that inadequate choice of input data sources can significantly underestimate or overestimate W_{opt}, number of days until W_{opt} is obtained, surface discharge and soil loss, and consequently the effect of e.g. climate change and measures.

1 Introduction

1.1 Background

Models have become inevitable tools for a wide range of applications in agricultural and environmental management, including e.g. assessment of land use and climate change effects on soil and water quality and flooding frequency, risk of water pollution by agrochemicals like nutrients and pesticides, risk of greenhouse gas emissions and soil degradation by compaction and erosion, assessment of sustainability of cropping and cultivation systems and efficiency of mitigation strategies, and for assessment of water use efficiency, crop productivity and food security. At the same time, it is widely recognized that modeling is associated with uncertainty. Quantification of uncertainty is important, because ignoring uncertainty may result in the choice of non-optimal strategies in decision making. There are several sources of uncertainty in the modeling process, including the model conceptualization (i.e. process representation, equations used), the availability, adequacy and quality of input data (meteorological, topographical, soil and crop data), choice of initial and boundary conditions, and parameterization/calibration of the model.

Error sources contributing to input data uncertainty include measurement error, inadequate sampling procedures, averaging and aggregation of data, interpolation and extrapolation of data, derivation of input data from maps and remotely sensed data, prediction of input variables from primary data through use of additional models, and variability. By notion, variability (heterogeneity, diversity) should be distinguished from uncertainty in that variability is a property of nature and not reducible through further measurements while uncertainty (or incertitude) is a property of the risk assessor and in theory reducible. But in practice, variability contributes to the total uncertainty when not adequately accounted for.

The soil physical properties are among the most fundamental properties determining water flow, energy and mass transport. Most simulation models therefore require soil physical data in one form or the other. Internationally, numerous studies the past couple of decades have documented and quantified spatial and/or temporal variability in soil physical properties like particle size distribution, bulk density, water retention characteristics, air permeability, infiltration capacity, sorptivity, hydraulic conductivity, aggregate stability, soil strength and penetrometer resistance (e.g. Ciollaro and Romano, 1995; Mallants et al., 1996; Stolte et al., 1996; Boix-Fayos et al., 1998; Falleiros et al., 1998; Tsegaye and Hill, 1998; van Es et al., 1999; Paz-Gonzales et al., 2000; Merz et al., 2002; Sauer and Logsdon, 2002; Iversen et al., 2003; Deeks et al., 2004; Nael et al., 2004; Regalado and Munoz-Carpena, 2004; Coquet et

al., 2005; Wendroth et al., 2006; Chirico et al., 2007; Duffera et al., 2007; Bormann and Klaassen, 2008; Zimmermann and Elsenbeer, 2008; Cantón et al., 2009; de Souza et al., 2009). Soil physical properties can be highly variable even on small scales, and can also be time consuming, difficult and costly to measure. In particular this applies to the important property of saturated hydraulic conductivity (K_s), being among those parameters to which models are most sensitive (Davis et al., 1999). Thus, it is difficult to obtain an adequate characterization of soil physical properties on scales relevant to managers like farmers and water management authorities, i.e. on field and catchment scale. Generalization and transferability of existing information on soil variability to other areas is difficult because the extent of variability and its degree of randomness or spatial and temporal correlation or continuity depends on many factors: which variables we are studying, the natural soil forming factors, anthropogenic influence, and the scale of interest.

In Norway there has been little emphasis on quantification of soil physical properties on arable land. Most of the work that has been done is not readily available, or it is even unavailable, forgotten or unknown. Typically, such data have been collected as part of the soil survey in relation to soil map production, or as part of characterizing the soil in plot studies of e.g. cropping systems (Haraldsen et al., 1994; Riley and Eltun, 1994; Sveistrup et al., 1994a,b) and runoff and nutrient transport (Myhr et al., 1996), and studying effects of e.g. tillage systems (e.g. Børresen, 1987; 1999; Kolsrud, 2001), subsurface drainage (Øygarden et al., 1997) and applications of manure or organic waste (Myhr et al., 1990; Sveistrup and Haraldsen, 1991; Haraldsen and Sveistrup, 1994; 1996; Øgaard et al., 2009) on various soil physical properties. Quantification of spatial and temporal variability in soil physical properties, at any scale, has received even less attention. The more comprehensive studies dealing with variability on arable soils in Norway include the quantification of variability in various soil physical properties between and/or within different soils (Høstmark, 1994; Olsen, 1999; Kværnø, 2000), the quantification of spatial patterns in hydraulic conductivity (Kværnø and Deelstra, 2002), and electrical conductivity as related to soil texture (Korsæth and Riley, 2003; Korsæth, 2008; Korsæth et al., 2008). The only known study attempting at quantifying seasonal variability in soil physical properties on arable soils in Norway, has been carried out by Øygarden (2000), focusing on aggregate stability.

Quantification of soil physical properties will strongly depend on other approaches and data sources than direct measurements. For most areas, a soil map will be the most informative source of primary soil physical data. In Norway soil maps exist only for arable land, which constitutes about 3 % of the total land area. Soil data for other land uses, e.g. for

forest, which is an important land use in Norway, are virtually absent all over the country. Only a few basic soil variables can be derived directly from a soil map and the underlying database. For the Norwegian soil maps, produced by the Norwegian Forest and Landscape Institute, this includes topsoil texture and organic matter content classes. Additional information can be derived from the national soil survey database, containing measured data on particle size distribution, gravel and organic matter content on different depths for soil profiles representative for various soil series. Currently, the soil map is a very important source of soil information in Norway. One of the thematic soil maps, the erosion risk map, is widely used in Norway for planning measures against soil erosion, and forms a basis for subsidies to farmers. The quality or accuracy of the soil map is unknown. Various studies have shown that variability within map units can be considerable (Young et al., 1997; Salehi et al., 2003), and that within-unit variability may be greater than between-unit variability (Lathrop et al., 1995). The resolution of the Norwegian soil map (1:5000) is small enough to provide some information about variability within a farm field. However, no information about variability within map units exists (apart from indicating the presence of complexes or inclusions).

The use of PTFs, or "pedotransfer functions" has become a popular approach for solving the problem with lack of measured data for the more difficult to obtain soil physical properties like hydraulic conductivity and soil water retention curve (SWRC). PTFs for SWRC and K_s are abundant in the literature, some popular PTFs being those of Rawls and Brakensiek (1989), Wösten et al. (1999) and Schaap et al. (2001). However, PTFs are themselves models, requiring input data (most often texture, SOM and sometimes bulk density), and using PTFs to provide model input data results in further uncertainty propagation. The PTF model error should not be neglected since it can be significantly larger than the soil heterogeneity (Vereecken et al., 1992; Christiaens and Feyen, 2001). It is often shown that measured and PTF predicted soil properties result in different model outputs (e.g. Timlin et al., 1996), that poor PTF predictions are inadequate inputs to models (Sobieraj et al., 2001), and that different PTFs result in different model outputs (Gijsman et al., 2003). Still, in cases where there are no data available, there are few or no alternatives to using PTFs. Assessment of the PTF error is therefore important, both by ways of direct statistical evaluation of predicted versus measured soil property (e.g. Tietje and Tapkenhinrichs, 1993; Wagner et al., 1998; Cornelis et al., 2001; Gijsman et al., 2003; Givi et al., 2004; Donatelli et al., 2004; Wagner et al., 2004; Børgesen and Schaap, 2005), and by ways of evaluating the errors resulting from using the PTF derived data in a model, termed a "functional evaluation"

(e.g. Wösten et al. 1990; Vereecken et al., 1992; Timlin et al., 1996; Sobieraj et al., 2001; Gijsman et al., 2003; Nemes et al., 2003; Soet and Stricker, 2003; Ma et al., 2009). In Norway, there has been developed PTFs for soil organic matter, mean particle density, dry bulk density, porosity, water content at specific matric potentials, available water capacity, air capacity and hydraulic conductivity (Riley, 1996), and for aggregate stability (Grønsten, 2008). The PTFs of Riley (1996) are part of the national soil survey database, and serve as basis for some thematic maps derived from the soil maps.

The practical importance of variability and uncertainty differs between different studies. Incorporating information about soil variability and increasing the resolution of soil data in simulation models have often shown to improve model predictions (Lathrop et al., 1995; Lilburne and Webb, 2002; Chaplot, 2005, Lindahl et al., 2005), but some studies have also shown little gain in precision using spatially variable data as compared to mean values or effective parameters (Peck et al., 1977; Lewan and Jansson, 1993; Bechini et al., 2003). The influence of variability has also shown to differ within single model studies (Merz and Plate, 1997; Vachaud and Chen, 2002).

To summarize, the use of models relies on the sparse information that exists, making assessment of uncertainty very important. It is therefore important to quantify uncertainties related to using what is generally available, compared to more detailed data sources that are generally NOT available. Published studies dealing with input data uncertainties show deviating conclusions with respect to effect of data source, data aggregation and use of pedotransfer functions. Transferability of results from other studies is therefore difficult.

1.2 Main objectives

The objective of this thesis is to quantify variability in soil physical properties on arable land, uncertainties related to data sources, and effects of variability and uncertainty on selected functional criteria. Specific objectives within this scope are to

- quantify spatial variability in topsoil texture and carbon content on arable land within a catchment, on within-field and catchment scales
- assess the uncertainty related to basic soil data (texture and carbon content) derived from the soil map
- validate PTFs for predicting the soil water retention curve, both those that are currently used as a basis for thematic soil maps in Norway, and alternative PTFs that are more useful in model simulations

- measure effect of soil moisture content and number of freeze-thaw cycles on aggregate stability of three different soils
- assess implications of variability and uncertainty in texture and carbon content on maximum water content for optimum workability and number of days until tillage after spring snowmelt, as predicted by simple models
- assess implications of variability and uncertainty in soil physical properties on catchment surface discharge and soil loss, as predicted by a process based simulation model, using different sources for basic soil properties and deriving hydraulic properties and soil stability variables using PTFs

2 Material and methods

2.1 Study site characteristics

The area of focus in this thesis is the Skuterud catchment (Figure 1) in the municipalities of Ås and Ski, approximately 30 km south of Oslo. The catchment can be considered representative of agricultural areas with cereal production on marine deposits in South-east Norway. The mean annual temperature and precipitation in the area (Ås) are 5.3˚C and 785 mm, respectively. The catchment has a size of approximately 450 ha (4.5 km^2). It is located at an altitude of 85–150 m above sea level, and the topography is undulating. Marine deposits cover most of the catchment. According to the soil map (covers arable land only), produced by the Norwegian Forest and Landscape Institute (www.skogoglandskap.no), the predominating soils in the central and level parts are marine silt loam and silty clay loam soils classified in World Reference Base for soil resources (WRB) as Albeluvisols and Stagnosols. The texture of the marine shore deposits is mainly sand and loamy sand, soils are classified as Cambisols , Arenosols, Umbrisols, Podzols and Gleysols. Land use in the catchment is 60 % arable land, 31 % forest, 2 % forested peatland, and 7 % urban area. The Skuterud catchment is part of the Environmental Agricultural Monitoring Programme in Norway (JOVA), and monitoring of discharge and water quality (concentrations of pesticides, suspended sediment, nutrients like nitrogen and phosphorus, and other elements) has been carried out at the outlet of the catchment since 1993 (Sørbotten, 2011). In 2008 a monitoring station was installed in the south-eastern part of the catchment (Figure 1), as part of a project on storm water runoff (Kramer and Stolte, 2009). Data and investigations in the Skuterud catchment are used in all the four papers that are part of this thesis.

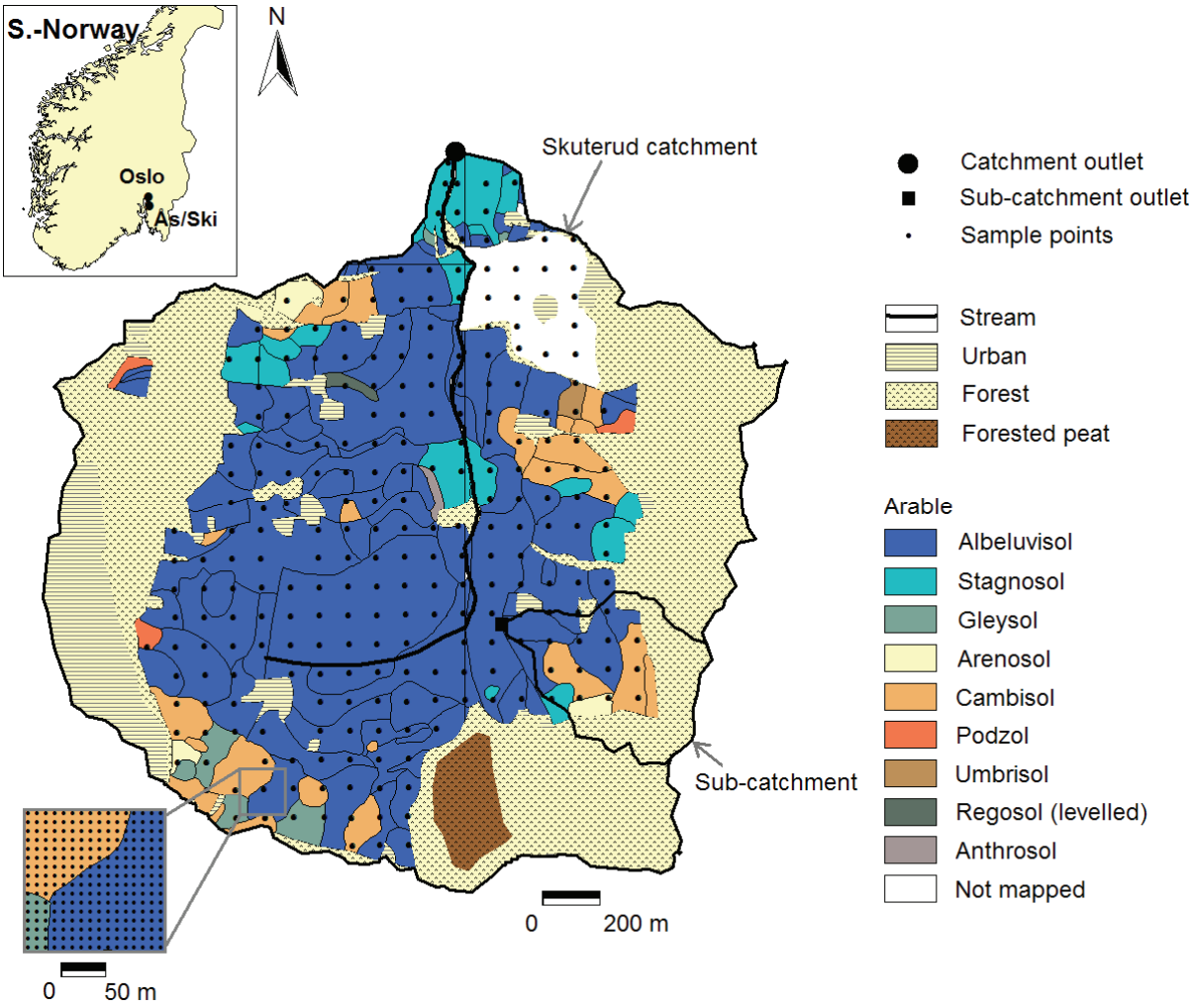

Figure 1. Combined land use map and soil map (WRB soil orders) for the Skuterud catchment, with locations of soil samples and catchment outlet monitoring stations.

In this thesis we also use data collected in other parts of Norway. Two soils for aggregate stability measurements (paper II) were collected from a small catchment (Vandsemb) located in the municipality of Nes, Akershus county, to represent soils with assumed lower aggregate stability than found for the clay soils in the Skuterud catchment: an artificially leveled soil with silty clay loam texture, and a Gleyic Cambisol with silt texture. For PTF performance evaluation (paper III), data from many parts of Norway were collected to form a database. Marine deposits, brackish flood sediments, fluvial deposits and glacial till are represented, all common parent material for arable soils in Norway. Textural composition of the samples varied from sand to heavy clay.

2.2 Measured data

The sampling schemes for topsoil (0-20 cm depth) particle size distribution and carbon content (papers I and IV) were selected to represent two different scales, for determining scale effects on soil variability. The large grid (247 samples, 100 m spacing), covered the total area of arable land (270 ha) in the Skuterud catchment (Figure 1). The small grid (256 samples, 10 m spacing) covered 2.25 ha of a 13.4 ha field (Figure 1). The bulked samples from each sample point were analysed for percentage of clay, silt, fine sand, medium sand and coarse sand using the pipette method (Gee and Bauder, 1986), and carbon content, using a Perkin Elmer 2400 CHN Elemental Analyzer.

For analyzing temporal variability, a laboratory approach was used to study effects of freezing and thawing on aggregate stability (paper II). The experiments were done in a controlled environment to be able to study the factors of interest only. Three topsoils on agricultural land were sampled for the study: a clay loam from the Skuterud catchment, and a silt soil and an artificially leveled silty clay loam from the Vandsemb catchment. The soil was treated by sieving into the fraction 1-4 mm, repacking into PVC cylinders, adjustment of soil matric potential using a sandbox apparatus, freezing and thawing at 0, 1, 3 and 6 cycles, and finally aggregate stability measurements using a rainfall simulator (Marti, 1984) on all samples and also a wet-sieving apparatus (Kemper and Rosenau, 1986) on selected samples. Aggregate stability was expressed as the percentage of dry material remaining on the sieve after the stability test relative to the initial amount of dry soil.

Shear strength (τ), representing the cohesion parameter in the LISEM model (paper IV), was measured in 22 selected sample points in the Skuterud catchment as a basis for developing a local PTF. We used a vane with four blades and made 10 replications in each of the 22 locations.

For validation of pedotransfer functions for the soil water retention curve (paper III) and dry bulk density (paper IV), we collected a dataset consisting of measured water content at different matric potentials (0, -5, -20, -100, -1000 and -15000 hPa) together with data on dry bulk density and content (%) of clay, silt, sand, gravel and carbon (or loss on ignition in some cases). These data were assembled from soil profile descriptions from the Norwegian Forest and Landscape Institute, and from various research projects at Bioforsk (the Norwegian Institute for Agricultural and Environmental Research) and the Norwegian University of Life Sciences. The total dataset contained 540 samples. The samples have been collected on agricultural land in different parts of Norway. The soils have formed on marine deposits, brackish flood sediments, fluvial deposits and glacial till, all common parent material for

arable soils in Norway. The database also included data from three soil profiles located within the Skuterud catchment, i.e. an Albeluvisol series Rk8, a Stagnosol series He8 and an Arenosol series Je3.

For calibration of a physically based soil erosion model (the LISEM model, see section 2.4), we used surface runoff and concentration of suspended solids measured at the outlet of the subcatchment (paper IV). A flume was installed to measure overland flow. Water depth (logged at 10-minute intervals) in the flume was measured using an ultrasonic sensor, and a conversion from depth to discharge was performed using a height-to-discharge relationship. ISCO water samplers were placed at the site to collect water samples from the flume during and after rainfall and snowmelt events. Water samples were used for determination of suspended sediments. This work was carried out in two projects funded by the NORKLIMA program of the Norwegian Research Council (the Climrunoff and ExFlood projects).

2.3 Derived data

The soil map was used as a source of basic soil physical properties (papers I and IV). The map contains information about soil order as classified in World Reference Base for Soil Resources, local soil series name, a figure referring to soil texture class, a letter referring to slope class and a figure referring to stone and block content class. The soil texture class corresponds to the classes presented in the Norwegian soil textural triangle (Sveistrup and Njøs, 1984). One of the thematic maps available also provide SOM class (0-1 %, 1-3 %, 3-6 %, 6-12 %, 12-20 %, >20 %). In addition, a description of the local soil series exists (Nyborg, 2003; 2008), and for each soil series mapped in Norway, this report gives typical horizon names and depths, typical texture classes and gravel content classes of all horizons, and typical carbon content of the topsoil. For the Skuterud catchment, we derived values for clay, silt, sand and SOM content in two ways: 1) by using the centroid of the soil texture class, together with the carbon and gravel contents reported by Nyborg (2003) (paper I), and 2) by using representative ("generic") soil profile data that are not publicly available, but are available in the database of the Norwegian Forest and Landscape Institute and in this case were provided upon request by Nyborg (pers.comm.) (paper IV). These profiles are currently used as basis for thematic maps developed by the Norwegian Forest and Landscape Institute, like the erosion risk map. The texture and SOM values of these generic profiles may be a

mean value from several profiles, or they may even come from a different soil type with the same texture.

PTFs were used for calculating several soil physical properties (papers I, III and IV). Common for all the PTFs used were that they required as input one or more of the following basic soil properties: percentage of clay, silt, sand and gravel, organic matter content, and bulk density. In paper I, the PTFs by Riley (1996) were used to predict bulk density and water content at field capacity, PTFs by Kretschmer (1996), as recommended by Mueller et al. (2003), to predict the functional criterium "maximum water content for optimum workability" (W_{opt}), and PTFs by Schindler, cited by Mueller et al. (2003), to predict the upper and lower plasticity limits (UPL and LPL).

PTFs for the soil water retention curve were statistically evaluated in paper III, and included the point PTFs of Riley (1996), which predict water contents at different matric potentials, and six parameter PTFs published by Rawls and Brakensiek (1989), Vereecken et al. (1989), Wösten et al. (1999) and Schaap et al. (1998, 2001), which predict parameters in the Brooks and Corey (1964) or van Genuchten (1980) equations (equation 1 and 2 respectively):

$$\theta(h)=\begin{cases}\theta_s, & h/h_a\leq 0\\ \theta_r+(\theta_s-\theta_r)\times(h/h_a)^{-\lambda}, & h/h_a>1\end{cases} \quad (1)$$

$$\theta(h) = \theta_r + (\theta_s - \theta_r) \times [1 + (\alpha h)^n]^{-m} \quad (2)$$

where $\theta(h)$ is the water content at matric potential h, θ_s is the saturated water content, θ_r is the residual water content, h_a is the air entry value or bubbling pressure, λ is the pore-size distribution index, and α, n and m are shape parameters. Four of the six parameter PTFs used continuous input data, while the remaining two provided parameter values for specified classes: texture class for the Schaap PTFs, texture class by topsoil and subsoil for the Wösten PTFs.

In paper IV an additional PTF performance evaluation was performed for dry bulk density, PTFs including Riley (1996), Leonaviciute (2000), Manrique and Jones (1991), Kätterer et al. (2006) and Rawls and Brakensiek (1989). The validation material was 186 topsoil samples from the dataset used in paper III for evaluating PTFs for the SWRC. Bulk density ranged between 0.63 and 1.8 g cm^{-3} in these samples. Clay content was 1.0 – 43 %,

silt content 2.0 – 90 %, sand content 1.8 – 97 %, gravel content 0 – 44 % and SOM content 0.10 – 17 %.

Based on the PTF evaluations in paper IV and III, the PTFs of Riley (1996) for bulk density and Wösten et al. (1999) for the SWRC, in addition to PTFs for hydraulic conductivity parameters K_s and l (Wösten et al., 1999), aggregate stability (Grønsten, 2008) and cohesion (local PTFs – see section 3.2.2), were chosen to predict input data to the LISEM model (paper IV).

2.4 Models for calculating functional criteria

The responses for which we evaluated effects of variability, uncertainty and data source (functional criteria) were W_{opt}, number of days until soil is workable (paper I), surface discharge and soil loss (paper IV).

W_{opt} was calculated using PTFs (section 2.3). The number of days from the last snowmelt until W_{opt} is reached was expressed as (only for soils with clay content > 10 %):

$$Number\ of\ days = D + (\theta_{FC} - W_{opt} \times \rho_b)/E_{pot} \quad (3)$$

where D is the number of days with free drainage (assumed = 2 days), θ_{FC} is the volume fraction water content at field capacity (defined at -100 hPa), ρ_b is the dry bulk density (calculated from Riley, 1996), W_{opt} is the gravimetric maximum water content for optimum workability, $W_{opt} \times \rho_b$ is the volume fraction of water at W_{opt}, and E_{pot} is the potential evaporation, assumed to equal 2.4 mm/day based on calculations using the Penman equation with data from the UMB meteorological station in Ås in the period April 15 to May 31 (median E_{pot} = 111 mm over 46 days). April 15 is the approximate date of the last day with snow cover in Ås. For non-cohesive soils it was assumed sufficient with two days of free drainage to obtain workable conditions.

Storm event driven surface discharge and soil loss were simulated by LISEM , the LImburg Soil Erosion Model (de Roo et al., 1996a; Jetten, 2002). It is a physically based model which simulates hydrology and sediment transport during and immediately after a single rainfall event on a catchment scale. LISEM is a spatially distributed model, completely incorporated in a raster geographical information system (PCRaster (Wesseling et al., 1995)). The basic processes incorporated in the model are rainfall, interception, surface storage in micro-depressions, infiltration, vertical movement of water in the soil, overland flow, channel

flow, detachment by rainfall and throughfall, transport capacity and detachment by overland flow. The catchment under study is divided in grid cells of equal sizes. For each grid cell for every time step, rainfall and interception by plants are calculated, after which infiltration and surface storage are subtracted to give net runoff. Subsequently, splash and flow erosion and deposition are calculated using the stream power principle and the water and sediment are routed to the outlet with a kinematic wave procedure. Infiltration can be calculated with various sub-models, according to the data available. In this study, a finite difference solution of the Richards' equation was used. This includes vertical soil water transport and the change of matric potential in the soil during a rainfall event. We calibrated the model using measured runoff and sediment data for the sub-catchment, for one storm event on August 13, 2009. Then, for obtaining a measure of uncertainty in simulated hydrograph and soil loss as related to variability and uncertainty in soil physical input data, the model was run for the Skuterud catchment, for a storm event on August 19, 2008. Basic input data taken were from two sources: locally measured data (section 2.2.), and soil map combined with generic soil profile data (section 2.3). The locally measured data were assigned in two ways: 1) randomly distributed within soil map texture class units, retaining information about variability, and 2) mean of measured data for each soil map texture class. Simulations were first run for the actual soil surface state, i.e. with crop cover, and then for a "worst case" situation with uncovered soil and with aggregate stability and cohesion reduced by 25 %, based on the findings from paper II.

2.5 Statistical methods

Various statistical methods were used in this study, including:

1) summary statistics like minimum, median, maximum, moments (mean, standard deviation, skewness) and coefficient of variation (CV) (all papers).
2) geostatistics with estimation of parameters from the variogram model: nugget, sill and range, and nugget to sill ratio (paper I).
3) regression analysis for removing trends before variogram analysis (paper I), for development of a shear strength PTF (paper IV) and for comparison of aggregate stabilities measured by wet-sieving and rainfall simulator (paper II).
4) the Tukey's multiple comparison test for comparing means (paper I and II), and the Brown-Forsythe test for unequal variances for comparing variances of different soil series (paper I).

5) the general linear model (GLM) procedure for determining treatment effects and differences between measurement methods in the freeze-thaw experiment (paper II).
6) various statistical indicators to evaluate PTF performance (papers III and IV): modeling efficiency (EF), the Pearson product-moment correlation coefficient (r), relative error (RE), root mean squared error (RMSE) and relative RMSE (RRMSE), and some of these statistical indicators combined into a fuzzy-based integrated index developed by Donatelli et al. (2004).

3 Main results and discussion

3.1 Spatial variability and soil map uncertainty

The two datasets with measured particle size distribution and carbon content of arable land topsoil in the Skuterud catchment were used to quantify spatial variability and uncertainty in thematic soil maps (paper I). Spatial variability in clay, silt, sand and carbon content showed to be considerable both for the large grid and the small grid. Spatial correlation parameters, which can be used for spatial interpolation (kriging) and for guidance with respect to sampling density, were scale dependent. The effective range for texture variables was 16 times larger in the large grid than in the small grid, and nugget to sill ratios were also higher in the large grid, indicating that more of the variation could be considered small scale and/or random. The data from the large grid were further used to quantify variability between and within soil map units. Clay, silt and sand content were significantly different between series having different texture class, but not between different series with the same texture class. Within a soil series, the span in clay content was up to 34 %, and for silt and sand content up to 45 and 67 %, respectively (Figure 2). The coefficients of variation (CV) for clay and silt was largest for two soil series located in parts of the catchment with a patchy spatial distribution of marine and shore deposits. The data from the small grid illustrated large variability on the border between two map units of different parent material and texture, and that the boundary between the two map units was fuzzy or gradual rather than crisp.

The data from the large grid also provided a measure of soil map uncertainty. The mean and median values for clay, silt, sand and carbon content mostly fell within the limits of the texture or SOM class of the soil series, but the total range of the four variables could span from below to above these limits (Figure 2). Comparison of actual and soil map texture class

(according to the Norwegian texture triangle) revealed that on the large grid scale, 42 % of the samples had a different texture class than the mapping units they were sampled from, but most of these samples (39 %) belonged to a neighboring texture class in the soil texture triangle. The deviating samples were generally located in areas with many soil series and different deposits, indicating higher uncertainty around the map unit delineations in this variable soilscape. In the small grid the mismatch was higher, 73 %, of which 57 % in neighbouring texture groups. Most prominent on both scales was the underrepresentation of texture class sandy loam/loam and overrepresentation of silt loam in the soil map compared to the sample measurements.

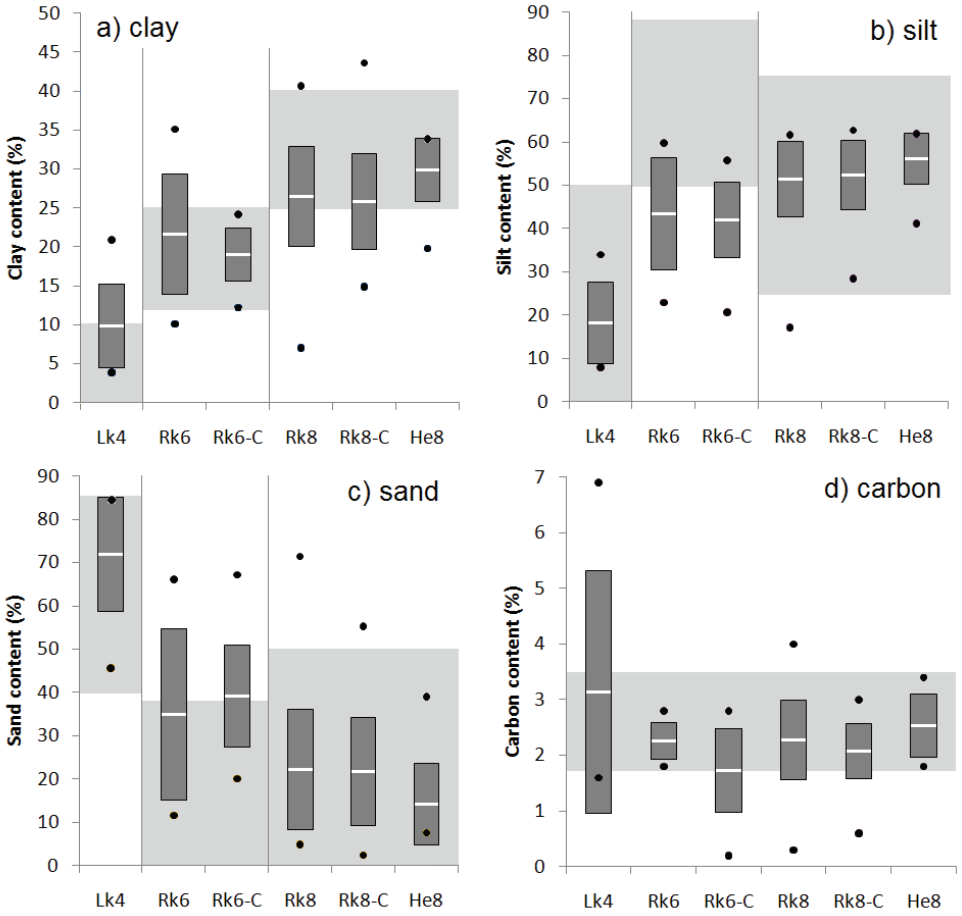

Figure 2. Boxplots for texture variables and carbon content for six soil series (-C denotes complexes, the others are concosiations) in the Skuterud catchment. White line is the mean, boxes represent ±standard deviation and dots min and max values. Light grey area shows the clay, silt and sand content ranges for classes 4 (loamy fine sand), 6 (silt loam) and 8 (clay loam, silty clay loam), and the carbon content range for SOM-class 3-6 %. Adapted from Table 2 in paper I.

From this it seems that the soil map can be a useful source of basic soil properties data on the larger scale, but not accurate enough for site-specific management like precision farming. In precision farming, the goal is to maximize yield and income and at the same time minimize costs and environmental pressure. Spatial variability in soil physical properties will be of utmost importance for e.g. the availability of water to plants and consequently drought stress, influencing crop yields, risk of nitrogen leaching and nitrous gas emissions, and thus fertilizer use efficiency. In precision farming the width of machinery for application of fertilizer, lime, pesticides, etc., determines the spatial resolution that can be managed. This width rarely exceeds 10 m, meaning that a spatial resolution corresponding to the small grid in this study needs to be characterized. In precision agriculture, several remote sensing techniques have become popular for fast and cheap characterization of variability, including in situ "on-the-go" measurements of electrical conductivity (EC_a) and near infrared reflectance spectroscopy (NIR), which can be related to soil properties if also direct measurements are available for making local transfer functions.

The conclusions from this investigation are not necessarily applicable to areas outside the Skuterud catchment, but since intensive sampling has not been carried out anywhere else in Norway, we do not know. According to Arnoldussen (pers. comm.), the soil map for Skuterud was made in the beginning of soil mapping in Norway, before 1991, and he claims that maps created after 1991 have better quality, particularly with respect to texture classes. However, no information about map accuracy or uncertainty is available to the users – the soil maps can be downloaded, and the poorer quality maps will be used indiscriminately in the same way as better quality maps. It would be useful if available soil maps could be supplemented with information about uncertainty and within map unit variability. This would require more investigations like the one presented here.

3.2 Temporal variability: freeze-thaw effects on aggregate stability

Freezing and thawing is one of the factors that can lead to temporal variability in soil physical properties. This was shown for aggregate stability of three different soils subjected to repeated freezing and thawing (paper II). The pre-freezing aggregate stability of the clays was around 80 %, and 31 % for the silt. It was expected that the artificially leveled clay would behave differently than the non-levelled clay because levelled soils often have low organic matter content and poor structure (e.g. Lundekvam and Skøyen, 1998), but the stabilities were similar. The leveled clay actually had similar organic matter content as the non-levelled, but

at visual inspection the structure seemed considerably poorer, and this was not reflected in these measurements. Freezing and thawing decreased the aggregate stability of all soils (Figure 3), corresponding to results from some other studies (Bullock et al., 1988; Edwards, 1991; Mulla et al., 1992; Staricka and Benoit, 1995; Dagesse et al., 1997; Bajracharya et al., 1998). The effect was more severe on the silt soil, as the relative decrease from none to 6 freeze-thaw cycles was 55 %, as opposed to approximately 20 % on the clay soils. There was no evident effect of water content on the stability, probably due to experimental limitations related to increased aggregate consolidation at high water contents (difficulties with sieving wet soil). These results show that the temporal variability in aggregate stability, induced by freeze-thaw cycles, should be accounted for in modeling soil erosion in areas with frozen soils part of the year. To date, few, if any, models include the process of freeze-thaw induced aggregate breakdown, partly because the models have been developed for areas where freezing and thawing is not important, and partly because of the lack of data, especially under natural field conditions. The importance of freeze-thaw induced aggregate breakdown will be particularly important in areas with unstable winter conditions, where freezing and thawing occurs several times during the winter season. Climate change can potentially lead to warmer and wetter winters, and maybe more frequent freezing and thawing. Combined with more precipitation as rainfall during the winter period both runoff and erosion may increase. Today's erosion risk maps in Norway do not take climatic conditions into account, but in further improvement and development of these maps freeze-thaw effects on soil erodibility should be accounted for.

In comparing wet-sieving to rainfall simulator, wet-sieving resulted in less aggregate breakdown than the rainfall simulator due to different energy levels. This has also been shown by Grønsten and Børresen (2009). Our study showed that the relationship between wet-sieving and aggregate stability was not linear - rainfall impact seemed to be relatively more detrimental than wet-sieving on more unstable soil, that is, on silt soil and soil subjected to many freeze–thaw cycles. This should be kept in mind if a model requires aggregate stability measured by one method, but only data measured by another method is available.

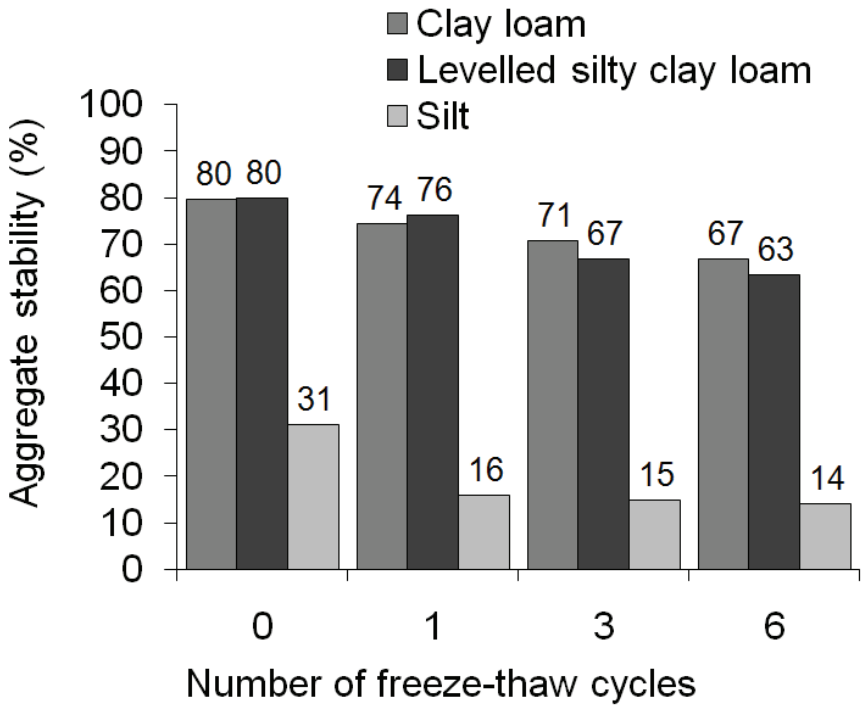

Figure 3. Aggregate stability measured by rainfall simulator, as influenced by various number of freeze-thaw cycles.

3.3 Uncertainties in data derived via pedotransfer functions

In the study concerning performance of PTFs to predict the SWRC (paper III), the Riley PTFs showed good overall performance. The most problematic point was predicting water contents in the wetter range of the SWRC, possibly because bulk density, which is strongly related to soil porosity and thus the saturated water content, is not used as a predictor in the PTFs for θ_s and $\theta(-20)$. The layer and soil specific versions of the Riley PTFs performed almost equally well, according to the small differences in performance indicators. However, we found that the soil specific version should be preferred over the layer specific at clay contents > 25 %, as the latter may introduce a negative change in water content with increasing matric potential (h). The main disadvantage with the Riley PTFs is that they predict water contents at six matric potentials only, making them of limited use in models that need more points or the SWRC function parameters as input. The Riley PTFs can still be useful for predicting porosity, field capacity, wilting point and derivatives like plant available water and drainable porosity, which is sometimes used as input to more simple models. Among the parameter PTFs, Wösten's continuous PTF showed the overall best performance (for all soils and in all matric potential ranges), closely followed by Rawls and Brakensiek and Vereecken. The Vereecken PTF performed slightly poorer in the matric potential range between -20 and -

60 hPa, possibly because Vereecken restricts the m parameter in the van Genuchten equation (equation 2) to 1, while in our fitting to the measured data m was restricted to 1-1/n, which also applies to the other PTFs. Rawls and Brakensiek was more problematic from saturation to -10 hPa, maybe relating to the way entrapped air is adjusted for and the exclusion of SOM as input. The latter may also be one explanation for the poorer performance of the ANN-based continuous PTF of Schaap compared to its regression based counterparts. The class PTFs of Wösten and Schaap often performed poorly, because of systematic errors related to particle size and organic matter: the same SWRC represents a range of particle size distributions, and SOM is not explicitly included as an input variable. The performance of these PTFs was particularly poor in the wet and moist range of the SWRC, an area much influenced by SOM. The Wösten class PTF performed slightly better than the Schaap class PTF for the full dataset, possibly because the Wösten class PTF provides separate PTFs for topsoils and subsoils. In addition to the main points noted above, we also concluded that: 1) The PTF performance showed little difference between soil groups, 2) water contents in the dry range of the SWRC were generally better predicted than water contents in the wet range, 3) PTFs including both SOM and measured bulk density as input, i.e. Wösten, Vereecken and Rawls and Brakensiek, performed best in the wet range, and 4) aggregation of multiple statistical indicators should be preferred over using single statistics as PTF evaluation criteria, and different methods of aggregating the statistics indicated slight, but not dramatic differences in ranking of PTFs.

Table 1. Statistical indicators for PTF performance, and ranking of PTFs according to the indicators.

Indicator	Riley (1996)	Kätterer et al. (2006)	Manrique and Jones (1991)	Leoniviciute (2000)	Rawls and Brakensiek (1989)
EF	0.47	0.22	0.12	0.42	0.19
rank	1	3	5	2	4
RRMSE	11	13	14	11	13
rank	1	3	5	1	3
RE	0.64	6.8	-7.4	3.4	3.8
rank	1	4	5	2	3
MAE	0.10	0.12	0.15	0.11	0.13
rank	1	3	5	2	4
R^2	0.50	0.44	0.46	0.50	0.33
rank	1	4	3	1	5
mean rank	1.0	3.4	4.6	1.6	3.8
Final rank	**1**	**3**	**5**	**2**	**4**

R^2 = coefficient of determination, EF = modeling efficiency, RRMSE = relative root mean squared error, MAE = mean absolute error, RE = relative error.

The results of a similar PTF performance test for dry bulk density were briefly presented in paper IV, as basis for choice of PTF to use for predicting input data to the LISEM model. The full results for all PTFs were not shown in the paper, but I show them here, in Table 1. All the evaluated PTFs showed relatively poor performance, as most evident from low EF and R^2. The Riley PTF, developed for soils in Norway, was ranked best. A possible implication of the poor performance of PTFs for bulk density can be increased error in predictions of hydraulic conductivity and SWRC by using PTFs to which bulk density is an input, and consequently higher uncertainty in simulation modeling.

As mentioned introductorily, a functional evaluation of PTFs is an alternative to pure statistical evaluation of predicted property versus observed property. The benefit of such an approach is that different models, model responses and environmental conditions may result in different uncertainties for the same PTF. This is partly linked to the model's sensitivity to the predicted variable or parameter: the choice of input data and PTFs are less important if the model is not sensitive to the inputs. Sometimes it can be beneficial to use an ensemble of PTFs instead of choosing one PTF: Guber et al. (2006) used an ensemble of 22 published pedotransfer functions for water regime simulations, and this approach resulted in smaller errors than when using actual measured data from the site. Brimelow et al. (2010) found that there appears to be merit in using a PTF ensemble to improve estimates of the soil's hydraulic properties for simulating soil moisture. There is also a question to which extent it pays off to use PTFs. Minasny and McBratney (2002) showed that in cases with large spatial variability it can pay off in terms of reduced uncertainty to conduct lots of cheap and imprecise measurements as input to PTFs instead of a few expensive and precise direct measurements of the hydraulic properties. Similarly, Deng et al. (2009) concluded from using PTF predicted hydraulic data in simulation of moisture flow that more input to the PTFs reduced parameter uncertainty more than collecting additional measurements for PTF development. As the data scarcity in Norway is large, we should put more work into functional evaluation of PTFs for different model applications and with various sources of PTF input data. This implies that also more measurements of soil physical properties must be carried out, so that we have appropriate data for such evaluation studies.

3.4 Implications of variability, uncertainty and data source on predicted functional criteria

3.4.1 Workability

The variability in texture and SOM was important in determining maximum water content for optimum workability (W_{opt}) and the number of days until soil is workable after spring snowmelt (paper I). W_{opt} for the most widespread soil series ERk8 varied between 15 and 38 % (mean 27 %) based on the large grid data, and between 17 and 38 (mean 21 %) based on the small grid data (Table 2). The calculated number of days to reach W_{opt} by drainage and evaporation for ERk8 varied between 2 and 6.4 days (mean 4.7 days) based on the large grid data, and between 2 and 6.0 days (mean 3.5 days) based on the small grid samples. Not presented in paper I were the figures for the other major soil series, For two other major soil series, ERk6 and EHe8, the variability was considerable (Table 2, data not presented in paper I). On average the number of days required to dry up the soil sufficiently for workable conditions was a little higher than the median length of dry periods in Ås within the relevant period (mid-April to end of May), which has been calculated to 3.7 days (range 1.5 – 9 days). Data source and spatial representation (soil map values, field averages, interpolated surface, and different scales) were also found to be important in calculating W_{opt} and number of days. As expected, the largest deviations were found in those areas where texture misclassification was most problematic, i.e. for the silt loam map units. This is summarized in Table 2, including an additional data source ("Generic") that was previously not available. The "Centroid-1" is the same source of texture and SOM as used in paper I, i.e. texture simply equal to the centroid of the class in the texture triangle, and soil series specific SOM from soil series definitions (Nyborg, 2003). The "Generic" has texture and SOM derived from the soil survey database (Nyborg, pers.comm.). W_{opt} from measured data was lower than for derived data. Maximum differences in W_{opt} were 3 % for THe8, 5 % for ERk8 and 9 % for ERk6. Differences in number of days were small for these three soil series.

Where dry periods are short, even small differences can be important. This was more evident within the area of the small grid. Comparing values interpolated from the large grid within the area of the small grid to point values in the small grid showed that the differences ranged from -2.8 to +4.5 % for W_{opt}. The difference for the water content between field capacity and W_{opt} ranged between -5.5 and 6.5 mm, corresponding to at least ±2–3 days of evaporation. Since the median number of consecutive dry days in spring was 3.7 only, this difference can be of significant importance.

Table 2. Values for W_{opt} and number of days until soil is workable, based on different input data sources.

	Measured		Derived	
Soil series	**Small grid**	**Large grid**	**Centroid-1**	**Generic**
		W_{opt}		
ERk8	21 (17-34)	27 (15-38)	33	28
ERk6	-	22 (13-32)	31	31
THe8	-	30 (20-34)	33	32
		Number of days		
ERk8	3.5 (2.0-6.0)	4.7 (2.0-6.4)	3.9	4.3
ERk6	-	5.0 (3.0-6.1)	4.8	4.2
THe8	-	4.5 (3.1-5.2)	3.9	3.6

With less information about the soil properties, wrong decisions can be made: tillage may be carried out too early, leading to poor seedbed preparation and compaction, or tillage may be carried out later than necessary, leading to delayed sowing and crop development and consequently lower crop yields, in addition to poor seedbed preparation. The functional criterias W_{opt} and number of days can be especially important with respect to climate change. In Norway, a wetter climate can lead to larger difficulties related to workability and trafficability. If the number of consecutive dry days decrease, margins become very small and good predictions of W_{opt} and Nd may be even more useful, but also more influenced by variability and uncertainty. Under such conditions more thorough predictions of workability limits and soil water content can be desirable. This also applies as more land is managed by contractors, since contractors usually have less detailed knowledge about the soil and have larger areas to manage. In this study the uncertainties related to the models for W_{opt} and Nd were not assessed. For Nd a simplistic approach was used, based on potential evaporation. The evaporation rate will usually be lower than the potential evaporation used in the calculations, meaning that the number of days are underestimated. The simple formulation could be substituted by a more complex water balance model to calculate the timing of W_{opt} (Hoogmoed et al., 2003), and also to calculate indicators like average workday probability (de Toro and Hansson, 2004), which could be an idea for a future thematic soil map. Further, PTFs for W_{opt} would need to be validated, as no such data were available for this study, except for the very limited data on lower and upper placticity limits (LPL and UPL). It is recommended that measured data for W_{opt}, LPL and UPL are collected, for getting more information about these variables that may become increasingly important with climate

change and with increased area managed by contractors, and for validation or further development of PTFs.

3.4.2 Discharge and soil loss

The effect of input data source showed to be very important when using the event based LISEM model to simulate catchment discharge (surface runoff) and soil loss (paper IV). Input data derived from the national soil survey database ("Generic run") resulted in a peak discharge that was almost 400 l/s higher than the peak discharge simulated using locally measured data ("Mean run" and "Stochastic runs"), time to peak was 130 minutes earlier and the soil loss was five times higher (Figures 4 and 5). In most circumstances measured data will not be available, and the only option is to use the soil survey database. It is therefore important to take uncertainty into account.

The value of K_s, derived from the basic input data using a pedotransfer function, was especially important in explaining the differences, as LISEM is highly sensitive to this parameter (De Roo et al., 1996b; Stolte et al., 2003). Less surface runoff simulated by the Mean run and Stochastic runs corresponded with higher area-weighted mean K_s (86 and 92 cm d-1, respectively) on arable land in these runs than in the Generic run (59 cm d-1). The predicted K_s will strongly depend on the basic soil properties as long as PTFs are used, emphasizing the importance of having access to adequate basic data and PTFs. K_s poses a large problem in modeling because it is often highly variable in time and space, it has a high degree of random variability (often resulting from macroporosity) and it is very difficult to measure correctly. Some authors have suggested that K_s is best represented as a calibration parameter (e.g. Davis et al., 1999), but this is inappropriate in distributed modeling, where the spatial distribution of K_s is important. In our study a "compromise" solution was chosen, where the PTF predicted K_s of all clay soils (because of macroporosity) was multiplied with a single calibration factor to get a good match between the measured and simulated hydrograph. More measured K_s data are required to come up with a more sophisticated and realistic approach.

The main reason for more soil loss simulated by the Generic run seemed to be that considerably more surface runoff was simulated by this approach. Differences in aggregate stability and cohesion were too small to explain the difference.

The two approaches of assigning locally measured input data, i.e. using a mean value on one hand and a stochastic distribution on the other hand, did not result in large differences in simulated discharge and soil loss. The variability in model output for the realizations in the

stochastic approach was negligible, especially for simulated surface runoff. The possibly small gain in precision by using the stochastic approach instead of the mean value approach cannot justify the extra effort made in input data generation, model runs and processing of results for multiple realizations. This needs to be verified also for other situations (surface cover, event size, season). Both of these approaches to assign measured data used the soil map as basis for spatial distribution of soil properties. This study should be followed up with alternative approaches where the spatial correlation of the locally measured data is retained. This might influence the result due to interactions between soil and terrain.

Running the model for both a low risk situation (crop covered surface) and a high risk situation (bare soil with freeze-thaw induced changes in aggregate stability and cohesion) showed that the variability in model output for the stochastic approach was similar in both cases, i.e., the uncertainty did not appear to depend on the erosion risk. Comparison of absolute and relative differences between the two risk situations and the three input data approaches showed that the uncertainty related to input data could result in larger differences between runs with different input data source than between runs with the same input data source but extreme differences in erosion risk. Effects of removing the crop cover and decreasing the structural stability varied between the input data approaches.

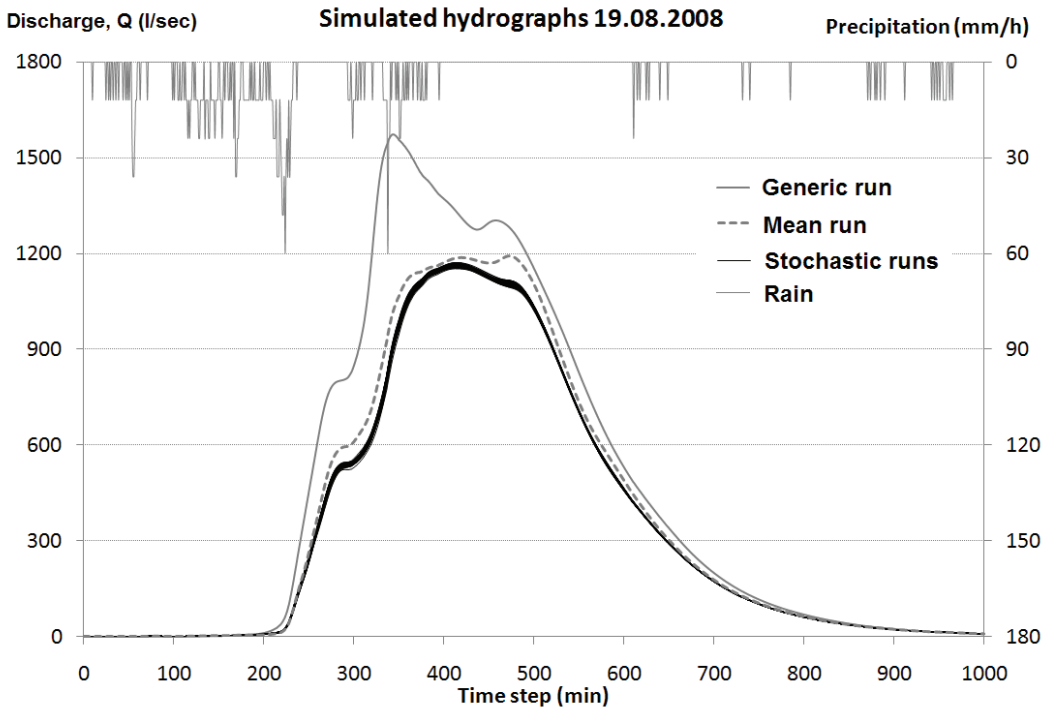

Figure 4. Simulated surface runoff for the Generic run, Mean run and 50 Stochastic runs, together with rainfall intensity.

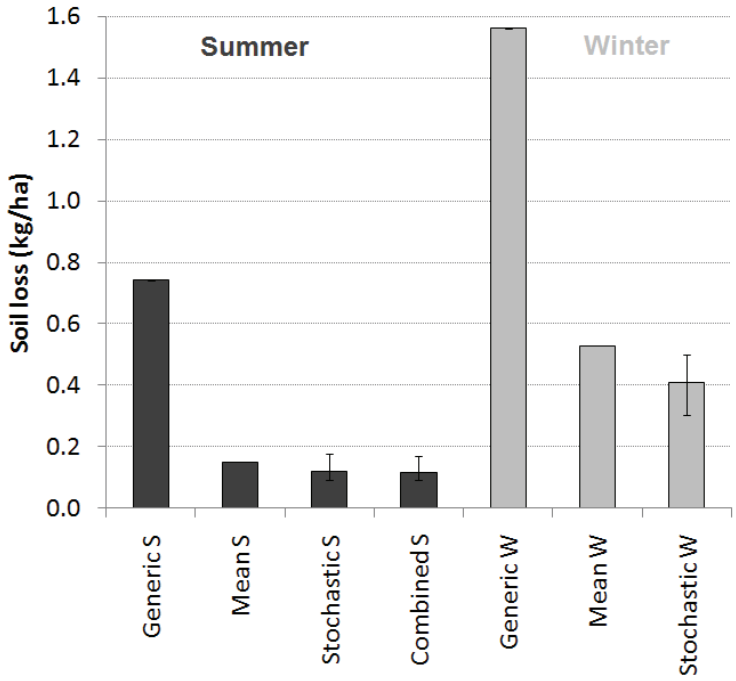

Figure 5. Simulated soil loss for the different input data approaches, summer conditions and "worst case" winter conditions. The bars shown for the Stochastic and Combined approach represent the mean of the 50 realizations, while the whiskers represent minimum and maximum values.

This study clearly showed that inadequate choice of input data sources can significantly underestimate or overestimate surface discharge, soil loss and consequently the effect of measures to reduce soil erosion. Clearly, this is only a first step towards quantifying uncertainty in simulated responses of catchments in Norway. Other studies dealing with input data uncertainty in modeling show that the effects of input data source, variability and uncertainty differ between models, type of response, spatial and temporal resolution, thresholds for certain parameters, event size, etc. (e.g. Merz and Plate, 1997; Vachaud and Chen, 2002; Lindahl et al., 2005).

Unfortunately, we cannot find out which of the approaches used in this study produced the most realistic results at the main catchment scale, because only total discharge is measured at the catchment outlet. The total discharge is a mix of surface runoff, subsurface drainage water (both macropore and matrix flow), and groundwater flow/ baseflow. Investigations of uncertainty in relation to measured response should be investigated on a sub-catchment scale, with available precipitation and surface runoff data with high temporal resolution (sub-hourly or even sub-minute). The sub-catchment within the Skuterud catchment, successfully used for

calibration of LISEM, is the only site in Norway that can be used for this specific purpose. It is strongly recommended that more such experimental sites are established for more detailed research on effects of variability and uncertainty in input data on hydrological processes, soil and nutrient loss.

Lack of validation data can be an equally important problem in hydrological modeling as lack of input data – we need to have some confidence that the models produce realistic responses in order to use them in risk and scenario analyses. Spatially distributed models like LISEM have the advantage that they can be used to predict not only the magnitude of loss from a catchment, but also where the problems are largest and where it will be most beneficial to invest in measures. At the same time, it is more difficult and costly to obtain appropriate input data and validation data. A study by Takken et al. (1999) clearly showed that it is not possible to evaluate the performance of spatially distributed erosion models by using catchment outlet data alone; such models' behavior can only be understood if they are evaluated using spatially distributed data. Poor reproduction of spatial erosion patterns was also found by Jetten et al. (2003) and Hessel et al. (2003). Hessel et al. (2006) has pointed out several reasons for overpredicted soil loss and poor match between simulated and observed erosion patterns: 1) the difficulty of obtaining enough accurate data to run the model, 2) the difficulty of obtaining accurate data for validation, both at the outlet and spatially, 3) the model could not deal correctly with complex events, i.e. those having double rainfall peaks, and 4) the model could not deal with events in which throughflow or baseflow played a role (those processes are not simulated). De Roo (1998) relates the disappointing results of spatial models in the uncertainty involved in estimating and measuring the large number of input variables at a catchment scale. Presently model performance in predicting spatial erosion patterns cannot be carried out for the Skuterud catchment or any other place in Norway, due to lack of both erosion pattern observations and spatially distributed model input data. It is recommended that future research on soil erosion puts strong emphasis on prediction of spatial patterns, because, as stated by Jetten et al. (2003): "It is much more cost effective to over-dimension an erosion control measure than to put it in the wrong spot". Sometimes the benefit from using a complex, process based model is counteracted by the increasing error due to uncertainty on the soil information for such models (Van Rompaey and Govers, 2002; Schoups and Hopmans, 2006). Thus, simpler (e.g. lumped, regression based) models may actually outperform the more complex models.

4 Conclusions

The main focus of this thesis has been on variability and uncertainty in soil physical properties on arable land.

Spatial variability in measured topsoil texture and carbon content on arable land within a 450 ha catchment was considerable, and spatially correlated. Variability within the major soil series was quantified – the CVs ranged between 10 and 69 %, and the span in variable values was large for all soil series. Comparison of actual and soil map texture class revealed substantial misclassification in the soil map, with underrepresentation of loam and sandy loam soils, and overrepresentation of silt loam soil. Misclassification was particularly high in a the small sample grid located on the border between a sandy shore deposit soil and a clayey marine deposit soil, indicating fuzzy boundaries between map units and high uncertainty in these areas.

A specific aspect of temporal variability was investigated, i.e. effects of freezing and thawing on aggregate stability. The study showed that aggregate stability decreased with repeated freezing and thawing. The decrease was larger for the initially more unstable silt soil than the two more stable clay soils. Different measurement techniques yielded different aggregate stability values, and the difference in aggregate stability measured by the two techniques was greater the more unstable the soil was (silt soil, many freeze-thaw cycles).

Performance of pedotransfer functions for the soil water retention curve was evaluated on a dataset of 540 soil samples from different soils in Norway. The point PTFs developed for soils in Norway showed overall good performance. The parameter PTFs showed variable performance. One of the PTFs that performed well in most cases, was the one by Wösten et al. (1999). The PTFs of Vereecken et al. (1989) and Rawls and Brakensiek (1989) also performed well. The class PTFs showed poorer performance, especially if SOM was not an input to the PTF.

Implications of variability, uncertainty and data source were investigated for selected functional criteria, i.e. the maximum water content for optimum workability (W_{opt}), the number of days until workable conditions is obtained after spring snowmelt (Nd), catchment discharge and catchment soil loss. The effect of variability on W_{opt} and Nd appeared to be important, considering small margins with respect to the usually low number of consecutive dry days in spring. The effect of data source on simulations of storm event driven surface discharge and soil loss was large, with higher values simulated using input data derived from the soil map and soil survey database than when using locally measured input data. In this

particular study, there was no merit in retaining information about spatial variability within map units by stochastic assignment of measured data, as compared to simply using a mean value for each map unit. This study also showed that differences related to choice of data source can be larger than differences as a result of different risk of runoff and erosion (crop covered situation versus "worst case" situation with reduced soil stability and without crop cover).

The major conclusion of this study is that inadequate choice of input data sources can significantly underestimate or overestimate W_{opt}, number of days, surface discharge, soil loss and consequently the effect of climate change and measures.

4.1 Future perspectives and research needs

In this work attention has been put to the great lack of data on soil physical properties of soils in Norway. This applies not only to high-quality data for difficult to measure-properties like e.g. hydraulic conductivity, soil water retention curve and aggregate stability, but also to more basic data that can serve as input to pedotransfer functions (texture and SOM). Almost no study in Norway has focused on the magnitude and effects of uncertainty and spatial and temporal variability in soil physical properties. Considering the necessity of using models for land management planning and risk assessment, this is a significant problem. Inadequate model input data, whether measured or derived from other data sources and via PTFs, can lead to erroneous response predictions and thereby non-optimal decision making with respect to increasing crop productivity and economic income, and reducing environmental pressure. In addition, gaining knowledge about processes also depends on data on soil physical properties, and thus the lack of data hampers further improvement of prediction tools and their adaptation to various conditions. Acquisition of new data and compilation of existing data is therefore utterly important and should be given high priority. I recommend that systematic collection of measured data on soil physical properties is carried out for a wide range of soils in Norway, both on arable land and under other land use types as well. Efforts should be made to further characterize variability within and between soil series, both spatial and temporal variation and on different scales. Without these data, the importance of variability cannot be further investigated. More emphasis should also be put on alternative sources of information, like remote sensing techniques, as supplement to direct measurements.

The uncertainty in soil map derived properties needs further attention, as the soil map will continue to be one of the most important sources of soil information in the future. Only one soil map from a small area in South-east Norway, mapped during the infancy of soil mapping in Norway, was considered in this thesis. Soil maps from other areas, representing different terrain, climate and parent material, should also be evaluated. Today the erosion risk map, derived from the soil map, is important for management panning and determining farmers' subsidies. Both the basic soil map and the derived thematic soil maps should be accompanied with some measure of uncertainty. This requires data collection, and additionally that already existing data in the soil survey database are made available for assessment of uncertainty. Soil mapping should also be extended to other land use in addition to arable land.

A good start is to carry out surveys in areas where also responses (crop growth, yields, runoff, erosion, nutrient loss, gas emissions, etc) are measured, as an important goal is to calibrate and validate models, and to quantify and reduce uncertainty in model output. The network of catchments in the National Environmental and Agricultural Monitoring Programme in Norway is very well suited for this purpose: Discharge and concentrations of nutrients, particles and pesticides have been monitored at the catchment outlet since the early 1990'es, and detailed information about farming practices has also been collected. But soil data are virtually non-existent for most of these catchments, making modeling difficult and associated with high uncertainty. These catchments are supposed to represent important agricultural areas in Norway, with respect to soils, climate, farming practices, and agricultural pollution loads. Therefore, supplementing these catchments with high-quality soil data can dramatically increase the potential use of the already available data in modeling e.g. effects of land management and climate change, and for planning measures against pollution. However, a catchment response does not say anything about where risks are highest and where measures will be most beneficial, and it gives little information about processes at work. Therefore, more emphasis should also be put on collecting within-catchment response data. For erosion models like LISEM, this would include e.g. registration of erosion features (rills, gullies, sedimentation), in addition to sub-catchment monitoring of flow pathways (surface runoff versus subsurface drainage). Moreover, continuous monitoring of subsurface drainage can be one indirect method for obtaining information about e.g. hydraulic conductivity. Currently, there are only a few sites in Norway where runoff and flow paths are measured on the small scale. It is strongly advised to establish more such sites, for increasing process understanding and for model calibration purposes.

Uncertainties related to the use of PTFs also require further attention, primarily because PTFs may be unavoidable means of obtaining model input data in areas with limited data availability, and because there is little consistency in the literature regarding the statistical and functional performance of PTFs. The statistical evaluation presented in this thesis should therefore be followed up with functional evaluation of PTFs for various model applications. Existing PTFs are usually developed using data from large regions, and are therefore often best suited for large scale applications as small scale variability tends to be lost or smoothed. Thus, the potential for developing local PTFs should be investigated in more detail.

Because of the high sensitivity to K_s of many models, including LISEM, special attention should be given to measurement and prediction of K_s. This has been a topic of research for decades, but still it is one of the soil physical properties that is most difficult to measure and predict. Another property that should be given more attention is W_{opt}, because of its potentially greater importance if climate change leads to increased precipitation in autumn and spring. The PTF for W_{opt} was not validated in this thesis because there were no available data to validate against. Just a few data for the placticity limits LPL and UPL (input PTFs to the W_{opt} PTF) were available for validation. Such data should be collected, both for PTF validation and for studies concerning effects of climate change on workable conditions in Norway.

Temporal variability in soil physical properties is even less understood than spatial variability, and more research is needed. Under Norwegian climatic conditions, temporal variability is particularly influenced by freeze-thaw processes, as illustrated for aggregate stability in this thesis. More research on the influence of frost action on soil properties is needed, and also inclusion of temporal variability in models.

The model uncertainty was not a topic in this thesis, but it must be stressed that future modeling studies dealing with uncertainty ideally should include all sources of uncertainty in the modeling process. The models used here were the simple functions for W_{opt} and Number of days, and the process-based LISEM model, and it was implicitly assumed that these models were correct. For LISEM, there are several features and processes that are not accounted for in the model, and that can be recommended to include: artificial drainage, man-holes (works as short cuts for surface water to the stream), preferential flow (part of the soil loss can occur through drains via macropores, and bypass flow can reduce surface runoff), frozen soil and snow dynamics (partly included, but snowmelt is included as an input and a simple K-reduction is used to represent frozen soil).

5 References

Bajracharya, R.M., Lal, R., 1992. Seasonal soil loss and erodibility variation on a Miamian silt loam soil. *Soil Sci. Soc. Am. J. 65*, 1560– 1565.

Bechini, L., Bocchi, S., Maggiore, T., 2003. Spatial interpolation of soil hydraulic properties for irrigation planning. A simulation study in northern Italy. *Eur. J. Agron. 19*, 1-14.

Boix-Fayos, C., Calvo-Cases, A., Imeson, A.C., Soriano-Soto, M.D., Tiemessen, I.R., 1998. Spatial and short-term temporal variations in runoff, soil aggregation and other soil properties along a mediterranean climatological gradient. *Catena 33*, 123–138.

Bormann, H., Klaassen, K., 2008. Seasonal and land use dependent variability of soil hydraulic and soil hydrological properties of two Northern German soils. *Geoderma 145*, 295-302.

Brooks, R.H., Corey, A.T., 1964. Hydraulic properties of porous media. *Hydrology Paper No. 3*. Colorado State Univeristy, Fort Collins.

Brimelow, J.C., Hanesiak, J.M., Raddatz, R., 2010. Validation of soil moisture simulations from the PAMII model, and an assessment of their sensitivity to uncertainties in soil hydraulic parameters. *Agr. Forest Meteorol. 150*, 100-114.

Bullock, M.S., Kemper,W.D., Nelson, S.D., 1988. Soil cohesion as affected by freezing, water content, time and tillage. *Soil Sci. Soc. Am. J. 52*, 770– 776.

Børgesen, C.D. & Schaap, M.G., 2005. Point and parameter pedotransfer functions for water retention predictions for Danish soils. *Geoderma, 127*, 154-167.

Børresen, T., 1987. Tre jordarbeidingssystemer for korn kombinert med ulik pakking og halmdekking, virkning på avling, jordtemperatur og fysiske egenskaper på leirjord i Ås og Tune, 1983-1984 (Effects of three tillage systems combined with different compaction and mulching treatments, on cereal yields, soil temperature and physical properties on clay soil in South-Eastern Norway). *Norw. Agr. Res.* Supplement No. 3, 178 pp (in Norwegian with English abstract). ISSN: 0801-5333.

Børresen, T., 1999. The effect of straw management and reduced tillage on soil properties and crop yields of spring-sown cereals on two loam soils in Norway. *Soil Till. Res. 51*, 91-102.

Cantón, Y., Solé-Benet, A., Asensio, C., Chamizo, S., Puigdefábregas, J., 2009. Aggregate stability in range sandy loam soils. Relationships with runoff and erosion. *Catena 77*, 192-199.

Chaplot, V., 2005. Impact of DEM mesh size and soil map scale on SWAT runoff, sediment and NO3-N loads predictions. *J. Hydrol. 312*, 207–222.

Chirico, G.B., Medina, H., Romano, N., 2007. Uncertainty in predicting soil hydraulic properties at the hillslope scale with indirect methods. *J. Hydrol. 334*, 405-422.

Christiaens, K., Feyen, J., 2001. Analysis of uncertainties associated with different methods to determine soil hydraulic properties and their propagation in the distributed hydrological MIKE SHE model. *J. Hydrol. 246*, 63-81.

Ciollaro, G., Romano, N., 1995. Spatial variability of the hydraulic properties of a volcanic soil. *Geoderma 65*, 263-282.

Coquet, Y., Vachier, P., Labat, C., 2005. Vertical variation of near-saturated hydraulic conductivity in three soil profiles. *Geoderma 126*, 181-191.

Cornelis, W.M., Ronsyn, J., van Meirvenne, M., Hartmann, R., 2001. Evaluation of Pedotransfer Functions for Predicting the Soil Moisture Retention Curve. *Soil Sci. Soc. Am. J. 65*, 638-648.

Dagesse, D.F., Groenevelt, P.H., Kay, B.D., 1997. The effect of freezing cycles on water stability of soil aggregates. In: Iskandar, I.K., Wright, E.A., Radke, J.K., Sharratt, B.S., Groenevelt, P.H., Hinzman, L.D. (Eds.), International Symposium on Physics, Chemistry, and Ecology of Seasonally Frozen Soils, Fairbanks, Alaska, June 10– 12, 1997. Special Report 97-10. U.S. Army Cold Regions Research and Engineering Laboratory, Hanover, NH, pp. 177– 181.

Davis, S.H., Vertessy, R.A., Silberstein, R.P., 1999. The sensitivity of a catchment model to soil hydraulic properties obtained by using different measurement techniques. *Hydrol. Process. 13*, 677-688.

Deeks L.K., Bengough A.G., Low D., Billett M.F., Zhang X., Crawford J.W., Chessell J.M. and Young I.M., 2004. Spatial variation in effective porosity is related to discharge response. *J. Hydrol. 209*, 217-228.

Deng, H., Ming, Y., Schaap, M.G., Khaleel, R., 2009. Quantification of uncertainty in pedotransfer function-based parameter estimation for unsaturated flow modeling. *Water Resour. Res. 45*, 1-13.

De Roo, A.P.J., Wesseling, C.G., Ritsema, C.J., 1996a. LISEM: a single-event physically based hydrological and soil erosion model for drainage basins. I: Theory, Input and Output. *Hydrol. Process. 10*, 1107-1117.

De Roo, A.P.J., Offermans, R.J.E., Cremers, N.H.D.T., 1996b. LISEM: a single-event physically-based hydrological and soil erosion model for drainage basins: II. Sensitivity analysis, validation and application. *Hydrol. Process. 10*, 1119– 1126.

De Roo, A.P.J., 1998. Modelling runoff and sediment transport in catchments using GIS. *Hydrol. Process. 12*, 905-922.

de Souza, Z.M., Junior, J.M., Pereira, G.T., Saenz, C.M.S., 2009. Spatial variability of aggregate stability in Latosols under sugarcane. *R. Bras. Ci. Solo 33*, 245-253.

de Toro, A., Hansson, P.-A., 2004. Analysis of field machinery performance based on daily soil workability status using discrete event simulation or on average workday probability. *Agric. Syst. 79*, 109–129.

Donatelli, M., Wösten, J.H.M., Belocchi, G., 2004. Chapter 20. Methods to evaluate pedotransfer functions. In Ya. Pachepsky & W.J. Rawls (Eds), Development of Pedotransfer Functions in Soil Hydrology. Developments in Soil Science – Volume 30, pp. 357-411. Elsevier, Amsterdam.

Duffera, M., White, J.G., Weisz, R., 2007. Spatial variability of Southeastern U.S. Coastal Plain soil physical properties: Implications for site-specific management. *Geoderma 137*, 327-339.

Edwards, L.M., 1991. The effect of alternate freezing and thawing on aggregate stability and aggregate size distribution of some Prince-Edward-Island soils. *J. Soil Sci. 42*, 193–204.

Falleiros, M.C., Portezan, O., Oliveira, J.C.M., Bacchi, O.O.S., Reichardt, K., 1998. Spatial and temporal variability of soil hydraulic conductivity in relation to soil water distribution, using an exponential model. *Soil Technol. 45*, 279–285.

Gee, G.W., Bauder, J.W., 1986. Particle-size Analysis. In: Klute, A. (Ed.), Methods of Soil Analysis, Part 1–Physical and Mineralogical Methods, second ed., vol. 9. Agronomy Monograph, Madison, WI, pp. 383–411.

Gijsman, A.J., Jagtap, S.S., Jones, J.W., 2003. Wading through a swamp of complete confusion: how to choose a method for estimating soil water retention parameters for crop models. *Eur. J. Agron. 18*, 77-106.

Givi, J., Prasher, S.O., Patel, R.M., 2004. Evaluation of pedotransfer functions in predicting the soil water contents at field capacity and wilting point. *Agr. Water Manage. 70*, 83-96.

Grønsten, H.A., 2008. Prediction of soil aggregate stability and water induced erosion on agricultural soils in Southeast Norway. PhD Thesis 2008:54. Department of Plant and

Environmental Sciences, Norwegian University of Life Sciences, Ås. ISBN: 978-82-575-0856-2.

Grønsten, H.A., Børresen, T., 2009. Comparison of two methods for assessment of aggregate stability of agricultural soils in southeast Norway. *Acta Agric. Scand. Sect B 59*, 567-575.

Guber, A.K., Pachepsky, Ya.A., van Genuchten, M.Th., Rawls, W.J., Simunek, J., Jacques, D., Nicholson, T.J., Cady, R.E., 2006. Field-Scale Water Flow Simulations Using Ensembles of Pedotransfer Functions for Soil Water Retention. *Vadose Zone J. 5*, 234–247.

Haraldsen, T.K., Sveistrup, T.E., 1994. Effects of cattle slurry and cultivation on infiltration in sandy and silty soils from northern Norway. *Soil Till. Res. 29*, 307-321.

Haraldsen, T.K., Sveistrup, T.E., 1996. Influence of cattle slurry application and soil faunal activity on infiltration in soils from northern Norway. *Norw. J. Agr. Res. 10*, 43-54.

Haraldsen T.K., Sveistrup, T.E., Engelstad, F., 1994. Dyrkingssystemforsøk i økologisk landbruk. Startkarakterisering, jordundersøkelser på Apelsvoll forskingsstasjon, avd. Landvik. Statens forskingsstasjoner i landbruk, Holt forskingsstasjon, Trykk 3/94. 23 pp.

Hoogmoed, W.B., Cadena-Zapata, M., Perdok, U.D., 2003. Laboratory assessment of the workable range of soils in the tropical zone of Veracruz. Mexico. *Soil Till. Res. 74*, 169–178.

Høstmark, A.-K.S., 1994. Variasjon i noen kjemiske og fysiske parametre på 4 jordtyper i Sør-Øst-Norge (Variation in Some Chemical and Physical Parametres on 4 Soiltypes in South-Eastern Norway). Doctor Scientiarum Theses 1994:3, Agricultural University of Norway, 212 pp (in Norwegian with English abstract).

Hessel, R., Jetten, V., Baoyuan, L., Yan, Z., Stolte, J., 2003. Calibration of the LISEM model for a small Loess Plateau catchment. *Catena 54*, 235-254.

Hessel, R., van den Bosch, R., Vigiak, O., 2006. Evaluation of the LISEM soil erosion model in two catchments in the East African Highlands. *Earth Surf. Proc. Land. 31*, 469-486.

Iversen, B.V., Moldrup, P., Schjønning, P., Jacobsen, O.H., 2004. Field Application of a Portable Air Permeameter to Characterize Spatial Variability in Air and Water Permeability. *Vadose Zone J. 2*, 618-626.

Jetten, V., 2002. LISEM user manual, version 2.x. Draft version January 2002. Utrecht Centre for Environment and Landscape Dynamics, Utrecht University, 48 pp.

Jetten, V., Govers, G., Hessel, R., 2003. Erosion models: quality of spatial predictions. *Hydrol. Process. 17*, 887-900.

Kätterer, T., Andrén, O., Jansson, P.-E., 2006. Pedotransfer functions for estimating plant available water and bulk density in Swedish agricultural soils. *Acta Agric. Scand. Sect B 56*, 263-276.

Kemper, W.D., Rosenau, R.C., 1986. Aggregate stability and size distribution. In: Klute, A. (Ed.), Methods of Soil Analysis: Part 1. Physical and Mineralogical Methods. SSSA Book Series No. 5, Madison, Wisconsin, pp. 425– 442.

Kolsrud, E., 2001. Lagelighet for jordarbeiding og jordfysiske forhold i fem jordarbeidingssystemer på siltig mellomleire (Workability and soil physical properties in five tillage systems on a silty clay loam). Master thesis, Agricultural University of Norway, 67 pp (in Norwegian with English abstract).

Korsæth, A., Riley, H., Kværnø, S., Vestgarden, L. 2008. Relations between a Commercial Soil Survey Map Based on Soil Apparent Electrical Conductivity (EC_a) and Measured Soil Properties on a Morainic Soil in Southeast Norway. In: Barry J. Allred, Jeffrey J. Daniels, M. Reza Ehsani (Eds.). Handbook of Agricultural Geophysics, p. 225-231. CRC Press, Taylor & Francis Group. New York.

Korsæth, A., Riley, H., 2003. Relations between electrical conductivity, soil texture and SOM content: Experiences with EM38 on morainic soil in SE Norway. DIAS REPORT Plant Production vol. 100, 139-142.

Korsæth, A., 2008. Dependence of Soil Apparent Electrical Conductivity (ECa) upon Soil Texture and Ignition Loss at Various Depths in Two Morainic Loam Soils in Southeast Norway. Handbook of Agricultural Geophysics, p. 217-222.

Kretschmer, H., 1996. Koernung und Konsistenz. In: Blume, H.-P., Felix-Henningsen, P., Fischer, W.R., Frede, H.G., Horn, R., Stahr, K. (Eds.), Handbuch der Bodenkunde, first ed., vol. I. Ecomed.

Kramer, G.J., Stolte, J., 2009. Cold-Season Hydrologic Modeling in the Skuterud Catchment. An Energy Balance Snowmelt Model Coupled with a GIS-based Hydrology Model. Bioforsk Report 4(126), 46 pp. ISBN: 978-82-17-00548.

Kværnø, 2000. Måling og estimering av jordas hydrauliske egenskaper på fem ulike jordarter (Measurement and estimation of soil hydraulic properties on five different soils). Master thesis, Agricultural University of Norway, 136 pp. (in Norwegian with English abstract).

Kværnø, S.H., Deelstra, J., 2002. Spatial variability in hydraulic conductivity and soil water content of a silty clay loam in the Skuterud catchment. Jordforsk report 62/02, 30 pp. ISBN: 82-7467-433-2.

Lathrop Jr., R.G., Aber, J.D., Bognar, J.A., 1995. Spatial variability of digital soil maps and its impact on regional ecosystem modeling. *Ecol. Model. 82*, 1–10.

Leonaviciute, N., 2000. Predicting soil bulk and particle densities by pedotransfer functions from existing soil data in Lithuania. *Geogr. Metrast. 33*, 317–330.

Lewan, L., Jansson, P.-E., 1993. Implications of spatial variability of soil physical properties for simulation of evaporation at the field scale. *Water Resour. Res. 32*, 2067-2074.

Lilburne, L.R., Webb, T.H., 2002. Effect of soil variability, within and between soil taxonomic units, on simulated nitrate leaching under arable farming. New Zealand. *Aust. J. Soil Res. 40*, 1187–1199.

Lindahl, A.M.L., Kreuger, J., Stenström, J., Gärdenes, A.I., Alavi, G., Roulier, S., Jarvis, N.J., 2005. Stochastic Modeling of Diffuse Pesticide Losses from a Small Agricultural Catchment. *J. Environ. Qual. 34*, 1174-1185.

Lundekvam, H., Skøyen, S., 1998. Soil erosion in Norway. An overview of measurements from soil loss plots. *Soil Use Manage. 14*, 84– 89.

Ma, L., Hoogenboom, G., Saseendran, S.A., Bartling, P.N.S., Ahuja, L.R., Green, T.R., 2009. Effects of Estimating Soil Hydraulic Properties and Root Growth Factor on Soil Water Balance and Crop Production. *Agron. J. 101*, 572-583.

Mallants, D., B.P. Mohanty, D. Jaques, J. Feyen, 1996. Spatial variability of soil hydraulic properties in a multi-layered soil profile. *Soil Sci. 161*, 167-181.

Manrique, L.A., Jones, C.A., 1991. Bulk density of soils in relation to soil physical and chemical properties. *Soil Sci. Soc. Am. J. 55*, 476-481.

Marti, M., 1984. Kontinuierlicher Getreidebau ohne Pflug im Südosten Norwegens-Wirkung auf Ertrag, physikalische und chemische Bodenparameter (Continuous cereal production with ploughless cultivation in Southeastern Norway – Effects on yields and soil physical and chemical parameters). Doctoral thesis, Agricultural University of Norway, ISBN: 82-576-3502-2, 155 pp. (in German with English summary).

Merz, B., Plate, E.J., 1997. An analysis of the effects of spatial variability of soil and soil moisture on runoff. *Water Resour. Res. 33*, 2909-2922.

Merz, B., Bardossy, A., Schiffler, G.R., 2002. Different methods for modeling the areal infiltration of a grass field under heavy precipitation. *Hydrol. Process. 16*, 1383-1402.

Minasny, B., McBratney, A.B., 2002. The efficiency of various approaches to obtaining estimates of soil hydraulic properties. *Geoderma 107*, 55-70.

Mueller, L., Schindler, U., Fausey, N.R., Lal, R., 2003. Comparison of methods for estimating maximum soil water content for optimum workability. *Soil Till. Res. 72*, 9–20.

Mulla, D.J., Huyck, L.M., Reganold, J.P., 1992. Temporal variations in aggregate stability on conventional and alternative farms. *Soil Sci. Soc. Am. J. 56*, 1620–1624.

Myhr, K., Håland, Å., Nesheim, L., 1990. Verknad av våtkompostert og ubehandla blautgjødsel, og av jordpakking, på infiltrasjonen av vatn i dyrka jord. *Norsk Landbruksforskning 4*, 161-172.

Myhr, K., Oskarsen, H., Haraldsen, T.K., 1996. The Kvithamar field lysimeter I. Objectives, methods and results of soil analyses. *Norw. J. of Agr. Sci. 10*, 197-210.

Nael, M., Khademi, H., Hajabbasi, M.A., 2004. Response of soil quality indicators and their spatial variability to land degradation in central Iran. *Appl. Soil Ecol. 27*, 221-232.

Nemes, A., Schaap, M.G. & Wösten, J.H.M., 2003. Functional evaluation of pedotransfer functions derived from different scales of data collection. *Soil Sci. Soc. Am. J. 67*, 1093-1102.

Nyborg, Å ., 2003. Seriedefinisjoner vår 2003. NIJOS dokument 5/03 (in Norwegian).

Nyborg, Å., 2008. Seriedefinisjoner Våren 2008. Håndbok fra Skog og landskap 03/2008. ISBN: 978-82-311-0039-3.

Olsen, P.A., 1999. Estimation and Scaling of the Near-Saturated Hydraulic Conductivity. *Nord. Hydrol. 30*, 177- 190.

Paz-Gonzalez, A., Viera, S. R., Toboada-Castro, M. T., 2000. The effect of cultivation on the spatial variability of selected properties of an umbric horizon. *Geoderma 97*, 273-292.

Peck, A.J., Luxmoore, R.J., Stoltzy, J.L., 1977. Effects of Spatial Variability of Soil Hydraulic Properties in Water Budget Modeling. *Water Resour. Res. 13*, 348-354.

Rawls, W.J., Brakensiek, D.L., 1989. Estimation of soil water retention and hydraulic properties. In H.J. Morel-Seytoux (Ed.), Unsaturated Flow in Hydrologic Modeling - Theory and Practice. Kluwer Academic Publishers, Boston. 275-300.

Regalado, C.M., Munoz-Carpena, R., 2004. Estimating the saturated hydraulic conductivity in a spatially variable soil with different permeameters: a stochastic Kozeny–Carman relation. *Soil Till. Res. 77*, 189-202.

Riley, H., 1996. Estimation of physical properties of cultivated soils in southeast Norway from readily available soil information. *Norw. J. Agr. Sci.*, Supplement No. 25, 1-51.

Riley, H. & Eltun, R., 1994. The Apelsvoll cropping system experiment II. Soil characteristics. *Norw. J. Agr. Sci. 8*, 317-333.

Salehi, M.H., Eghbal, M.K., Khademi, H., 2003. Comparison of soil variability in a detailed and a reconnaissance soil map in central Iran. *Geoderma 111*, 45–56.

Sauer, T.J., Logsdon, S.D., 2002. Hydraulic and physical properties of stony soils in a small watershed. *Soil Sci. Soc. Am. J. 66*, 1947–1956.

Schaap, M.G. & Leij, F.J. (1998). Using neural networks to predict soil water retention and soil hydraulic conductivity. *Soil Till. Res. 47*, 37-42.

Schaap, M.G., Leij, F.J., van Genuchten, M.Th., 2001. ROSETTA: a computer program for estimating soil hydraulic parameters with hierarchical pedotransfer functions. *J. Hydrol. 251*, 163-176.

Schoups, G., Hopmans, J.W., 2006. Evaluation of Model Complexity and Input Uncertainty of Field-Scale Water Flow and Salt Transport. *Vadose Zone J. 5*, 951-962.

Soet, M., Stricker, J.N.M., 2003. Functional behaviour of pedotransfer functions in soil water flow simulation. *Hydrol. Process. 17*, 1659-1670.

Sorbieraj, J.A., Elsenbeer, H., Vertessy, R.A., 2001. Pedotransfer functions for estimating saturated hydraulic conductivity: implications for modeling storm flow generation. *J. Hydrol. 251*, 202-220.

Staricka, J.A., Benoit, G.R., 1995. Freeze-drying effects on wet and dry soil aggregate stability. *Soil Sci. Soc. Am. J. 59*, 218-223.

Stolte, J., Ritsema, C.J., Veerman, G.J., Hamminga, W., 1996. Establishing temporally and spatially variable soil hydraulic data for runoff simulation in a soil erosion study in the loess region of the Netherlands. *Hydrol. Process. 10*, 1027-1034.

Stolte, J., van Venrooij, B., Zhang, G., Trouwborst, K.O., Liu, G., Ritsema, C.J., Hessel, R., 2003. Land-use induced spatial heterogeneity of soil hydraulic properties on the Loess Plateau in China. *Catena 54*, 59-75.

Sveistrup, T., Njøs, A., 1984. Kornstørrelser i mineraljord, Revidert forslag til klassifisering. *Jord og myr 8*, 8–15 (in Norwegian).

Sveistrup, T.E., Haraldsen, T.K., 1991. Virkninger av jordpakking og blautgjødsel på jordfysiske egenskaper i jordtyper fra Nord-Norge. SFFL faginfo 3, 251-269.

Sveistrup, T.E., Haraldsen, T.K., Engelstad, F., 1994a. Dyrkingssystemforsøk i økologisk landbruk. Startkarakterisering, jordundersøkelser på Østre Voll, Norges landbrukshøgskole. Statens forskingsstasjoner i landbruk, Holt forskingsstasjon, Trykk 4/94, 25 pp.

Sveistrup, T.E., Haraldsen, T.K., Engelstad, F., 1994b. Dyrkingssystemforsøk i økologisk landbruk. Startkarakterisering, jordundersøkelser på Kvithamar forskingsstasjon. Statens forskingsstasjoner i landbruk, Holt forskingsstasjon, Trykk 5/94, 24 pp.

Sørbotten, L.-E. (Ed.), 2011. Jord- og vannovervåking i landbruket (JOVA). Feltrapporter fra programmet i 2009. Bioforsk rapport 6(38), 54 pp. (In Norwegian). ISBN: 978-82-17-00768-5.

Takken, I., Beuselinck, L., Nachtergaele, J., Govers, G., Poesen, J., Degraer, G., 1999. Spatial evaluation of a physically-based distributed erosion model (LISEM). *Catena 37*, 431-447.

Tietje, O., Tapkenhinrichs, M., 1993. Evaluation of pedotransfer functions. *Soil Sci. Soc. Am. J. 57*, 1088-1095.

Timlin, D.J., Pachepsky, Ya.A., Acock, B., Whisler, F., 1996. Indirect estimation of soil hydraulic properties to predict soybean yield using GLYCIM. *Agric. Syst. 52*, 331-353.

Tsegaye, T., Hill, R.L., 1998. Intensive tillage effects on spatial variability of soil physical properties. *Soil Sci. 163*, 143-154.

Vachaud, G., Chen, T., 2002. Sensitivity of computed values of water balance and nitrate leaching to within soil class variability of transport parameters. *J. Hydrol. 264*, 87-100.

van Es, H.M., Ogden, C.B., Hill, R.L., Schindelbeck, R.R., Tsegaye, T., 1999. Integrated Assessment of Space, Time, and Management-Related Variability of Soil Hydraulic Properties. *Soil Sci. Soc. Am. J. 63*, 1599–1608.

van Genuchten, M.Th., 1980. A closed form equation for predicting the hydraulic conductivity of unsaturated soils. *Soil Sci. Soc. Am. J. 44*, 892-898.

Van Rompaey, A.J.J., Govers, G., 2002. Data quality and model complexity for regional scale soil erosion prediction. *Int. J. GIS 16*, 663–680.

Vereecken, H., Maes, J., Feyen, J., Darius, P., 1989. Estimating the soil moisture retention characteristic from texture, bulk density and limited data. *Soil Sci. 148*, 389-403.

Vereecken, H., Diels, J., van Orshoven, J., Feyen, J., Bouma, J., 1992. Functional evaluation of pedotransfer functions for the estimation of soil hydraulic properties. *Soil Sci. Soc. Am. J. 56*, 1371-1378.

Wagner, B., Tarnawski, V.R., Wessolek, G., Plagge, R., 1998. Suitability of models for the estimation of soil hydraulic parameters. *Geoderma 86*, 229-239.

Wagner, B., Tarnawski, V.R., Stöckl, M., 2004. Evaluation of pedotransfer functions predicting hydraulic properties of soils and deeper sediments. *J. Plant Nutr. Soil Sci. 167*, 236-245.

Wendroth, O., Koszinski, S., Pena-Yewtukhiv, E., 2006. Spatial Association among Soil Hydraulic Properties, Soil Texture, and Geoelectrical Resistivity. *Vadose Zone J. 5*, 341-355.

Wesseling, C.G., Karssenberg, D., Van Deursen, W.P.A., Burrough, P.A., 1995. Integrating dynamic environmental models in GIS: the development of a dynamic modelling language, *Trans. GIS 1*, 40-48.

Wösten, J.H.M., Schuren, C.H.J.E., Bouma, J., Stein, A., 1990. Functional sensitivity analysis of four methods to generate soil hydraulic functions. *Soil Sci. Soc. Am., J. 54*, 832-836.

Wösten, J.H.M., Lilly, A., Nemes, A., Le Bas, C., 1999. Development and use of a database of hydraulic properties of European soils. *Geoderma, 90*, 169-185.

Young, F.J., Hammer, R.D.,Williams, F., 1997. Estimation of map unit composition from transect data. *Soil Sci. Soc. Am. J. 61*, 854–861.

Zimmermann. B, Elsenbeer, H., 2008. Spatial and temporal variability of soil saturated hydraulic condcutivity in gradients of disturbance. *J. Hydrol. 361*, 78-95.

Øgaard, A., Grønsten, H., Sveistrup, T., Bøen, A., Haraldsen, T., 2009. Effekt av 3 ulike slamtyper på avling, jordas innhold av tilgjengelig fosfor, pH og jordstruktur. Bioforsk FOKUS 4(1), 14-20.

Øygarden, L., 2000. Soil erosion in small agricultural catchments, south-eastern Norway. Doctor Scientiarum Thesis 2000:8. Norges Landbrukshøgskole, Ås.

Øygarden, L., Kværner, J., Jenssen, P.D., 1997. Soil erosion via preferential flow to drainage systems in clay soils. *Geoderma 76*, 65-86.

Paper I

Kværnø, S.H., Haugen, L.E., Børresen, T., 2007. Variability in topsoil texture and carbon content within soil map units and its implications in predicting soil water content for optimum workability. *Soil & Tillage Research 95*, 332-347.

Available online at www.sciencedirect.com
ScienceDirect
Soil & Tillage Research 95 (2007) 332–347
Soil & Tillage Research
www.elsevier.com/locate/still

Variability in topsoil texture and carbon content within soil map units and its implications in predicting soil water content for optimum workability

S.H. Kværnø [a,*], L.E. Haugen [b], T. Børresen [b]

[a] *Norwegian Institute for Agricultural and Environmental Research (Bioforsk), Soil and Environment Division, Frederik A. Dahls vei 20, 1432 Ås, Norway*

[b] *Norwegian University of Life Sciences, Department for Plant and Environmental Sciences, P.O. Box 5003, 1432 Ås, Norway*

Received 6 October 2006; received in revised form 2 January 2007; accepted 6 February 2007

Abstract

The ability to predict the timing of optimum soil workability depends on knowledge of the extent and structure of variability in main physical characteristics of the soil. Our objectives were to quantify the variability in texture and carbon content within soil map units in a small agriculture-dominated catchment in South-east Norway and to assess implications of variability in texture and carbon content on land management operations, using the predicted maximum water content for optimum workability as an example. Information from three different sources were used: a soil map (1:5000), a large sample grid (100 m spacing, 270 ha extent), and a small sample grid (10 m spacing, 2.25 ha extent). Readily available information on texture and organic matter content from the soil map was found to be of limited use for soil management due to broad textural classes together with deviations from the mapped main textural classes. There were significant differences in clay, silt and sand content between the different soil textural classes on the soil map. Statistical distributions within soil map units were generally either positively or negatively skewed and the coefficient of variation was intermediate, 15–50%. Most of the variation in both grids was spatially correlated. The large grid was dominated by a patchy structure, whilst the small grid showed a systematic trend with a gradual transition indicating fuzzy boundaries between map units in this catchment. The effective range for texture was 16 times larger in the large grid. Implications of variability in texture and carbon content on land management operations were assessed for the maximum water content for optimum workability (Wopt), predicted using pedotransfer functions. Wopt was usually in the same range as the water content at–100 kPa matric potential, indicating that considerable evaporation in addition to drainage is required for obtaining workable conditions in the field. The time required for obtaining the water content was estimated to about 5 days, which is longer than an average length of periods without precipitation in the area, median 3.7 days. Wopt predicted from the soil map deviated strongly from Wopt predicted from the sample grids. Comparing estimates of Wopt from the large grid with measurements in the small grid showed differences corresponding to ±2–3 days of evaporation.

Keywords: Soil texture; Carbon content; Variability; Workability; Pedotransfer function; Soil map

1. Introduction

The ability to predict and select optimal management strategies to maximize crop productivity and economic income, and minimize environmental risk, is restrained by the fact that the physical characteristics of the soil

* Corresponding author. Tel.: +47 92643599; fax: +47 64948110.
E-mail address: sigrun.kvaerno@bioforsk.no (S.H. Kværnø).

0167-1987/$ – see front matter © 2007 Elsevier B.V. All rights reserved.
doi:10.1016/j.still.2007.02.001

may vary over short distances and time periods. Soil variability is caused by different combinations of the soil forming factors. The extent of variability and its degree of randomness or spatial and temporal correlation or continuity also depends on the variables themselves and the scale of interest (Goderya, 1998; Western and Blöschl, 1999; Lin et al., 2005). Incorporating information about soil variability and increasing the resolution of soil data in simulation models have often shown to improve model predictions (Lathrop et al., 1995; Lilburne and Webb, 2002; Chaplot, 2005). Quantification of the nature and extent of variability in soil properties is particularly important from the viewpoint of precision agriculture, defined as ''the application of technologies and principles to manage spatial and temporal variability associated with all aspects of agricultural production for the purpose of improving crop performance and environmental quality'' (Pierce and Nowak, 1999).

Although important, quantification of soil physical properties is rarely prioritized due to high costs of analysis. The most comprehensive source of information on soil properties is the soil map and databases from soil surveys. Only a few soil variables can be derived directly from the map and the underlying database. For the Norwegian soil maps, produced by the Norwegian Forest and Landscape Institute, this includes texture and organic matter content classes. Variability and uncertainty within map units is not included in the soil map. Various studies have shown that variability within map units can be considerable (Young et al., 1997; Salehi et al., 2003), and that within-unit variability may be greater than between-unit variability (Lathrop et al., 1995).

More detailed information about variability must be obtained from additional data sources, e.g., soil sampling. Basic soil properties like particle size distribution and organic matter content are simple and relatively inexpensive to measure, and often available from soil surveys and research projects. Therefore, they are the most frequently used input variables in pedotransfer functions (PTFs), intended for estimating properties that are more costly and difficult to measure. Numerous PTFs have been developed for, e.g., water retention parameters and hydraulic conductivity, whilst PTFs for other physical properties are less common.

One particular characteristic of the soil for which both spatial and temporal variability must be taken into account, is soil workability. Information on workability limits is important for the farmer in deciding when and how to carry out tillage on different soils. Soil workability is defined as ''the optimum water content at which agricultural tillage produces the greatest proportion of small aggregates'' (Dexter and Bird, 2001). Tilling at higher or lower water contents than this optimum (Wopt) may produce large clods (e.g., Tisdall and Adem, 1986), eventually leading to structural damage (compaction) and poor seedbed preparation, resulting in decreased crop growth and higher runoff and erosion risk. The optimum water content is highly dependent on particle size distribution and organic matter content, and PTFs for Wopt and the upper and lower plasticity limits (UPL and LPL) have been presented by, e.g., Mueller et al. (2003) and Dexter and Bird (2001).

The objective of this work is to quantify the extent and nature of variability in texture and carbon content within soil map units using a publicly available soil map from the Norwegian Forest and Landscape Institute in combination with soil sample grids at two scales. We also evaluate some limitations (resolution, informativity, quality) of the Norwegian soil map with respect to agricultural management, and assess implications of variability in texture and carbon content on agricultural management, using the maximum water content for optimum workability, estimated from pedotransfer functions, as an example. The study area is a small catchment in South-east Norway, where soils are developed on marine and shore deposits, and agriculture is conventional with spring and winter cereals as main crops.

2. Materials and methods

2.1. Site and soil description

This project was carried out in the Skuterud catchment (450 ha), located in the municipality of Ås, approximately 30 km south of Oslo, in South-east Norway. The major part of the catchment is arable land (270 ha), the main crops being spring and winter sown cereals. The catchment is part of the Environmental Agricultural Monitoring Programme in Norway (JOVA, Skjevdal and Vandsemb, 2005). The average annual temperature and precipitation in the area are 5.3 °C and 785 mm, respectively. The topography of the catchment is undulating. The slopes are the steepest (up to 30 %) in the eastern and western parts, while the central areas near the stream are more level. The elevation is 85–150 m above sea level. Marine deposits, occasionally rich in gravel and stone cover most of the catchment. Coarser marine shore deposits predominate on the fringes of the agricultural land near and in the forested area. The catchment is transected by marginal moraine ridges

(“Raet”) originating from the ice cap melting at the end of the last glaciation. In the northern and southern part smaller morainic ridges are visible. A soil map for arable land in the catchment, developed by the Norwegian Forest and Landscape Institute, is shown in Fig. 1. Reference soil groups are classified according to the World Reference Base for Soil Resources (WRB), and local soil series names are provided. The soil map contains 34 local soil series. The predominating soils in the central and level parts are marine silt loam and silty clay loam soils (Albeluvisols and Luvisols). The texture of the shore deposits is mainly sand and loamy sand (Umbrisols, Podzols, Cambisols, Gleysols). Lighter clay soils (loam, sandy loam) are found in the transition zones between marine and shore deposits, and on the moraine ridges.

2.2. Soil sampling and analyses

Our sampling schemes were selected to represent two different scales, for determining scale effects on soil variability. Soil sampling (0–20 cm depth) was carried out in regular grids (Fig. 2) using a vehicle mounted soil auger. In each point nine samples were collected along a one meter line and bulked into one sample. The samples were positioned using a Trimble AgGPS 114. The large grid covered the total area of arable land (270 ha) in the catchment, with 100 m spacing between the samples. With a total of 247 topsoil samples, the sampling density was approximately one sample per ha and on average five samples per field. This corresponds to what is normally recommended for farmers’ fertiliser planning on conventional farms in Norway. The small grid (256 samples, 10 m spacing) covered 2.25 ha of a 13.4 ha field belonging to a farm where precision agriculture was planned. The grid was located on the boundary between two representative soil series, Rk8 and Ir3. The small grid provided data for a more detailed characterisation of variability on the transition between marine and shore deposits.

The bulked samples from each sample point were analysed for particle size distribution (percentage of clay, silt, fine sand, medium sand and coarse sand) and carbon content. Particle size distribution was determined using the pipette method (Gee and Bauder, 1986). Soil organic carbon was determined using a Perkin Elmer 2400 CHN Elemental Analyzer.

2.3. Statistical analyses

The data were analysed statistically with respect to moments (skewness, mean, and standard deviation), coefficient of variation (CV) and spatial dependency.

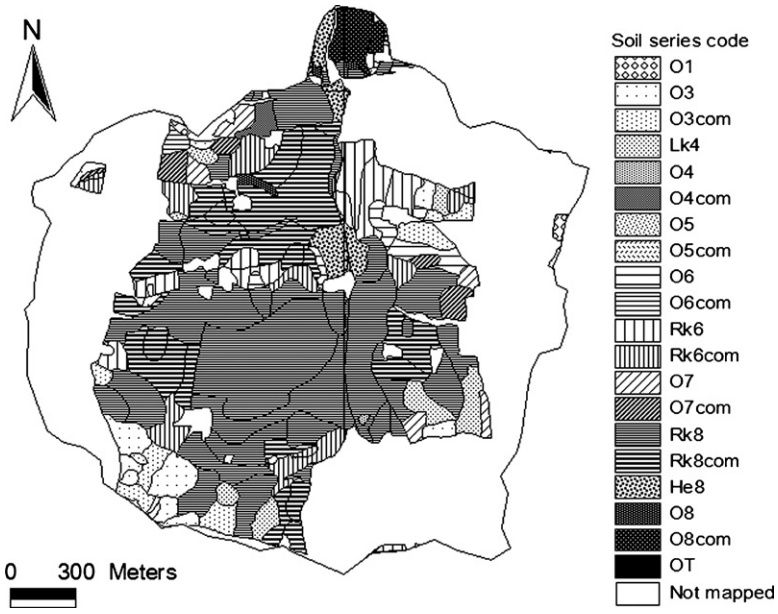

Fig. 1. Soil map (the Norwegian Forest and Landscape Institute) for arable land in the Skuterud catchment. The soil series code is a simplified soil series signature. The code consists of the soil series name, simplified to “O” for all series except those discussed in this paper, a figure indicating the soil map texture group, and the suffix “com” if the map unit is a complex (more than one series within the unit). The soil map texture group (Fadnes, 2003) corresponds to the texture classes in the Norwegian soil texture triangle (Sveistrup and Njøs, 1984): 1 = sand, 3 = loamy medium sand, 4 = loamy fine sand, 5 = silt, 6 = silt loam, 7 = (sandy) loam, 8 = (silty/sandy) clay loam. The “not mapped” area includes some agricultural fields, forest, peat/bog and urban areas.

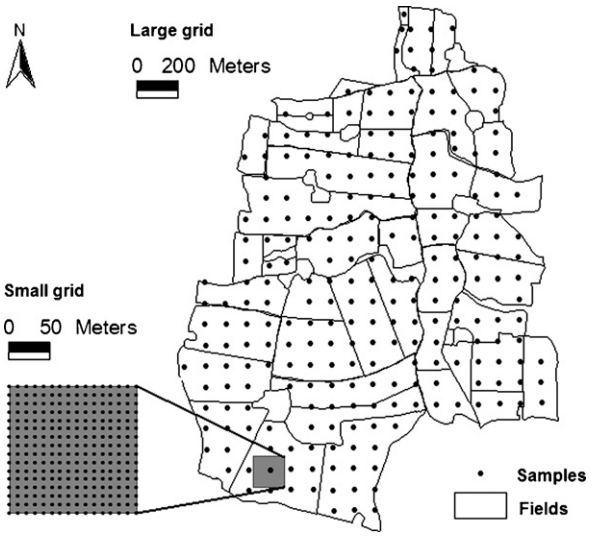

Fig. 2. Sample postings in the small grid and large grid, and field boundaries in the Skuterud catchment.

For analyses of variation between and within mapped soil series, the soil samples from the large grid and small grid were used. Mapped soil series with nine grid samples or more were included. Consociations (map units that are dominated by a single soil taxon, e.g., local soil series, and soils that are so similar that the major interpretations are not significantly affected. The dominating soil component provides name to the map unit (Soil Survey Division Staff, 1993)) and complexes (map units consisting of two or more components with significant dissimilarities in morphology or behaviour (Soil Survey Division Staff, 1993)) were treated separately for testing possible differences in variability. No partitioning based on soil series or texture class of the complexes were made. Consequently, the analyses included map units labelled Lk4 (Endostagnic Umbrisol, Låke loamy fine sand, area extent 8.3 ha), Rk6 (Stagnic Albeluvisol, Rokke silt loam, 15 ha), Rk8 (Stagnic Albeluvisol, Rokke silty clay loam, 112 ha), He8 (Stagnic Luvisol, Hellerud silty clay loam, 7.4 ha), Rk6com (Rk6 complex, including series with texture groups 6 and 8, 15 ha) and Rk8com (Rk8 complex, texture groups 6, 7 and 8, 48 ha) in the large grid, and Ir3 (Endogleyic Umbrisol, Hildrum loamy medium sand) and Rk8 in the small grid. The Brown-Forsythe test was used for testing unequal variances, and the Tukey HSD multiple comparison test was used for testing differences between means. Both tests were carried out in JMP 6.0 (SAS Institute Inc., 2005).

The spatial structure and continuity was examined by computing experimental variograms from the semivariances of all variables. Prior to computing the variogram, data with skewness <-0.5 or >0.5 were transformed by square roots or logarithms for approximation to normality. Negative skewness was made positive by reflecting the variable (subtracting the data values from a number one greater than its maximum value (Tabachnick and Fidell, 2001)). The semivariance (Matheron, 1965) is given by

$$\gamma(h) = \frac{1}{2 \times N(h)} \times \sum_{i=1}^{N(h)} [z(x_i) - z(x_i + h)]^2 \quad (1)$$

where $N(h)$ is the number of pairs separated by the distance or lag h, $z(x_i)$ and $z(x_i + h)$ are the values of the variable z, measured at any location x_i and $x_i + h$. Spatial dependence can be described in terms of parameters characterising the variogram, namely the nugget variance, sill variance and effective range, estimated by fitting different authorized models (Webster and Oliver, 2001) to the sample variograms.

The degree of systematic variation (non-stationarity) in the grids was analysed by simple linear regression with the measured value as response and the coordinates as regressors. In cases where significant ($p < 0.05$ and $R^2 > 0.20$) spatial trends were present in the data, the sample variogram was computed on the residuals from the regression analysis.

2.4. Derived variables using pedotransfer functions

Workability and water retention variables were estimated using pedotransfer functions (PTFs) requiring depth (D) in cm, clay (Cl), silt (Si), sand (Sa), organic matter (SOM = 1.724 × carbon content, where 1.724 is the Van Bemmelen factor (Nelson and Sommers, 1982)) and gravel (G) content in % as input. The maximum water content for optimum workability (Wopt) was calculated using the PTF of Kretschmer (1996), as recommended by Mueller et al. (2003):

$$\text{Wopt} = \text{LPL} - 0.15 \times (\text{UPL} - \text{LPL}) \quad (2)$$

where LPL and UPL are the lower and upper plasticity limits, respectively. LPL and UPL were not measured in this study, instead they were calculated using the PTFs of Schindler, cited by Mueller et al. (2003), valid for SOM < 10% and clay < 33%:

$$\text{UPL} = 10.5 + 0.355 \times \text{Cl} + 0.01 \times \text{Cl}^2 + 0.002 \times \text{Si}^2 + 2.11 \times \text{SOM} \quad (3)$$

$$\text{LPL} = 14.73 + 0.008 \times \text{Cl}^2 + 0.261 \times \text{Si} + 0.005 \times \text{Si}^2 + 1.93 \times \text{SOM} \quad (4)$$

Before using these equations with our data, the equations were validated on experimental data from Kolsrud (2001) and Eich-Greatorex and Børresen (pers. comm.). Those data had been collected on a site 3 km away from our site. The soils had clay contents ranging from 20% to 36%, silt 40–51%, sand 24–29% and organic matter 3.7–6.2%. The concept of LPL and UPL is not applicable to non-cohesive soils and for soils with clay content <10% Wopt was assumed to equal the water content at −10 kPa matric potential (''field capacity''), estimated from the topsoil specific PTF of Riley (1996):

$$\theta(-10) = 23.5 - 0.22 \times \mathrm{Sa} + 2.1 \times \mathrm{SOM} - 0.29 \times G + 11.3 \times \mathrm{BD} \quad (5)$$

where BD is the bulk density, defined as:

$$\mathrm{BD} = 1.522 - 0.065 \times \mathrm{SOM} + 0.0064 \times G + 0.0026 \times D - 0.0015 \times \mathrm{Si} + 0.0022 \times \mathrm{Cl} \quad (6)$$

The necessary input variables for calculating Wopt were not explicitly available from the soil map. The soil map provides soil texture classes related to the classes of the Norwegian soil texture triangle (Sveistrup and Njøs, 1984). The values for sand, silt and clay were selected by choosing the approximate midpoint of the relevant groups in the texture triangle. Soil map group 8, representing sandy clay loam, clay loam and silty clay loam (Fadnes, 2003), was restricted to represent silty clay loam only in this study, based on common texture classes listed in the local soil series definitions manual (Nyborg, 2003) for the soil series in our study area. The soil series specific values for gravel and SOM content were also derived from Nyborg (2003). The gravel content was assumed to be low and set to 5% for soil series where no gravel content range was reported. The values for sand, silt, clay, gravel and SOM contents for different soil map units are summarized in Table 1.

3. Results and discussion

3.1. Soil information from the soil map

The scale of the Norwegian soil map is 1:5000, and the minimum size of a map unit is 0.4 ha (roughly 65 by 65 meters) (Fadnes, 2003). When considering, e.g., precision agriculture, the required map resolution would depend on the width of the machinery used. The width of combine harvesters, equipment for application of lime, fertilizer, etc. rarely exceeds 10 m, indicating that a more appropriate limit for map units would be less than 0.04 ha. It is of course not feasible to include such detail in conventional soil maps, and additional information (e.g., soil sampling, remote sensing) is commonly used to increase the level of detail.

As mentioned introductorily, the soil map lacks information about variability within soil map units. In the Norwegian soil map, the signature of a map unit may contain up to three soil series, and together they should comprise at least 75% of the area (Fadnes, 2003). Inclusions (areas within a map unit that are too small to be delineated separately, or their location is difficult to identify, and they are therefore not identified in the name of the map unit (Soil Survey Division Staff, 1993)) may comprise up to 25% of the area if non-limiting for agricultural management, 10% if limiting (Fadnes, 2003). Information about the area extent and location of the different soil series used in the signature of the unit is missing.

Quantitative figures for particle size distribution and carbon content are not readily available from the soil map, and have to be deduced from soil map texture groups and organic matter classes. Based on the soil map and the texture triangle, a map unit labelled with e.g. texture group 8 (predominating in the catchment), covering both sandy clay loam, clay loam and silty clay loam, could theoretically have a clay content from 25%

Table 1
Clay, sand, gravel and carbon contents of soil map units, represented by texture groups 1–8 and T, corresponding to texture classes in the Norwegian soil texture triangle (Sveistrup and Njøs, 1984)

Soil map texture group (corresponding texture class)	Area (ha)	Clay (%)	Sand (%)	Gravel (%)	Carbon (%)
1 (sand)	1.9	2	93	5	2–2.5
3/4 (loamy medium/fine sand)	30.7	5	65	5–25	2.5–4
5 (sandy silt)	1.1	7	28	5	2.5–10
6 (silt loam)	38.6	19	15	5	2.5–3
7 (sandy loam + loam)	10.7	18	45	5–25	2–3
8 (silty clay loam)	173.3	34	8	5	1–10
T (organic soil)	0.018	5	65	5	10

Clay and sand content are given as % of material < 2 mm, gravel as % of total soil sample.

to 50%, silt 0–75% and sand 0–75%. Adding information from the series definitions manual, indicating that the soil series in group 8 mainly had silty clay loam texture, reduced the ranges to 50–75% and 0–30% for silt and sand, respectively. Still, these are rather large differences, and even small changes in static variables like particle size distribution may generate large changes in dynamic properties (Warrick, 1998) such as infiltrability and compactability. Regarding carbon content, most of the area has been mapped into the 3–6% organic matter class (carbon content 1.7–3.5%).

3.2. Soil information from the large grid

3.2.1. Comparison with soil map

The texture class of the samples from the large grid is plotted into the Norwegian texture triangle in Fig. 3. The texture classes of the samples were concentrated along rather straight lines from sand via loamy sand and loam/sandy loam to silty clay loam, indicating a linear relationship between clay and sand or silt content and gradual changes in topsoil texture in space.

Comparing the soil map texture class and soil sample texture class showed that 42% of the large grid-samples had a different texture class than the mapping units they were sampled from. However, most of these samples (39%) belonged to a neighbouring texture class in the soil texture triangle. Interestingly, the largest deviations (disregarding the texture class of complexes) from the real texture class were found for map units classified as group 6 – silt loam (90% deviation), group 4 – loamy fine sand (80% deviation) and group 3-loamy medium sand (61% deviation). The most prominent deviation was that group 7-sandy loam/loam was underrepresented in the soil map compared to the sample measurements. Fourteen sample points only were located within group 7 map units (consociations and complexes). In reality, 83 of the samples had texture group 7. The deviating samples were generally located in areas with many soil series and different deposits, indicating a possible lack of accuracy in map unit delineations in this variable soilscape, at least with respect to topsoil texture group. Note that the soil map for Skuterud was made in the beginning of soil mapping in Norway, before 1991. According to Arnoldussen (pers. comm.), maps created after 1991 have better quality, particularly with respect to texture classes. However, soil maps from the early period are still available to the public today, and they are used in the same way as the better quality maps.

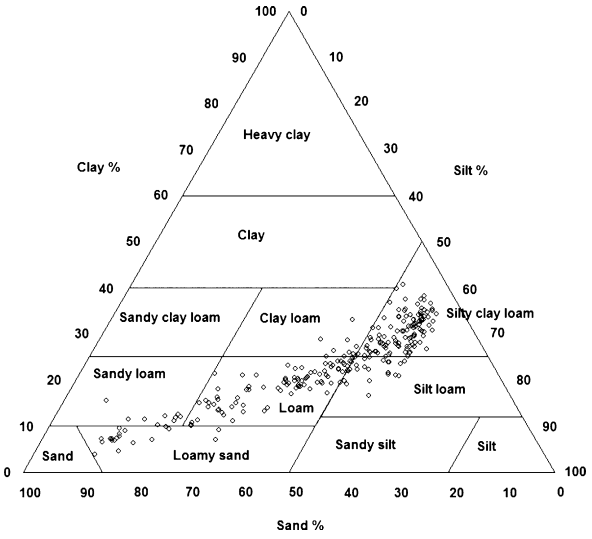

Fig. 3. Soil textural composition of samples from the large grid plotted in the Norwegian soil texture triangle (Sveistrup and Njøs, 1984).

3.2.2. Variability within map units

Summary statistics for mapped soil series with more than 9 samples are presented in Table 2. The order of average percentages of clay, silt and sand were as expected, with clay and silt content being lowest for the sand series Lk4 and highest for He8, with Rk6 and Rk6com, Rk8 and Rk8com as transitions between these extremes. This is illustrated for clay content in Fig. 4, together with the texture group limits from the texture triangle. The median clay content fell within the group limits for all of the mapped series. The same was true for sand and silt content, except for Rk6 and Rk6com where the median silt content was lower (limits 50–85%). The Tukey HSD test showed that there were significant differences ($p < 0.0001$) in clay, silt and sand contents between series having different texture groups, but not between different series with the same texture group (Table 2). Series Lk4 and He8 had the highest arithmetic means for carbon content, but for Lk4 the high value was due to three samples with unusually high carbon content (5.2–6.9%). Those samples were collected in shore deposit areas less than 60 m from the forest edge. Considering the median instead of the arithmetic mean, there were small differences in carbon content between mapped soil series. Fig. 4 shows that the median carbon content of the mapped series were within the carbon content class available from the soil map (1.7–3.5% carbon), but primarily in the lower range of the class.

Rk6 was the only soil series where all variables were close to normally distributed ($-0.5 <$ skewness < 0.5). Apart from this distributions were generally either positively or negatively skewed. The lack of normality

Table 2
Summary statistics for clay, silt, sand and carbon content of important soil map soil series covering the large grid

Map unit	Lk4	Rk6	Rk6com	Rk8	Rk8com	He8
n	9	11	15	105	40	10
Clay						
Min–max	3.9–20.9	10.1–35.1	12.2–24.2	7.0–40.7	14.9–43.6	19.8–33.8
Median	7.2	21.9	18.5	26.3	25.9	30.7
Arithm. mean	9.89 [d]	21.6 [bc]	19.0 [c]	26.5 [ab]	25.8 [ab]	29.9 [a]
Std. dev.	5.33	7.63	3.29	6.41	6.13	4.00
Skewness	1.0	−0.0024	−0.12	−0.43	0.69	−1.99
CV	53.9	35.2	17.3	24.2	23.7	13.4
Silt						
Min–max	7.9–34.0	22.9–59.7	20.7–55.8	17.2–61.7	28.5–62.7	41.2–61.7
Median	13.8	45.8	42.5	53.3	53.9	56.7
Arithm. mean	18.3 [c]	43.3 [b]	41.9 [b]	51.3 [a]	52.4 [a]	56.1 [a]
Std. dev.	9.42	12.7	8.62	8.42	7.83	5.66
Skewness	0.87	−0.43	−0.94	−1.51	−1.21	−2.30
CV	51.3	29.2	20.6	16.4	14.9	10.1
Sand						
Min–max	45.7–84.5	11.6–66.1	20.1–67.2	4.9–71.4	2.4–55.3	7.6–39.0
Median	76.5	32.3	38.7	19.2	19.9	12.2
Arithm. mean	71.8 [a]	35.0 [b]	39.1 [b]	22.1 [c]	21.7 [c]	14.1 [c]
Std. dev.	13.0	19.7	11.5	13.8	12.3	9.14
Skewness	−1.1	0.38	0.88	1.31	0.89	2.70
CV	18.1	56.2	29.3	62.1	56.7	65.0
Carbon						
Min-max	1.6–6.9	1.8–2.8	0.2–2.8	0.3–4.0	0.6–3.0	1.8–3.4
Median	1.9	2.3	2.0	2.3	2.1	2.55
Arithm. mean	3.13 [a]	2.25 [ab]	1.73 [b]	2.28 [b]	2.08 [b]	2.54 [ab]
Std. dev.	2.16	0.305	0.75	0.708	0.488	0.566
Skewness	1.1	−0.49	−0.99	−0.55	−1.00	0.26
CV	69.1	13.6	43.2	31.1	23.5	22.3

Numbers 4, 6 and 8 denote textures loamy fine sand, silt loam and (silty/sandy) clay loam, respectively. Arithmetic mean values grouped by the same letters are not significantly different at the $p < 0.05$ significance level.

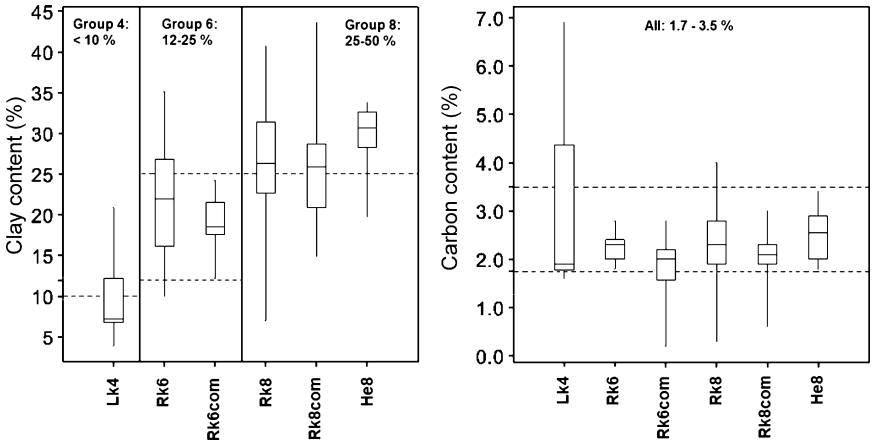

Fig. 4. Clay (left) and carbon (right) content for different soil map units on arable land in the Skuterud catchment. The box spans the interquartile range of the variables so that the middle 50% of the data lie within the box, with a line indicating the median. The whiskers represent minimum and maximum values. Clay content ranges for map texture groups are given in the clay content boxplot. Group 4 = loamy fine sand, 6 = silt loam, 8 = (sandy/silty) clay loam. Dashed lines show limits of texture group clay content and carbon content classes from the soil map.

here can partly be related to, e.g. the mentioned ''misclassifications'', uncertainties in map unit delineation and the presence of inclusions. Young et al. (1998) also found skewed distributions for soil physical properties within map units, and thus concluded that the median was a better measure of central tendency than was the mean.

Coefficients of variation (CV) ranged from 10% to 69% for the different soil series and variables, classified as low to high variation according to Warrick (1998) (low: CV < 15%, intermediate: CV = 15–50%, high: CV > 50%). The majority of the series/variables had CVs for particle size fractions and carbon content corresponding to intermediate variation. This is similar to what has been reported by, e.g., Goderya (1998), Warrick (1998), Lopez-Granados et al. (2002), Kiliç et al. (2004) and Duffera et al. (2007). For the soils mapped with clay content higher than 10 %, CVs ranged from 13% to 35 % for clay content and 29–65% for sand content. Lk4 showed highest CVs (>50%) for clay, silt and carbon content. For clay and silt this high variability primarily relates to a rather high degree of misclassification. For carbon it originates from the mentioned samples with high carbon contents.

The Brown-Forsythe test for unequal variances showed that the variances of different map series were not significantly different for the particle size fractions ($p = 0.069$, 0.20 and 0.14 for clay, silt and sand, respectively), suggesting that the complexes were not more variable than the consociations. Significant difference was found for carbon content ($p = 0.0002$), due to the high variance of Lk4. The sand series Lk4 and the Rk6 silt loam series, which had highest CVs for clay, are found in parts of the catchment with a patchy spatial distribution of marine and shore deposits, implying higher variability and larger uncertainties in the soil map. Lower CVs for the clay content were found for the series with texture group 8, which predominate in the lower-lying, central parts of the catchment.

3.3. Soil information from the small grid

3.3.1. Comparison with soil map

The texture class of the 256 samples from the small grid are plotted in the texture triangle (Fig. 5). We found the same tendency as for the large grid towards a linear relationship between clay and sand or silt. The soil map indicated the predominance of texture classes (silty/sandy) clay loam (25–50% clay) and loamy medium sand, as local soil series were Rk8 and Ir3. However, only two samples had more than 25% clay, and many samples were loams and sandy loams. The mismatch between mapped and sampled texture class was 73%, and 57% of the samples were located in neighbouring texture groups relative to the group expected from the map. A detailed soil survey carried out by the Norwegian Forest and Landscape Institute in the small grid has revealed six WRB reference soil groups and 29 soil series, and the extent of the series Rk8 and Ir3 was smaller in reality than apparent from the soil map (Nyborg, pers.comm.), correspondent to the mentioned mismatch in texture class.

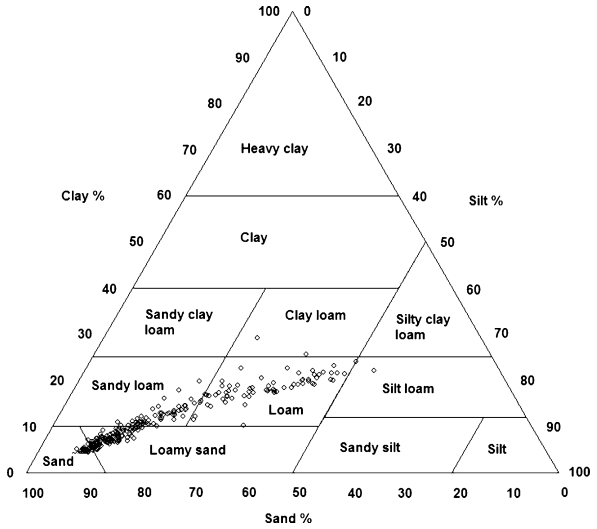

Fig. 5. Soil textural composition of samples from the small grid plotted in the Norwegian soil texture triangle (Sveistrup and Njøs, 1984).

3.3.2. Variability within map units

Summary statistics for particle size distribution variables and carbon content for the map units covering the small grid (Rk8 and Ir3) is presented in Table 3. The median clay, silt and sand content of Rk8 did not fall within the texture class limits, but for Ir3 they did. All variables were significantly different for the two soil series (Tukey HSD test, $p < 0.0001$ for particle size fractions and $p = 0.04$ for carbon). The particle size fractions were close to normally distributed for Rk8. Skewness was higher for the Ir3 map units, with positive skewness for clay and silt, and negative for sand. Carbon was positively skewed for both map units. Coefficients of variation (CV) ranged from 8% to 47% for the map soil series and variables, which classifies to intermediate variability. Rk8 had the highest CV for most variables, except clay content. Comparison with the CVs for Rk8 in the large grid shows that CVs for clay and silt were higher in the small grid, a result of the larger proportion of ''misclassified'' samples in the

Table 3
Summary statistics for clay, silt, sand and carbon content of soil map soil series covering the small grid

	Min–max	Median	Arithm. mean	Std. dev.	Skewness	CV (%)
Rk8 (n = 152)						
Clay (%)	6.10–29.2	13.5	14 [a]	5.09	0.29	36.3
Silt (%)	8.30–54.3	21.8	25.1 [a]	11.8	0.55	47
Sand (%)	23.6–84.7	64.4	60.9 [a]	16.5	−0.41	27.1
Carbon (%)	1.40–6.70	2.2	2.26 [a]	0.63	2.71	27.7
Ir3 (n = 104)						
Clay (%)	3.40–17.2	6.45	6.98 [b]	2.61	1.64	37.4
Silt (%)	7.1–27.6	11	12.1 [b]	4	1.89	33
Sand (%)	55.2–89.2	82.8	80.9 [b]	6.49	−1.78	8.01
Carbon (%)	1.40–4.10	2	2.11 [b]	0.56	1.62	26.6

Numbers 3 and 8 denote textures loamy medium sand and (silty/sandy) clay loam, respectively. Arithmetic mean values grouped by the same letters are not significantly different at the $p < 0.05$ significance level.

small grid (73% mismatch compared to 42% in the large grid). For carbon the CV was almost equal in the two grids. The variances of the particle size fractions were significantly higher for Rk8 than for Ir3 (Brown-Forsythe test, $p < 0.0001$), for carbon there was no significant difference ($p = 0.48$).

When combining the sample values with soil series determined in all 256 sample points by Nyborg (pers. comm.), distributions were more clearly normally distributed (for 70% of the soil series/variables), and the variation within soil series was slightly smaller. Sand had CV = 1.3–25%, silt 10–31%, clay 11–21% and carbon 10–24%.

Since the small grid was located on the boundary between two map units having different parent material and very different texture groups, it is hypothesised that similar scale variability in other parts of the catchment will rarely exceed what was reported for the small grid and that variability decreases when moving farther from the map unit boundary. In classical soil mapping, map unit delineations are considered abrupt, though it is well known that transition zones may be broad and ''fuzzy''/diffuse. From our data it appears that transition zones between marine and shore deposit units in this area may be around 100–200 m broad.

3.4. Spatial structures

The variogram describes the spatial structure of variables quantitatively. Both large grid and small grid particle size fractions were described by spherical variograms (Table 4, Figs. 6 and 7). The spherical variogram is widely used in geostatistics, and it represents transition features that have a common extent and which appear as patches (Webster and Oliver, 2001). The average range of the model represents the diameter of the patches. The distribution of texture classes in the arable area of the catchment was indeed patchy, with sandy shore deposits on the fringes and silty clay loam in the central area.

Due to the patchiness there was no significant spatial trend (systematic variation) in the large grid. The range

Table 4
Variogram model parameters

	Model	Nugget	Sill or slope	Range (m)	Nugget/sill (%)	R^2
Large grid						
Clay	Spherical	9.3	73.6	726	12.6	99.1
Silt [a,d]	Spherical	0.098	0.716	656	13.7	99.6
Sand [b]	Spherical	0.031	0.620	689	5.00	98.8
Carbon [c]	Linear	0.058	0.0000198	–	–	74.9
Small grid						
Clay [b,d]	Spherical	0.00001	0.01382	44.3	0.072	99.4
silt [b,d]	Spherical	0.00001	0.02132	44.0	0.047	93.1
Sand [a,b,d]	Spherical	0.0001	0.0537	44.4	0.19	98.1
Carbon [b,d]	Spherical	0.00183	0.0068	38.5	26.9	99.0

Transformations: [a] (maximum + 1 − value), [b] $\log_{10}$, [c] square root. Trend removal: [d] residuals.

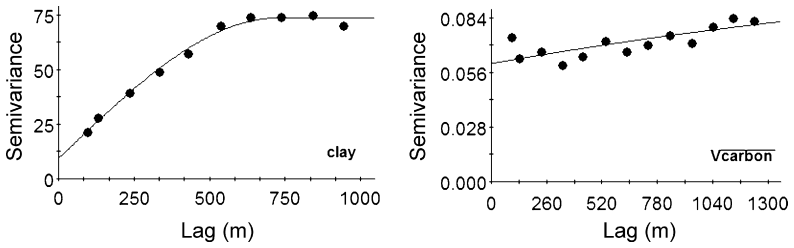

Fig. 6. Experimental and model variograms for clay (left) and square root of carbon (right) in the large grid.

for particle size fractions varied between 656 and 726 m. There was no sill and range for carbon content and an unbounded linear model (no range and sill) was fitted to the variogram. This suggests that the variability in carbon content continues to increase outside the surveyed region. The variogram seemed to have weak periodicity (period approximately 300 m), indicating a repeating pattern. The patchy structure of carbon content in the catchment could be a result of different farming practices on different farms, but also carbon translocation by erosion.

The small grid represented a 100–200 m broad transition zone between marine and shore deposits, with gradual changes in texture classes. The gradual change was evident also from the spatial trend analysis, where a significant trend ($p < 0.0001$) was found for all particle size fractions and carbon content. Clay and silt increased and sand decreased towards south-east. Carbon content increased towards the southern part of the grid, which was cleared of forest and cultivated quite recently (within the last 50 years) compared to the northern part (arable land for hundreds of years). Considering the random component (the residuals) of the spatial variation, the range was estimated to 44 m for the particle size fractions and 39 m for carbon content.

The nugget to sill ratio was nearly zero for the particle size fractions in the small grid, indicating that almost all of the variability was non-random. For carbon content in the small grid, random/small scale variation constituted 26.9% of the total variation. In the large grid, 5–13.7% of the variability could be considered random/small scale.

3.5. Implications of variability for predicted maximum water content for optimum workability

As described in previous sections, the coefficient of variation for sand, silt, clay and organic matter within soil map units ranged between 8% and 69% for both grids. The majority of the CVs were in the range 15–50% (intermediate variation). The variation within a map unit also reflects eventual errors in delineation of the map unit in the field, as shown by comparing topsoil texture classes from the map with measured data from the two grids. With respect to agricultural management the next question arising is: Will the variation have influence on the soil management operations and if so, how? In the following we consider the effect of variability on soil workability through the predicted "maximum water content for optimum workability" (Wopt).

3.5.1. Pedotransfer function validation

Wopt is a function of the lower and upper plastic limits (LPL and UPL), which both were calculated from clay, silt and organic matter (carbon) content in the topsoil (see Section 2.4). Measured and estimated LPL and UPL from two sites close to the catchment are shown in Fig. 8. Even if there are few points the relationship was relatively good and it was concluded that their performance was acceptable.

3.5.2. Variability in Wopt

Summary statistics for the predicted maximum soil water content for optimum workability (Wopt) are

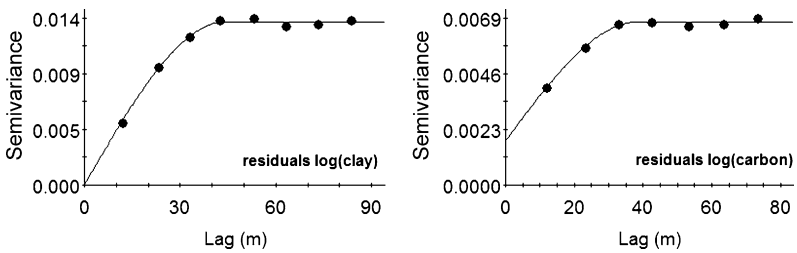

Fig. 7. Experimental and model variograms for residuals of log clay (left) and residuals of log carbon (right) in the small grid.

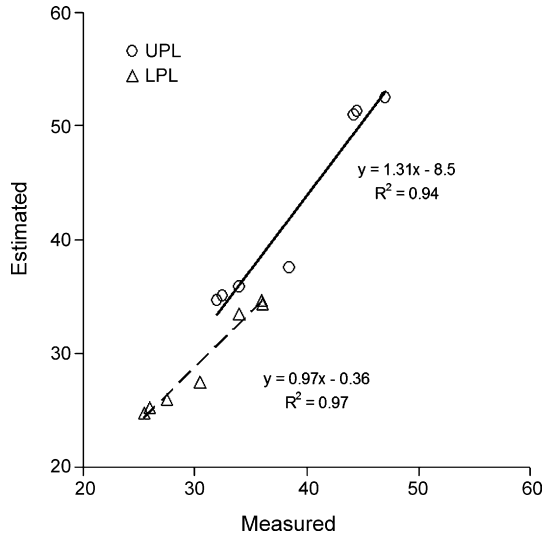

Fig. 8. Upper (UPL) and lower (LPL) plasticity limits (in weight% water) estimated from the equations of Schindler, cited by Mueller et al. (2003), vs. measured values.

presented in Table 5. Mean Wopt was smaller in the small grid (20.5 weight %) than in the large grid (25.1 weight %) due to lower clay and silt content in the small grid samples. Wopt in the large grid had higher CV (20%) than in the small grid (11%). When looking at the statistics for samples falling into the mapped soil series Rk8, mean Wopt and CVs were similar to the figures for the total dataset, for both grids. Recall that CVs for clay, silt and carbon content, from which Wopt was calculated, were 24%, 16% and 31%, respectively, for Rk8 in the large grid (Table 2) and 36%, 47% and 28%, respectively, for Rk8 in the small grid (Table 3). Considering the water amount in mm between a matric potential of −10 kPa (“field capacity”) and Wopt, the CV was 43% in the large grid and 124% in the small grid (Table 5). For the Rk8 map units CVs were slightly smaller, 31% and 82% in the large grid and small grid, respectively.

3.5.3. Wopt in relation to field water conditions and tillage timing

Predicted Wopt was compared to water contents at different soil matrix potentials estimated from the pedotransfer functions of Riley (1996). For samples with more than 10% clay the volumetric Wopt was usually in the same range as the water content at −100 kPa matric potential (Fig. 9). This agrees well with the predictions of Mueller et al. (2003), where the average matric potential at Wopt ranged from −16 to −500 kPa (−100 kPa for the total dataset), with higher matric potentials for high silt and clay contents. The consequence of Wopt corresponding to such high matric potentials is that a large proportion of the catchment area will not reach the optimum water content through drainage only, and soil water losses through soil evaporation will be an important process for reaching the requirements concerning workability.

Through the environmental agricultural monitoring programme in Norway (JOVA) information about farming practices in the Skuterud catchment has been collected since 1993. An overview of the timing of

Table 5
Summary statistics for the maximum water content for optimum workability (Wopt), and the water storage (mm) between matric potentials −2 and −10 kPa ($\theta(-2)$–$\theta(-10)$) and −10 kPa and Wopt ($\theta(-10)$–θ(Wopt)) in the top 10 cm of the soil

	Min–max	Median	Mean	Std.dev.	Skewness	CV
Large grid						
Wopt (weight %)	11.9–49.0	24.6	25.1	5.04	0.53	20.0
$\theta(-2)$–$\theta(-10)$ (mm)	1.46–8.58	3.60	3.83	0.95	1.34	24.7
$\theta(-10)$–θ(Wopt) (mm)	0.00–10.7	6.80	6.12	2.64	−1.00	43.1
Small grid						
Wopt (weight %)	16.7–34.1	19.9	20.5	2.33	1.53	11.4
$\theta(-2)$–$\theta(-10)$ (mm)	3.61–7.41	5.32	5.16	0.61	−0.21	11.8
$\theta(-10)$–θ(Wopt) (mm)	0.00–8.48	0.00	2.33	2.89	0.73	124
Rk8 large grid						
Wopt (weight %)	15.2–38.0	26.6	26.6	4.71	0.072	17.7
$\theta(-2)$–$\theta(-10)$ (mm)	1.89–5.26	3.46	3.53	0.57	0.55	16.1
$\theta(-10)$–θ(Wopt) (mm)	0.00–10.7	7.05	6.72	2.07	−1.24	30.8
Rk8 small grid						
Wopt (weight %)	16.7–34.1	19.9	20.7	2.54	1.55	12.3
$\theta(-2)$–$\theta(-10)$ (mm)	3.61–7.41	4.95	4.87	0.57	0.17	11.8
$\theta(-10)$–θ(Wopt) (mm)	0.00–8.48	3.70	3.62	2.98	0.0044	82.3

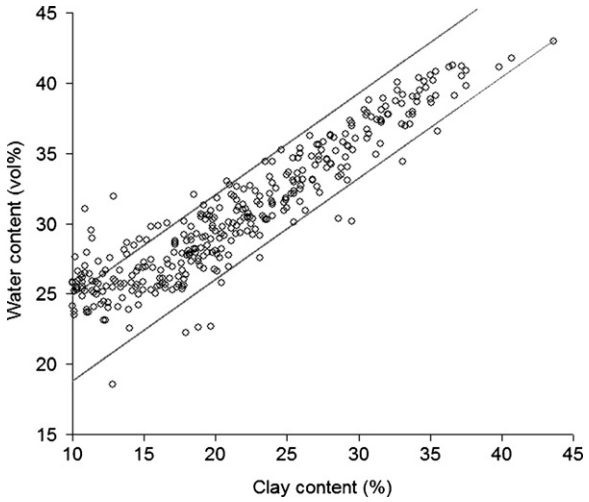

Fig. 9. The predicted maximum water content for optimum workability and 95% confidence lines for the predicted (Riley, 1996) water content at −100 kPa matric potential, as a function of clay content.

spring harrowing in the Skuterud catchment in the period 1993–2002 is shown in Fig. 10. The earliest observed harrowing date was April 11, and the latest was May 25, with a median of May 2. The last day with snow cover, based on measured data from a meteorological station (IMT-UMB: Department for Mathematics and Technology, Norwegian University of Life Sciences) approximately 3 km from the Skuterud catchment, varied from March 21 to April 20, with a median of April 10. Accordingly farmers harrow their fields about three weeks after snowmelt, on average.

Field observations on a silty clay loam located approximately 3 km from the Skuterud catchment showed that the groundwater level was between 20 and 60 cm below the soil surface in mid-April, and that the soil matric potential, as measured using electrical resistance blocks was between −5 and −7 kPa (Colleuille and Gillebo, 2002). Similar conditions can be assumed to prevail after spring snowmelt also on the clayey soil series in the Skuterud catchment. Assuming an initial groundwater level of 20 cm below soil surface, an initial soil matric potential of −2 kPa and drainage ceasing at a matric potential of −10 kPa (field capacity), the amount of drainable water in the top 10 cm of the soil was, as estimated using the pedotransfer functions of Riley (1996), approximately 4 and 5 mm for Rk8 in the large grid and small grid, respectively. The amount of water between field capacity and Wopt was 7 mm (0–10.7 mm) for Rk8 in the large grid and 4 mm (0–8.5 mm) for Rk8 in the small grid, and this amount would have to be evaporated for reaching Wopt.

Analyses of weather data from Ås (IMT-UMB) for the years 1961–1990, show that the median precipitation was 65.5 mm (range 26.4–200 mm) in the period April 15 to May 31. The median potential evapotranspiration calculated by the Penman equation was 111 mm for the same period (range 85–138 mm). The length of periods without precipitation is important with respect to spring tillage operations. The probability of a dry day following a dry day ranged from 0.33 to 0.89, on average 0.75 and the median length of a dry period during spring was 3.7 days (1.5–9 days). With a potential evaporation of 2.4 mm/day, evaporating the soil from −10 kPa to Wopt would take more than 0 and 5 days, considering that the actual soil evaporation is lower than the potential evaporation. If adding 2 days for draining the soil from

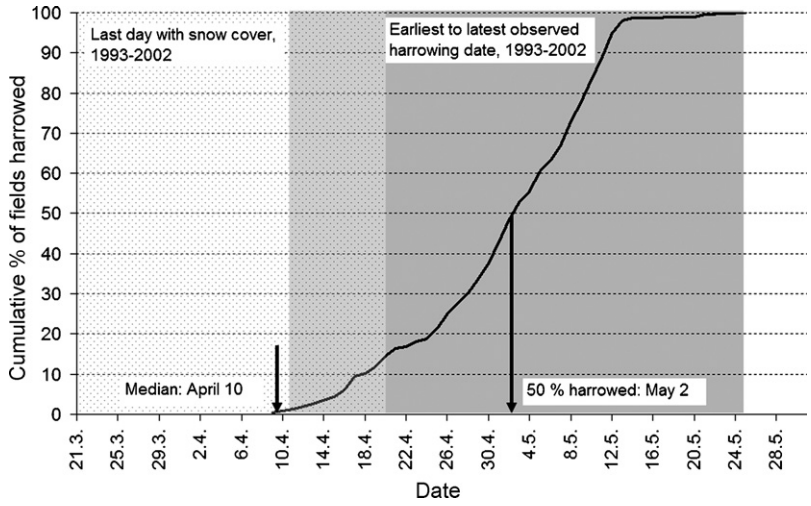

Fig. 10. The cumulative percentage of harrowed fields relative to date in the Skuterud catchment. The curve is calculated from observations in the period 1993–2002.

−2 kPa to field capacity, the time required would be at least 2–7 days, on average 4–5. The median length of dry periods (3.7 days) lies within the interval for required number of days, and it is slightly lower than the average. This implies that an intermediate variability in texture and carbon content can be very important for workability because the margins are small. The results also agree with the observation that farmers wait for three weeks before harrowing.

The effect of clay content on the water amounts available for drainage and evaporation is illustrated in Fig. 11. The amount of water between −2 and −10 kPa decreases linearly with increasing clay content, as the amount of large pores is lower. The amount of water between −10 kPa and Wopt, on the other hand, showed a weak polynomial relationship, indicating that the required time for reaching Wopt increases up to around 25% clay and thereafter decreases. This trend is in accordance with what can be experienced under field conditions, as it has been noted that soils with high clay contents tend to be workable after shorter periods of time.

3.5.4. Comparison of data sources for predicting and mapping Wopt

The maps shown in Fig. 12 show the spatial pattern of Wopt as calculated from soil map and soil samples. The Wopt map derived from the soil map (area weighted mean Wopt = 31%) deviated strongly from the maps derived from soil samples in the large grid (mean Wopt = 25% (Table 5)). One reason for this is the discrepancy between mapped and actual texture classes, as discussed in Sections 3.2.1 and 3.3.1. Mean clay content of the widespread Rk8 and Rk8inc map units was 26–27%, whilst the clay content assigned from the soil map by using the midpoint of the silty clay loam class in the texture triangle was 34%. The silt content of a large proportion of the samples was also lower than expected from the soil map, as loams and sandy loams were more common than silt loams. Clay and silt both increase the value of Wopt, and therefore Wopt was overestimated when using the soil map and available information about texture, SOM and gravel. It should be noted here that standard thematic maps produced by the Norwegian Forest and Landscape Institute and published on the web are based on representative soil profiles in the soil survey database, but these data were not easily accessible. Using the representative soil profiles may possibly have resulted in yet another different Wopt map.

The map with mean values for individual fields (mean of samples from the large grid) is representative of conventional agriculture, where (in Norway) the common sample density is one per hectare and soil samples are mixed to obtain average values for the individual fields, and fields are managed uniformly. Uniform tillage must be adapted to the parts of the field where the risk of compaction and poor seedbed preparation is largest. This map does not represent differences between different soils, and may lead to erroneous decisions about when the field should be tilled if the farmer's in situ evaluation of workability were to be replaced by pedotransfer estimates.

The interpolated map provides information about variability within fields and soil map units, and as such partly provides a better basis for decisions. It is more oriented towards precision agriculture: The farmer can choose to divide the field into management units that are tilled at different times. Alternatively, tillage timing of

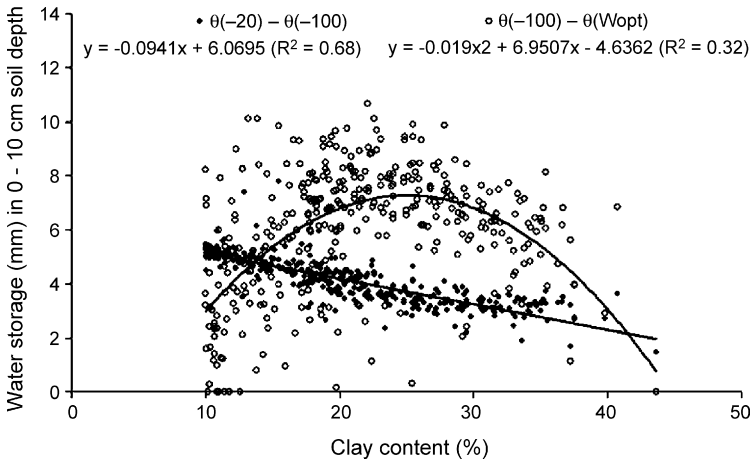

Fig. 11. Water storage (mm) between the matric potentials in the upper 10 cm of the soil as a function of clay content for sample postings in the small grid and large grid with clay content >10%.

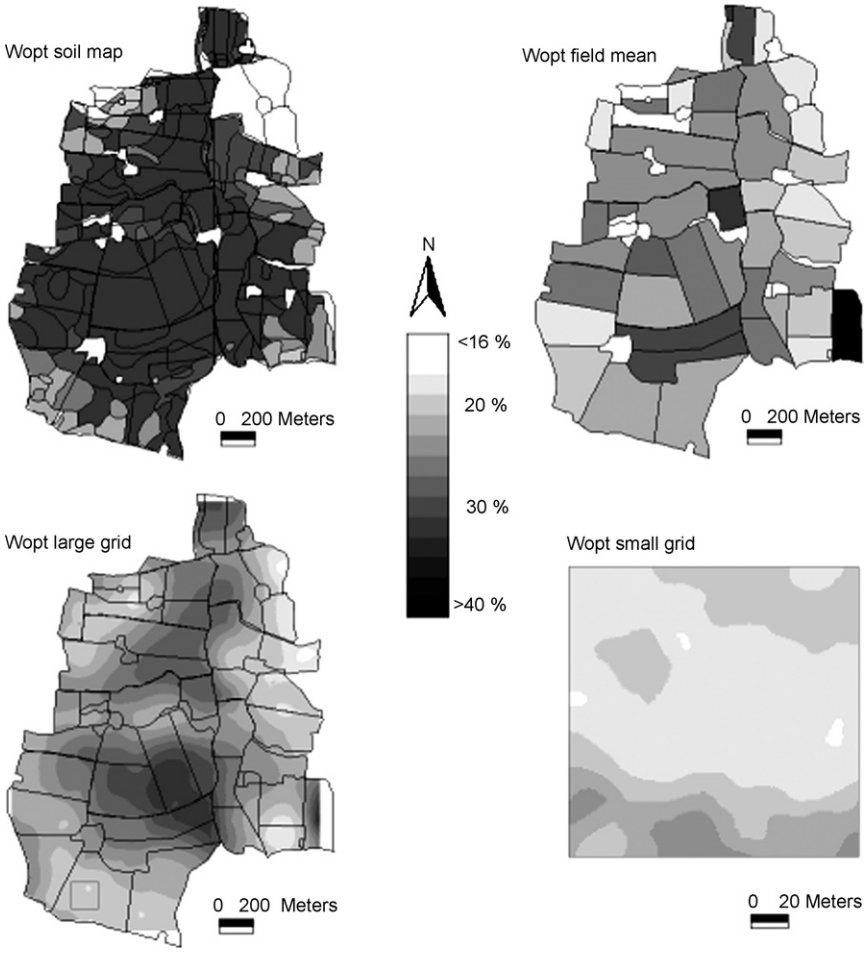

Fig. 12. Maximum soil water content for optimum workability (Wopt, in weight %) in the Skuterud catchment estimated from the soil map, mean values for individual fields calculated from samples in the large grid, interpolated surface from samples in the large grid and interpolated surface from samples in the small grid.

the entire field can be determined by the workability of the most problematic area of the specific field. The interpolated map indicates that all variation in Wopt is gradual, but possible abrupt boundaries between different soil types are lost using simple kriging on samples separated by such large distances. Techniques have been developed to integrate soil maps and ordinary kriging (Heuvelink and Bierkens, 1992; Boucneau et al., 1998), but this would require better characterization of the nature of soil map delineations. The data for the small grid, which was located directly on a transition zone between shore and marine deposits, showed that the boundary between the topsoil properties, including Wopt, of the two deposition types is indeed very gradual. Comparing values interpolated from the large grid within the area of the small grid to point values in the small grid showed that the differences ranged from −6.5–16.4% for clay content and −2.8–4.5 weight % (−3.2–5.7 volume %) for Wopt. The difference for the water content between −10 kPa and Wopt ranged between −5.5 and 6.5 mm, corresponding to at least 2–3 days of evaporation. Since the median number of consecutive dry days in spring was 3.7 only, this difference is of significant importance.

The Norwegian Forest and Landscape Institute have several thematic maps today, on e.g. erosion risk, available water capacity, recommended tillage, etc., but no maps for soil workability factors. It could be of interest for farmers, and maybe even more so for contractors, to have such maps, e.g. maps showing Wopt and typical values for the number of days from spring snowmelt or autumn harvest until tillage at different soil series, and the average number of workable days on different soils. If pursuing this, one should also include the subsoil in the calculations, as the wetness of the subsoil also contributes to both workability and

trafficability. As suggested by Hoogmoed et al. (2003), workability limits can be used in combination with water balance models to determine the number of workable days under a certain weather/climate regime, or the "average workday probability" (de Toro and Hansson, 2004). Real-time simulations is another possibility, if the soil map, or the farmer's site-specific information is coupled with a model that continuously estimates soil water content using information about soil physical properties and daily incoming climatic data.

4. Summary/conclusions

The readily available information on texture and organic matter content from the Norwegian soil map was found to be of limited usefulness for agricultural management, particularly for site-specific operations (precision agriculture). Firstly, provided texture and organic matter classes cover broad intervals, e.g., 25% for clay and 3% for organic matter for the most important soil series in the studied catchment. Secondly, the smallest size of a map unit is about 10 times the size of the manageable area in precision agriculture, and variability within map units is unknown. Thirdly, we found a considerable degree of "misclassification" of texture class in this particular soil map at comparison with analysed topsoil samples, and the most prominent deviation was that sandy loam and loam texture was underrepresented in the map. The problem was largest in areas with different deposits, many soil series and at the boundary between different series (e.g. in the small sample grid). The coefficients of variation were also higher for map units in this area. The variability within and between soil map units was carried out using data from the two sample grids together with the soil map. The major findings was that there were significant differences in both clay, silt and sand content between soil series having different texture classes on the map, but not for different series having the same texture class. Carbon content was similar for all map units, and all median values were in the lower range of the map class. The median clay, silt, sand and carbon content of the map units generally fell within the limits of the map texture class, except for Rk8 in the small grid (all variables outside class) and Rk6 and Rk6com (silt outside class). Furthermore, the statistical distributions were generally non-normal, that is positively or negatively skewed. The coefficients of variation were usually between 15% and 50%, classified as "intermediate" variability. There were no indications that the complexes had higher variability than the consociations. CVs were higher for map units in the small grid than in the large grid, except for carbon for which CVs were similar. Most of the variation in both the small grid and large grid was non-random, showing spatial dependency or continuity. The large grid was dominated by a patchy structure, whilst the variables in the small grid showed a systematic trend with gradual transition perpendicularly on the boundary between the two map units. The calculated range for variables in the large grid was 16 times larger than for the small grid, underlining the importance of scale (area extent, sample spacing and sample support) in determining spatial dependency. The gradual change in variable values in the small grid indicated that boundaries between different soils/deposits in reality are fuzzy or non-existent in this catchment, at least as far as the topsoil is concerned.

Implications of the variability in particle size distribution and carbon content on land management operations were assessed for one specific case: the maximum water content for optimum workability (Wopt), predicted from pedotransfer functions. The variability in weight% Wopt, expressed in terms of the CV, was 10–20%. The CV for the water amount between −10 kPa and Wopt was higher, 31–124%. Wopt was usually in the same range as the predicted water content at −100 kPa matric potential, indicating that evaporation in addition to drainage is required for obtaining workable conditions in the field. The time required for obtaining Wopt was estimated in a simplistic way to an average of at least 5 days, which is longer than the median length of a dry period in the area (3.7 days). This agreed with the observation that farmers in the area often harrow their fields as late as three weeks after spring snowmelt. Using different data sources for estimating Wopt also yielded different results. Wopt predicted from the soil map deviated strongly from Wopt predicted from the sample grids, due to higher clay and silt content than in reality. A comparison of Wopt predicted for the sample points in the small grid and interpolated Wopt from the large grid samples within the area covered by the small grid, showed the importance of high-resolution sampling for e.g. precision agriculture purposes, as errors related to using the large grid data corresponded to ±2–3 days with evaporation, a significant error considering the short period of consecutive dry days in the area.

Acknowledgements

This study was part of the Strategic Institute Programme "Soil Quality and Precision Agriculture", funded by the Norwegian Research Council (project number 143294/I10). We give our thanks to the farmers

in the Skuterud catchment for getting access to their fields, to Konrad Bjoner (Bioforsk) for assistance with soil sampling, to Dr. Lillian Øygarden (Bioforsk) for comments to the manuscript, to Dr. Marianne Bechmann (Bioforsk) for access to the data from the large grid and Åge Nyborg (the Norwegian Forest and Landscape Institute) for access to soil classifications in the small grid.

References

Boucneau, G., van Meirvenne, M., Thas, O., Hofman, G., 1998. Integrating properties of soil map delineations into ordinary kriging. Eur. J. Soil Sci. 49, 213–229.

Chaplot, V., 2005. Impact of DEM mesh size and soil map scale on SWAT runoff, sediment and NO_3-N loads predictions. J. Hydrol. 312, 207–222.

Colleuille, H., Gillebo, E., 2002. Nasjonalt observasjonsnett for markvann: etablering og vedlikehold av målestasjoner: Måleprosedyrer: Datautarbeiding og dataformidling. NVE-rapport 2002:6, 58 p (in Norwegian). ISBN 82-410-0466-4.

de Toro, A., Hansson, P.-A., 2004. Analysis of field machinery performance based on daily soil workability status using discrete event simulation or on average workday probability. Agric. Syst. 79, 109–129.

Dexter, A.R., Bird, N.R.A., 2001. Methods for predicting the optimum and the range of soil water contents for tillage based on the water retention curve. Soil Till. Res. 57, 203–212.

Duffera, M., White, J.G., Weisz, R., 2007. Spatial variability of Southeastern U.S. Coastal Plain soil physical properties: implications for site-specific management. Geoderma 137, 327–339.

Fadnes, K., 2003. Feltinstruks for jordsmonnkartlegging 2003. NIJOS dokument 4/03, 36 pp. (in Norwegian).

Gee, G.W., Bauder, J.W., 1986. Particle-size Analysis. In: Klute, A. (Ed.), Methods of Soil Analysis, Part 1–Physical and Mineralogical Methods, second ed., vol. 9. Agronomy Monograph, Madison, WI, pp. 383–411.

Goderya, F.S., 1998. Field scale variations in soil properties for spatially variable control: a review. J. Soil Contam. 7, 243–264.

Heuvelink, G., Bierkens, M.F.P., 1992. Combining soil maps with interpolation from point observations to predict quantitative soil properties. Geoderma 55, 1–15.

Hoogmoed, W.B., Cadena-Zapata, M., Perdok, U.D., 2003. Laboratory assessment of the workable range of soils in the tropical zone of Veracruz. Mexico. Soil Till. Res. 74, 169–178.

Kiliç, K., Özgöz, E., Akbas, F., 2004. Assessment of spatial variability in penetration resistance as related to some soil physical properties of two fluvents in Turkey. Soil Till. Res. 76, 1–11.

Kolsrud, E., 2001. Lagelighet for jordarbeiding og jordfysiske forhold i fem jordarbeidingssystemer på siltig mellomleire/Workability and soil physical properties in five tillage systems on a silty clay loam. Master thesis at the Agricultural University of Norway, Department for soil and water sciences, 67 p. (in Norwegian).

Kretschmer, H., 1996. Koernung und Konsistenz. In: Blume, H.-P., Felix-Henningsen, P., Fischer, W.R., Frede, H.G., Horn, R., Stahr, K. (Eds.), Handbuch der Bodenkunde, first ed., vol. I. Ecomed.

Lathrop Jr., R.G., Aber, J.D., Bognar, J.A., 1995. Spatial variability of digital soil maps and its impact on regional ecosystem modeling. Ecol. Model. 82, 1–10.

Lilburne, L.R., Webb, T.H., 2002. Effect of soil variability, within and between soil taxonomic units, on simulated nitrate leaching under arable farming. New Zealand. Aust. J. Soil Res. 40, 1187–1199.

Lin, H., Wheeler, D., Bell, J., Wilding, L., 2005. Assessment of spatial variability at multiple scales. Ecol. Model. 182, 271–290.

Lopez-Granados, F., Jurado-Exposito, M., Atenciano, S., Garcia-Ferrer, A., de la Orden, M.S., Garcia-Torres, L., 2002. Spatial variability of agricultural soil parameters in southern Spain. Plant Soil 246, 97–105.

Matheron, G., 1965. Les variables régionalisées et leur estimation. Masson, Paris.

Mueller, L., Schindler, U., Fausey, N.R., Lal, R., 2003. Comparison of methods for estimating maximum soil water content for optimum workability. Soil Till. Res. 72, 9–20.

Nelson, D.W., Sommers, L.E., 1982. Total Carbon Organic Carbon and Organic Matter. In: Page, A.L., Miller, R.H., Keeny, D.R. (Eds.), Methods of Soil Analysis, Part 2-Chemical and Microbiological Properties, second ed., 9, Part 2. Agronomy Monograph, Madison, WI, pp. 539–579.

Nyborg, Å., 2003. Seriedefinisjoner vår 2003. NIJOS dokument 5/03 (in Norwegian).

Pierce, F.J., Nowak, P., 1999. Aspects of precision agriculture. Adv. Agron. 67, 1–85.

Riley, H., 1996. Estimation of physical properties of cultivated soils in southeast Norway from readily available soil information. Norwegian J. Agric. Sci., Suppl. 25, 1–51.

Salehi, M.H., Eghbal, M.K., Khademi, H., 2003. Comparison of soil variability in a detailed and a reconnaissance soil map in central Iran. Geoderma 111, 45–56.

SAS Institute Inc. 2005. JMP 6.0.

Skjevdal, R.M., Vandsemb, S.M., 2005. Jord-og vannovervåking i landbruket. Feltrapporter fra programmet i 2004. Jordforsk report 84/05, 251 pp (in Norwegian).

Soil Survey Division Staff, 1993. Soil Survey Manual Soil Conservation Service. U.S. Department of Agriculture Handbook, pp. 18.

Sveistrup, T., Njøs, A., 1984. Kornstørrelser i mineraljord, Revidert forslag til klassifisering. Jord og myr 8, 8–15 (in Norwegian).

Tabachnick, B., Fidell, L., 2001. Using multivariate statistics, fourth ed. Allyn and Bacon, Boston.

Tisdall, J.M., Adem, H.H., 1986. Effect of water content at tillage on size-distribution of aggregates and infiltration. Aust. J. Exp. Agric. 26, 193–195.

Warrick, A.W., 1998. Spatial variability. In: Hillel, D. (Ed.), Environmental Soil Physics. Academic Press, San Diego, USA, pp. 655–675.

Webster, R., Oliver, M., 2001. Geostatistics for Environmental Scientists. John Wiley & Sons Ltd., Chichester.

Western, A.W., Blöschl, G., 1999. On the spatial scaling of soil moisture. J. Hydrol. 217, 203–224.

Young, F.J., Hammer, R.D., Williams, F., 1997. Estimation of map unit composition from transect data. Soil Sci. Soc. Am. J. 61, 854–861.

Young, F.J., Hammer, R.D., Williams, F., 1998. Evaluating central tendency and variance of soil properties within map units. Soil Sci. Soc. Am. J. 62, 1640–1646.

Paper II

Kværnø, S.H., Øygarden, L., 2006. The influence of freeze–thaw cycles and soil moisture on aggregate stability of three soils in Norway. *Catena 67*, 175-182.

Available online at www.sciencedirect.com
ScienceDirect
Catena 67 (2006) 175 – 182
CATENA
www.elsevier.com/locate/catena

The influence of freeze–thaw cycles and soil moisture on aggregate stability of three soils in Norway

Sigrun Hjalmarsdottir Kværnø *, Lillian Øygarden

Norwegian Institute for Agricultural and Environmental Research (Bioforsk), Soil and Environment Division, Frederik A. Dahls vei 20, N-1432 Ås, Norway

Received 5 November 2004; received in revised form 21 March 2006; accepted 27 March 2006

Abstract

Winter conditions with seasonally frozen soils may have profound effects on soil structure and erodibility, and consequently for runoff and erosion. Such effects on aggregate stability are poorly documented for Nordic winter conditions. The purpose of this study was to quantify the effect of variable freeze–thaw cycles and soil moisture conditions on aggregate stability of three soils (silt, structured clay loam—clay A and levelled silty clay loam—clay B), which are representative of two erosion prone areas in southeastern Norway. A second purpose was to compare aggregate stabilities measured by the Norwegian standard procedure (rainfall simulator) and the more widely used wet-sieving procedure. Surface soil was sampled in autumn. Field moist soil was sieved into the fraction 1–4 mm and packed into cylinders. The water content of the soil was adjusted, corresponding to matric potentials of −0.75, −2 and −10 kPa. The soil cores were insulated and covered, and subjected to 0, 1, 3 or 6 freeze–thaw cycles: freezing at −15 °C for 24 h and thawing at 9 °C for 48 h. Aggregate stability was measured in a rainfall simulator (all soils) and a wet-sieving apparatus (silt and clay B). The rainfall stability of silt was found to be significantly lower than of clay A and clay B. Clay A and clay B had similar rainfall stabilities, even though it was expected that the artificially levelled clay B would have lower stability. Freezing and thawing decreased the rainfall stability of all soils, but the effect was more severe on the silt soil. There was no evident effect of water content on the stability, probably due to experimental limitations. The same effects were observed for wet-sieved soil, but the wet-sieving resulted in less aggregate breakdown than the rainfall simulator. Rainfall impact seemed to be more detrimental than wet-sieving on more unstable soil, that is, on silt soil and soil subjected to many freeze–thaw cycles. Such conditions are expected to occur frequently during field conditions in unstable winters.

Keywords: Aggregate stability; Freezing and thawing; Winter; Erosion; Rainfall simulator; Wet-sieving; Norway

1. Introduction

Under Norwegian climatic conditions, runoff and erosion are documented to be highest in late autumn and in the winter season, especially during the snowmelt period (Lundekvam and Skøyen, 1998; Øygarden, 2000). Erosion can be particularly severe in connection with rain and snowmelt on partially thawed soil (Øygarden, 2000). Under such conditions, infiltration of meltwater is impeded by the frozen soil and surface runoff which is generated has the potential of detaching particles from the thawed soil surface.

In addition, temporal variation in the soil erodibility (the soil's inherent susceptibility to detachment and transport by rain and runoff (Ellison, 1945)) may result from alternating freezing and thawing. Several studies have shown that erodibility increases under winter conditions (e.g. Kirby and Mehuys, 1987; Kok and McCool, 1990; Bajracharya and Lal, 1992). This has lead to an increased interest in how individual factors determining erodibility are influenced by frost action. One such factor is the aggregate stability (the soil's ability to retain its structural arrangement and void space when exposed to mechanical stresses (Angers and Carter, 1996)).

* Corresponding author. Tel.: +47 64948159; fax: +47 64948110.
E-mail addresses: sigrun.kvaerno@bioforsk.no (S.H. Kværnø), lillian.oygarden@bioforsk.no (L. Øygarden).

0341-8162/$ - see front matter © 2006 Elsevier B.V. All rights reserved.
doi:10.1016/j.catena.2006.03.011

Most of the studies of effects of freezing and thawing on aggregate stability show that an increased number of freeze–thaw cycles tends to decrease the stability (Bullock et al., 1988; Edwards, 1991; Mulla et al., 1992; Staricka and Benoit, 1995; Dagesse et al., 1997; Bajracharya et al., 1998). However, there also exists evidence that frost action may actually increase the stability (Perfect et al., 1990; Lehrsch, 1998). The initial moisture conditions of the soil at freezing has been pointed out as a key factor in the freeze–thaw process. In general, aggregate stability has shown to be inversely proportional to soil water content at the time of freezing (Perfect et al., 1990; Staricka and Benoit, 1995; Lehrsch, 1998). On the other hand, freeze-drying of soil can also be highly detrimental to the aggregates (Staricka and Benoit, 1995). Different soils also respond differently to freezing and thawing due to e.g. differences in texture, structure, organic matter content, chemical properties and root development (Lehrsch et al., 1991; Oztas and Fayetorbay, 2002).

Lundekvam and Skøyen (1998) found higher stability for artificially levelled soils than for non-levelled soils, but these measurements did not include any seasonal variations. Øygarden (2000) found that soil shear strength and aggregate stability was lowest after the winter period, before spring tillage. Low stability and shear strength coincided with the periods of highest measured soil losses. Apart from this, there exist no detailed studies on how different freezing/thawing conditions normally occurring during winters in Norway influence aggregate stability. Norwegian studies concerning erosion in the winter season have primarily focused on quantifying particle loss from plots (Lundekvam and Skøyen, 1998) and catchments (Øygarden, 2000) and on effects of measures like constructed wetlands/sedimentation ponds (Braskerud, 2001) and bufferzones (Syversen, 2002). Erosion risk maps and soil prediction models (e.g. USLE-based) are used for planning of measures for reducing erosion in Norway, but they are not fully developed for describing winter conditions. Increased knowledge about the effect of frost action on soil physical properties like aggregate stability could help improving soil erosion prediction models also for winter conditions.

The Norwegian standard method for measuring aggregate stability includes using a rainfall simulator (Marti, 1984), while the wet-sieving procedure (Kemper and Rosenau, 1986) has been more widely used internationally. This makes it difficult to compare results.

The main goals of this study were to:

1. Investigate the effect of variable freeze–thaw cycles and soil moisture conditions on aggregate stability of three soils, which are representative of erosion prone areas in Norway.
2. Compare stability measured using the Norwegian standard method (rainfall simulator) with stability measured using the wet-sieving procedure.

2. Materials and methods

2.1. Site description

The experiments were carried out on three different soils from two agricultural areas in southeastern Norway: Ås, approximately 30 km southeast of Oslo, and Nes, 80 km northeast of Oslo (Fig. 1). The mean annual temperature and precipitation in Ås are 5.3 °C and 785 mm, respectively, and in Nes 4.3 °C and 665 mm. January is the coldest month, with mean temperatures of −4.8 °C and −6.9 °C in Ås and Nes, respectively. Winters in both areas are usually relatively unstable, with alternating periods of freezing and thawing and several snowmelt events. Below-zero temperatures occur frequently in the period November–April.

2.2. Soil sampling and treatments

The soil sampled in Ås ("clay A") was a clay loam (Stagnic Albeluvisol). The soils sampled in Nes were an artificially levelled silty clay loam ("clay B", Anthrosol) and a silt soil ("silt", Gleyic Cambisol). Some properties of the soils are presented in Table 1. The soil was sampled from arable fields in September/October 2001 (all soils) and September 2002 (clay B). Plant residues (stubble) were removed and a shovel was used to break loose the top 15–20 cm of the soil. The soil clods were carefully broken apart and placed in cardboard boxes. The boxes were covered

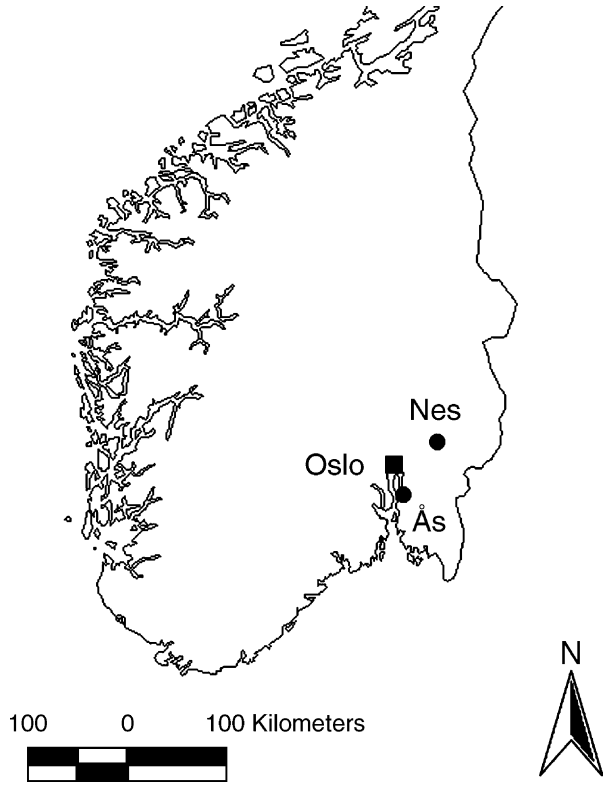

Fig. 1. South Norway, with the capital Oslo, and the two experimental sites—Ås and Nes.

Table 1
Physical and chemical properties of the three soils studied

Soil	Texture class	Sand (%)	Silt (%)	Clay (%)	Org C (%)	Base saturation (%)	pH (H_2O)
Clay A	Clay loam	24.3	48.4	27.4	1.6	71	6.6
Clay B	Silty clay loam	15.8	57.9	26.3	1.1	80	6.5
Silt	Silt	7.0	86.2	6.8	2.5	70	6.5

with plastic and stored at a temperature of approximately 9 °C.

The soil was sieved to obtain aggregates of size 1–4 mm (a fraction also used in similar studies, e.g. Lehrsch et al., 1991; Lehrsch and Jolley, 1992; Lehrsch, 1998). The aggregates were packed into PVC cylinders (diameter = 10 cm and height = 5.5 cm). The lower end of the cylinder was covered with a permeable nylon cloth. Packing was done by filling the cylinder with aggregates and tapping it gently against the table, little by little until the soil core was 4.5 cm thick and weighing 400 g. Three replicates for each of the treatments described below were prepared.

The water content of the repacked soil was adjusted using a sandbox apparatus from Eijkelkamp Agrisearch Equipment. The samples were placed in the sandbox, and saturated slowly from below over a 3-day period. Only slight slaking was observed during this wetting procedure. After saturation was obtained, a negative pressure was applied to obtain water contents corresponding to matric potentials $h = -0.75$ kPa ("near saturated"), $h = -2$ kPa ("intermediate") and $h = -10$ kPa ("field capacity"). These water contents were assumed to represent different moisture conditions in autumn, before soil freezes.

After adjusting the water content, the soil cores were insulated in expanded polyester, 3 cm at the sides and 5 cm at the bottom, to simulate one-dimensional freezing. The soil was covered with aluminium foil to prevent evaporation and freeze-drying during the freeze–thaw treatment. The numbers of freeze–thaw cycles selected were 0, 1, 3 and 6 (one cycle consists of one freezing and the thawing period until next freezing). The samples were frozen at −15 °C for 24 h and thawed at 9 °C 48 h in a cabinet with automatic temperature control, the temperatures being applied with a fast progressive decrease-increase (within 1 h).

2.3. Additional samples

The samples had to be pre-treated and analysed in groups due to limited space in the sandboxes. During freezing and thawing of the 3 and 6 freeze–thaw cycles samples of clay B and silt, the temperature cabinet started malfunctioning and new samples had to be prepared. Unfortunately, the limited resources did not allow for the experiment to be repeated in its entirety for both silt and clay B. As there was not enough clay B soil left on storage, it was decided to sample a new supply of clay B the following autumn, and to prepare the missing silt samples from soil already on storage. We tested the effect of using silt that had been stored for 5 months, only partly covered by plastic and therefore not longer field moist. The samples had a matric potential = −0.75 kPa, and were subjected to 0 and 1 freeze–thaw cycle (three parallels each).

2.4. Aggregate stability measurements

The rainfall simulator (Marti, 1984) was used on all samples. The rainfall simulator consists of a horizontal, rotating disk inside a metal frame with four nozzles. The nozzles are connected to a water pressure regulator. The distance between the disk and the nozzles is 32 cm. Two replications of 25 g each, from each of the treatment replications, were placed on sieves which were 15 cm in diameter, with a mesh width of 0.5 mm. The sieves were placed on the rotating disk and the water (tap water with pH 7.5 and total hardness 2.9°dH) was turned on so that "rain" fell from the nozzles. The rain intensity was approximately 1 l/min for 3 min, with a water pressure of 150 kPa. The material remaining on the sieve was dried and weighed.

The wet-sieving apparatus (Kemper and Rosenau, 1986) was used on all clay B samples, on silt samples frozen 3 and 6 cycles, and on stored silt samples with matric potential −0.75, frozen 0 and 1 cycle. The wet-sieving apparatus raises and lowers sieves of stainless steel into water contained in small cans. The sieves are 3.7 cm in diameter and the standard mesh width is 0.26 mm. To enable comparison with the rainfall simulator, the standard sieves were substituted by sieves with mesh width 0.5 mm. Two replications of 4 g each, from each of the treatment replications, were placed on the sieves. The sieves were raised and lowered into 87 ml of tap water for 3 min and 45 s. The suspended material in the water was dried and weighed.

The aggregate stability was expressed as the percentage of dry material remaining on the sieve after the stability test relative to the initial amount of dry soil. The initial amount of dry soil was determined gravimetrically on 25-g samples from each treatment replication and dried at 105 °C for 48 h.

2.5. Statistical analyses

Statistical analyses were carried out in Minitab 14 (Minitab Inc., 2005). The general linear model (GLM) procedure was used to determine treatment effects, including soil, matric potential, number of freeze–thaw cycles and interactions between matric potential and number of freeze–thaw cycles. The Tukey's multiple comparison test was used for comparing means. The effect of water content and interactions were not analysed for wet-sieved silt due to the unbalanced design (0 and 1 freeze–thaw cycles missing at

Table 2
p-values from the GLM test of different treatment effects

	Soil	*h*	FTC	*h* * FTC	Soil * *h*	Soil * FTC	Soil * *h* * FTC
Rainfall simulator							
All soils	<0.0001	0.007	<0.0001	0.009	0.009	<0.0001	0.001
Clay A	–	0.012	<0.0001	<0.0001	–	–	–
Clay B	–	ns	<0.0001	<0.0001	–	–	–
Silt	–	0.024	<0.0001	ns	–	–	–
Wet-sieving							
Clay B	–	<0.0001	<0.0001	0.037	–	–	–
Relative difference between rainfall simulator and wet-sieving							
Clay B and silt[a]	<0.0001	ns	ns	ns	0.029	ns	ns
Clay B[b]	–	<0.0001	<0.0001	<0.0001	–	–	–
Silt[c]	–	–	ns	–	–	–	–

FTC = number of freeze–thaw cycles, *h* = matric potential and ns = not significant at the 0.05 level.
[a] Statistical analysis performed on samples with FTC = 3 and 6 only.
[b] All samples.
[c] Samples with *h* = −0.75 kPa.

matric potentials −2 and −10 kPa). The relationship between aggregate stability measured by rainfall simulator and wet-sieving was tested by linear regression analysis. The GLM procedure and Tukey test were used to test whether the differences between stabilities measured with the two methods differed significantly for different number of freeze–thaw cycles and water contents.

3. Results and discussion

The results of the GLM tests indicated that all treatment effects, including interaction terms, were significant at $p < 0.01$ (Table 2). Further results for the rainfall simulator are discussed in Sections 3.1–3.4. Results for the wet-sieved samples are discussed in Section 3.5.

3.1. Soil effect

The Tukey test showed that the aggregate stability of silt was significantly lower than the stability of clays A and B (Table 3). The stability of clays A and B was not significantly different (Table 3). This was a bit unexpected, as clay B is artificially levelled and clay A is not. Levelled soils often have low organic matter content and poor structure, and are therefore considered less stable than similar non-levelled

Table 3
Mean values, confidence intervals and sample size (*n*) from the general linear model test, and results from the Tukey multiple comparison test for the means: mean values grouped by different letters (a–d) at each level are significantly different at the $p < 0.05$ significance level

Main effects	Mean (confidence limits)[Tukey group]		
	Rainfall simulator	Wet-sieving	Relative difference rainfall simulator–wet-sieving
Soil	*n* = 108		*n* = 36
Clay A	73.2 (70.5, 75.9)[a]		–
Clay B	71.5 (68.9, 74.2)[a]		25.1 (20.6, 29.5)[a]
Silt	19.0 (16.4, 21.7)[b]		53.9 (49.4, 58.3)[b]

	Clay A	Clay B	Silt	Clay B	Silt[1]	Clay B	Silt[1]
n	36	36	36	36	12	36	12
FTC							
0	79.9 (77.2, 82.5)[a]	80.2 (76.9, 83.6)[a]	31.0 (26.7, 35.3)[a]	94.1 (91.4, 96.9)[a]	57.1 (44.3, 70.0)[a]	15.0 (11.1, 18.9)[a]	31.5 (16.9, 46.0)[a]
1	76.3 (73.7, 79.0)[b]	74.9 (71.5, 78.3)[b]	16.0 (11.7, 20.3)[b]	93.3 (90.6, 96.1)[a]	43.2 (30.0, 56.1)[a,b]	18.4 (14.3, 22.0)[a]	45.6 (31.1, 60.2)[a]
3	66.7 (64.0, 69.3)[c]	70.8 (67.4, 74.1)[c]	15.0 (10.7, 19.3)[b]	89.6 (86.8, 92.3)[b]	30.6 (23.2, 38.1)[c]	25.4 (21.5, 29.2)[b]	47.2 (32.7, 61.8)[a]
6	63.2 (60.6, 65.9)[c]	66.9 (63.5, 70.3)[d]	14.1 (9.86, 18.4)[b]	84.4 (81.7, 87.2)[c]	33.0 (25.6, 40.4)[b,c]	24.8 (20.9, 28.6)[b]	53.1 (38.6, 67.6)[a]
h (kPa)							
−0.75	72.8 (68.7, 76.9)[a]	70.3 (65.5, 75.0)[a]	15.3 (10.0, 20.6)[a]	94.3 (91.6, 97.0)[a]	36.1 (27.7, 44.4)	25.6 (22.0, 29.2)[a]	44.4 (36.4, 52.3)
−2	71.8 (67.7, 75.8)[a,b]	71.8 (67.0, 76.5)[a]	22.5 (17.2, 27.8)[b]	90.2 (87.5, 92.9)[b]	–	20.3 (16.7, 23.9)[b]	–
−10	75.0 (70.9, 79.1)[b]	72.6 (67.9, 77.3)[a]	19.3 (14.0, 24.5)[b]	86.6 (83.9, 89.3)[c]	–	16.5 (12.9, 20.1)[c]	–

FTC = number of freeze–thaw cycles and *h* = matric potential.
[1] Analysis on silt samples with *h* = −0.75 kPa only.

soils (Prestvik, 1974; Lundekvam and Skøyen, 1998). Clays A and B were quite similar in clay and organic matter content (Table 1), but at visual inspection, the structure of the levelled clay B clearly differed from that of clay A. Aggregates of the levelled soil were larger, more angular in shape and seemed more dense. When wet, clay B was more smeary.

3.2. Freezing and thawing effect

The initial aggregate stability (0 freeze–thaw cycles, representing the state of the soil before the first frost period in autumn) was high for clay A and clay B (both about 80%) due to the high clay content. The initial stability for silt was lower (31%), indicating that this soil is very susceptible to erosion even before freezing and thawing. Organic carbon content was high (2.5%) in the silt, but the highly erodible silt and fine sand fractions together constituted 93% of the mineral material.

Averaged over water contents, the effect of freezing and thawing was significant for all soils (Table 2) and the tendency was that stability decreased with increasing number of freeze–thaw cycles. Several other studies have shown the same (Bullock et al., 1988; Edwards, 1991; Mulla et al., 1992; Staricka and Benoit, 1995; Dagesse et al., 1997; Bajracharya et al., 1998).

The decrease in stability after the first freeze–thaw cycle was significant for all three soils (Table 3). This is contrary to the results of Mostaghimi et al. (1988), Lehrsch et al. (1991) and Lehrsch (1998), who observed that freezing and thawing usually increased stability with the first few freeze–thaw cycles.

Further decrease on the silt was not significant. However, the stability of silt at 3 and 6 cycles might have been somewhat overestimated because drier soil was used for these treatments (see Materials and methods). Additional tests on stored soil confirmed the suspicion: The stability of the unfrozen samples was increased from 27% to 38% at storage and for samples frozen once the increase was from 12% to 23%. It is therefore likely that there should be a more pronounced decline in stability between one and three cycles for the silt. This finding stresses the importance of avoiding storing and drying soil before aggregate stability tests. Drying tends to strengthen bondings and hence the aggregate stability increases (Amezketa, 1999). However, direct immersion of dry aggregates may also cause serious disintegration due to air entrapment (Lehrsch and Jolley, 1992).

For clay A, the decrease in stability was no longer significant after 3 freeze–thaw cycles, but for clay B also the decrease after 6 cycles was significant. The relative decrease in stability after 6 freeze–thaw cycles (the difference between stabilities at 0 and 6 cycles as a percentage of the stability at 0 cycles) was 21% and 17% for clays A and B, respectively, and 55% for silt, indicating that the effect of freezing is more severe on the silt.

Under natural conditions, the number of freeze–thaw cycles can be much higher than in our experiment, especially if diurnal temperature fluctuations are taken into account. The yearly mean number of freeze–thaw cycles (based on daily air temperatures) was 15 in Ås and Nes in the period 1994–2002, with an average duration of 6–9 days for frost periods and 4–5 days for thaw periods (Eggestad, 2003). Diurnal freeze–thaw cycles were more frequent: The number of days with minimum temperatures less than −2 °C and maximum higher than +2 °C is 48 for Ås and 37 for Nes. The number of cycles in surface soil will however be lower than this due to insulating plant residues and snow.

The temperature at freezing has also shown to be of relevance to structural breakdown. For instance, Oztas and Fayetorbay (2002) observed that the effect of freezing actually was more disruptive at −4 °C than at −18 °C.

In further studies of this type, more attention should also be paid to natural conditions for number, duration and temperatures of the frost and thaw periods. There should be no doubt that freeze–thaw cycles should be taken into account when using aggregate stability as an indicator for erodibility during winter periods.

3.3. Water content effect

The Tukey test gave weak evidence for a slight increase in aggregate stability at lower water contents for clay A and silt (Table 3), which corresponds to what other studies have shown (e.g. Perfect et al., 1990; Staricka and Benoit, 1995; Lehrsch, 1998). At visual inspection, the wettest silt was almost like a slurry and very unstable. A similar state of the soil surface can also be expected under field conditions, during snowmelt and/or rainfall on partly frozen soil where the thawed layer is almost water saturated or super-saturated. Under such conditions, the soil will be extremely erosion prone because the thawed soil literally flows away.

However, the confidence intervals were wide and overlapping, and no definitive conclusions could be drawn. Also, when looking at individual freeze–thaw cycles, it seemed that in several cases the stability actually increased with increasing water content. The general lack of consistent trends could be attributed to our methodology. After repacking and wetting, the sieved aggregates adhered to each other. The wetter soil was more consolidated than the drier soil and, therefore, more difficult to separate into the original 1–4 mm fraction, a problem also reported by Bullock et al. (1988). Clay B was more severely affected (extremely smeary/sticky) than clay A and silt, maybe because of the levelling. Hence, this may also explain the insignificant differences in stabilities of clays A and B (Section 3.1). The consolidation process is also a natural phenomenon that can occur under field conditions: Layton et al. (1993) noticed that aggregates from some of their plots consolidated into a highly stable structure during a wet winter.

3.4. Interaction between water content and freezing–thawing

The interaction term (matric potential * number of freeze–thaw cycles) was significant for clays A and B, but not for silt (Table 2). Interaction effects were difficult to separate because of the mentioned problems with determining effects of water content alone. When looking at the different combinations, no clear trends were revealed. The only unambiguous result was that the clay A samples with the lowest water content were not significantly affected by freezing and thawing.

3.5. Treatment effects on aggregate stability measured by wet-sieving

The GLM test showed that both freezing and thawing, water content and interaction between the two had a significant effect on the aggregate stability of clay B (Table 2). The stability of clay B decreased with increasing number of freeze–thaw cycles and also with increasing water content.

The GLM test on the silt with matric potential −0.75 kPa showed a significant decrease in stability with increasing number of freeze–thaw cycles, but there was an increase between 3 and 6 cycles. The relative decrease in stability after 6 cycles was 10% for clay B and 56% for silt.

3.6. Comparison of aggregate stabilities measured by rainfall simulator and wet-sieving

The regression analysis revealed a significant ($p < 0.0001$) exponential relationship between aggregate stabilities measured using rainfall simulator and wet-sieving (Fig. 2). For both clay B and silt, the stability measured by the wet-sieving procedure was higher than the stability measured by rainfall simulator. The relationship appeared however to be different for the two soils studied. On average, the relative difference between stabilities measured by wet-sieving and rainfall simulator was 25% for clay B and 54% for silt, and the difference was significant (Table 2). This suggests that the effect of raindrop impact relative to runoff (represented by wet-sieving) could be more severe for silt than for clay B.

For clay B, the difference at 0 and 1 freeze–thaw cycles was significantly lower than the difference at 3 and 6 cycles (Table 3), indicating that soil that has been frozen several times, is relatively more prone to raindrop impact than to runoff forces. The same trend was not revealed for the silt soil.

The wet-sieving and rainfall simulation methods can be regarded as representing different processes (breakdown by surface runoff and raindrop impact, respectively) and energy levels. The significant relationship between our results from using the two methods indicates that results from one can potentially be used to predict the outcome of the other. The two methods cannot substitute each other until the relationships for different soils, moisture contents, freeze–thaw treatments and aggregate sizes have been investigated in more detail.

4. Conclusions

The results of this study showed that silt had significantly lower aggregate stability than clays A and B. Clays A and B had similar stabilities, even though clay B was artificially levelled, and therefore expected to have lower stability. The

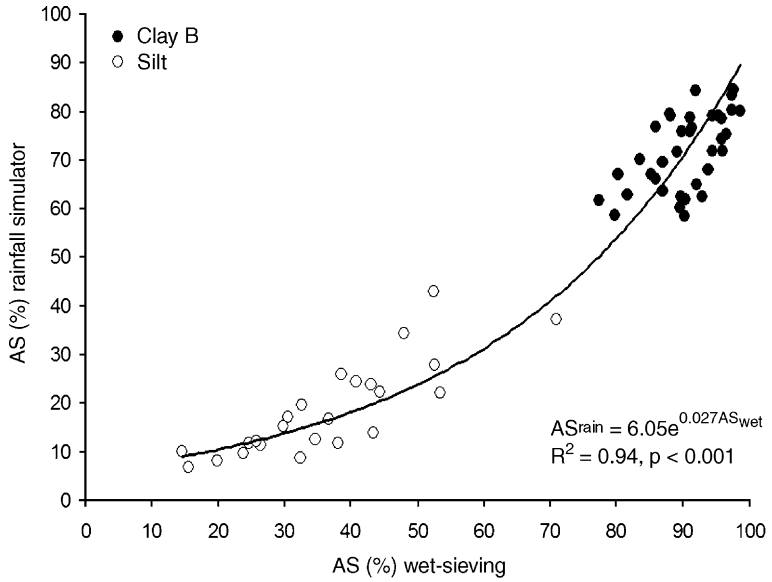

Fig. 2. Relationship between aggregate stability (AS) measured by rainfall simulator and wet-sieving for clay B and silt. FTC = number of freeze–thaw cycles and h = matric potential.

stabilities of all three soils were significantly decreased by increasing number of freeze–thaw cycles. The effect was more detrimental for the silt than for clay A and clay B. Some erosion prone areas in Norway have unstable winters with repeated freezing and thawing, and our results imply that freeze–thaw effects on aggregate stability should be taken more into consideration in future erosion experiments and modelling.

There was no strong or evident effect of water content on the stability, probably due to experimental limitations related to increased aggregate consolidation at high water contents. The method would therefore need further improvement to take initial water content and interaction between water content and freeze–thaw cycles into account.

Comparison of stabilities measured by rainfall simulator and the wet-sieving procedure (representing surface runoff) showed that the former was more detrimental, and the difference between stabilities measured by these methods was larger the more unstable the soil was (silt soil, many freeze–thaw cycles).

Climate change is expected to give more unstable winters with more freezing and thawing events. Combined with more precipitation as rainfall during the winter period both runoff and erosion will probably increase. In this context, more investigations should be put into documenting methods best suited for describing aggregate stability during natural conditions. It is also important to document effects on different soils for giving recommendations about measures to reduce erosion under such conditions.

Acknowledgements

The Norwegian Research Council has provided funding for the research (project number 133494/10). We also acknowledge Rut Skjevdal, Hege Bergheim and Geir Tveiti (Bioforsk), and Dr. Lars Egil Haugen (Dept. of Plant and Environmental Sciences, Agricultural University of Norway—IPM-UMB) for assistance with field and laboratory work, Prof. Trond Børresen (IPM-UMB) and Dr. Gary A. Lehrsch (USDA-ARS Northwest Irrigation and Soils Research Lab.) for general discussions regarding experimental methodologies, and Dr. Live Semb Vestgarden (IPM-UMB) and Heidi A. Grønsten (Bioforsk) for assistance with statistical analyses.

References

Amezketa, E., 1999. Soil aggregate stability: a review. Journal of Sustainable Agriculture 14, 83–151.

Angers, D.A., Carter, M.R., 1996. Aggregation and organic matter storage in cool, humid agricultural soils. In: Carter, M.R., Stewart, B.A. (Eds.). Structure and Organic Matter Storage in Agricultural Soils. Advances in Soil Science. Lewis Publishers, CRC Press Inc., Boca Raton, FL, pp. 193–211.

Bajracharya, R.M., Lal, R., 1992. Seasonal soil loss and erodibility variation on a Miamian silt loam soil. Soil Science Society of America Journal 65, 1560–1565.

Bajracharya, R.M., Lal, R., Hall, G.F., 1998. Temporal variation in properties of an uncropped, ploughed Miamian soil in relation to seasonal erodibility. Hydrological Processes 12, 1021–1030.

Bullock, M.S., Kemper, W.D., Nelson, S.D., 1988. Soil cohesion as affected by freezing, water content, time and tillage. Soil Science Society of America Journal 52, 770–776.

Braskerud, B., 2001. Sedimentation in small constructed wetlands. Retention of particles, phosphorus and nitrogen in streams from arable watersheds. Agricultural University of Norway, Ås. Doctor Scientiarium Thesis 2001: 10.

Dagesse, D.F., Groenevelt, P.H., Kay, B.D., 1997. The effect of freezing cycles on water stability of soil aggregates. In: Iskandar, I.K., Wright, E.A., Radke, J.K., Sharratt, B.S., Groenevelt, P.H., Hinzman, L.D. (Eds.), International Symposium on Physics, Chemistry, and Ecology of Seasonally Frozen Soils, Fairbanks, Alaska, June 10–12, 1997. Special Report 97-10. U.S. Army Cold Regions Research and Engineering Laboratory, Hanover, NH, pp. 177–181.

Edwards, L.M., 1991. The effect of alternate freezing and thawing on aggregate stability and aggregate size distribution of some Prince-Edward-Island soils. Journal of Soil Science 42, 193–204.

Eggestad, H.O., 2003. Værkarakteristika for JOVA-felter (in Norwegian). Jordforsk report 45/03. (25 pp.)

Ellison, W.D., 1945. Some effects of raindrops and surface flow on soil erosion and infiltration. Transactions of American Geophysical Union 24, 452–459.

Kemper, W.D., Rosenau, R.C., 1986. Aggregate stability and size distribution. In: Klute, A. (Ed.), Methods of Soil Analysis: Part 1. Physical and Mineralogical Methods. SSSA Book Series No. 5, Madison, Wisconsin, pp. 425–442.

Kirby, P.C., Mehuys, G.R., 1987. Seasonal variation of soil erodibilities in south-western Quebec. Journal of Soil and Water Conservation 42, 211–215.

Kok, H., McCool, D.K., 1990. Quantifying freeze/thaw-induced variability of soil strength. Transactions of the ASAE 33, 501–511.

Layton, J.B., Skidmore, E.L., Thompson, C.A., 1993. Winter-associated changes in dry-soil aggregation as influenced by management. Soil Science Society of America Journal 57, 1568–1572.

Lehrsch, G.A., 1998. Freeze–thaw cycles increase near-surface aggregate stability. Soil Science 163, 63–70.

Lehrsch, G.A., Jolley, P.M., 1992. Temporal changes in wet aggregate stability. Transactions of the ASAE 35, 493–498.

Lehrsch, G.A., Sojka, R.E., Carter, D.L., Jolley, P.M., 1991. Freezing effects on aggregate stability affected by texture, mineralogy, and organic matter. Soil Science Society of America Journal 55, 1401–1406.

Lundekvam, H., Skøyen, S., 1998. Soil erosion in Norway. An overview of measurements from soil loss plots. Soil Use and Management 14, 84–89.

Marti, M., 1984. Kontinuierlicher Getreidebau ohne Pflug im Südosten Norwegens-Wirkung auf Ertrag, physikalische und chemische Bodenparameter (in German). Department of Soil Fertility and Management. Agricultural University of Norway, ISBN: 82-576-3502-2 (155 pp.).

Minitab Inc.,, 2005. Minitab for Windows. Release 14.2. Minitab Inc., USA.

Mostaghimi, S., Young, R.A., Wilts, A.R., Kenimer, A.L., 1988. Effects of frost action on soil aggregate stability. Transaction of the ASAE 31 (2), 435–439.

Mulla, D.J., Huyck, L.M., Reganold, J.P., 1992. Temporal variations in aggregate stability on conventional and alternative farms. Soil Science Society of America Journal 56, 1620–1624.

Oztas, T., Fayetorbay, F., 2002. Effects of freezing and thawing processes on soil aggregate stability. Catena 52, 1–8.

Perfect, E., Van Loon, W.K.P., Kay, B.D., Groenevelt, P.H., 1990. Influence of ice segregation and solutes on soil structural stability. Canadian Journal of Soil Science 70, 571–581.

Prestvik, O., 1974. Bakkeplanering og vekstvilkår. Bakkeplanering-Aktuelt fra Landbruksdepartementets opplysningstjeneste nr 4, pp. 40–45 (in Norwegian).

Staricka, J.A., Benoit, G.R., 1995. Freeze-drying effects on wet and dry soil aggregate stability. Soil Science Society of America Journal 59, 218–223.

Syversen, N., 2002. Effect of a cold-climate buffer zone on minimising diffuse pollution from agriculture. Water Science and Technology 45, 69–76.

Øygarden, L., 2000. Soil erosion in small agricultural catchments, south-eastern Norway. Doctor Scientiarum Theses 2000:8. Agricultural University of Norway.

Paper III

Kværnø, S.H., Haugen, L.E., 2011. Performance of pedotransfer functions in predicting soil water characteristics of soils in Norway. *Acta Agriculturae Scandinavica Section B – Soil and Plant Science 61*, 264-280.

Acta Agriculturae Scandinavica Section B – Soil and Plant Science, 2011; 61: 264–280

Taylor & Francis
Taylor & Francis Group

ORIGINAL ARTICLE

Performance of pedotransfer functions in predicting soil water characteristics of soils in Norway

SIGRUN HJALMARSDOTTIR KVÆRNØ[1] & LARS EGIL HAUGEN[2]

[1]*Norwegian Institute for Agricultural and Environmental Research, Soil and Environment Division, Ås, Norway,*
[2]*Department of Plant and Environmental Sciences, Norwegian University of Life Sciences, Ås, Norway*

Abstract
Pedotransfer functions (PTFs), predicting the soil water retention curve (SWRC) from basic soil physical properties, need to be validated on arable soils in Norway. In this study we compared the performance of PTFs developed by Riley (1996), Rawls and Brakensiek (1989), Vereecken et al. (1989), Wösten et al. (1999) and Schaap et al. (2001). We compared SWRCs calculated using textural composition, organic matter content (SOM) and bulk density as input to these PTFs to pairs of measured water content and matric potential. The measured SWRCs and PTF input data were from 540 soil horizons on agricultural land in Norway. We used various statistical indicators to evaluate the PTFs, including an integrated index by Donatelli et al. (2004). The Riley PTFs showed good overall performance. The soil specific version of Riley is preferred over the layer specific, as the latter may introduce a negative change in water content with increasing matric potential (h). Among the parameter PTFs, Wösten's continuous PTF showed the overall best performance, closely followed by Rawls&B and Vereecken. The ANN-based continuous PTF of Schaap showed poorer performance than its regression based counterparts. Systematic errors related to both particle size and SOM caused the class PTFs to perform poorly; these PTFs do not use SOM as input, and are therefore inappropriate for soils in Norway, being highly variable in SOM. The PTF performance showed little difference between soil groups. Water contents in the dry range of the SWRC were generally better predicted than water contents in the wet range. Pedotransfer functions that included both SOM and measured bulk density as input, i.e. Wösten, Vereecken and Rawls&B, performed best in the wet range.

Keywords: *Soil water retention, matric potential, comparison, continuous parameter PTF, class PTF, soil texture, organic matter.*

Introduction

Simulation models concerned with water balance, water flow and solute transport in soils require data on soil hydraulic properties like the soil water retention curve (SWRC) and hydraulic conductivity as input. Unfortunately, these data are often difficult, time-consuming and expensive to measure, and are therefore rarely available. For purposes where extensive and spatially variable information on soil hydraulic properties is needed as model inputs, alternative methods for obtaining these data must therefore be used. This applies at a wide range of scales, from site-specific predictions of water and nutrient availability, yield potential and fertilizer requirements in precision agriculture, to, for example, regional water balance predictions for climate modelling.

Pedotransfer functions (PTFs) have been developed for estimating soil hydraulic properties from more readily available and routinely measured properties like particle size distribution, bulk density and organic matter content. Tietje and Tapkenhinrichs (1993) classified PTFs into three groups: Group 1, *point PTFs*, estimate water contents at specific matric potentials (Gupta & Larson, 1979; Rawls & Brakensiek, 1982; Pachepsky et al., 1996; Riley, 1996). Group 2, *functional parameter PTFs*, estimate parameters in a function for the relationship between water content and matric potential, most commonly the van Genuchten (1980) function (Vereecken et al., 1989; Pachepsky et al., 1996; Rajkai et al., 1996; Scheinost et al., 1997; Schaap & Leij, 1998; Wösten et al., 1999; Minasny & McBratney, 2002) or the Brooks and Corey (1964) function (Rawls & Brakensiek, 1989). In the

Correspondence: S.H. Kværnø, Norwegian Institute for Agricultural and Environmental Research, Soil and Environment Division, Frederik A. Dahls vei 20, NO-1432 Ås, Norway. E-mail: Sigrun.kvaerno@bioforsk.no

(Received 30 April 2009; revised 26 April 2010; accepted 28 April 2010)

ISSN 0906-4710 print/ISSN 1651-1913 online
DOI: 10.1080/09064710.2010.490233

studies cited so far continuous input data have been used to produce continuous output values, but another type of PTFs is the class PTFs, which generally provide data values for soil textural classes or similar (Wösten et al., 1999; Schaap et al., 2001). Group 3, *physical model PTFs*, are based on a physical-conceptual approach of the water retention phenomenon (e.g. Arya & Paris, 1981).

The importance of PTF performance becomes evident when applying a functional evaluation, which is a statistical examination of the variability in the outcome of a simulation model when the variability results from uncertainty in the PTFs only (Vereecken et al., 1992). Vereecken et al. (1992) found that prediction errors in hydraulic characteristics accounted for 90% of the variation in moisture supply capacity, while only 10% of the variability resulted from within map unit variability. Gijsman et al. (2003) used predictions from various PTFs as input to a crop model, and found 'a worrisome variability among methods in simulated crop yield'. As with other empirical functions, the PTFs must be used with care outside the region and range of soil characteristics they were developed for because different climatic and geological conditions lead to different soil types. A number of papers deal with evaluation and comparison of the performance of different PTFs by testing the relationship between predicted and measured data statistically (Tietje & Tapkenhinrichs, 1993; Kern, 1995; Wagner et al., 1998; Cornelis et al., 2001; Gijsman et al., 2003; Donatelli et al., 2004; Givi et al., 2004; Wagner et al., 2004; Børgesen & Schaap, 2005).

For soils in Norway, Riley (1996) developed point PTFs, and these are routinely used in the National Soil Survey database at the Norwegian Forest and Landscape Institute for predicting soil hydraulic properties. However, apart from the validation presented by Riley (1996), these PTFs have not been validated on independent datasets. One purpose of this study is therefore to validate the PTFs of Riley (1996) for a wide range of topsoils and subsoils from arable land in Norway. The main disadvantage with the Riley point PTFs is that they are not easily implemented in a simulation model, since parameters in an SWRC function is usually required. We therefore also test the performance of six parameter PTFs.

Materials and methods

The measured data

We assembled the dataset used in this study from soil profile descriptions from the Norwegian Forest and Landscape Institute, and from various research projects at the Norwegian Institute for Agricultural and Environmental Research and the Norwegian University of Life Sciences. The total dataset contains 540 samples for which the water content at different matric potentials and basic soil properties have been measured. Of the 540 samples 186 are from the topsoil, i.e. the A-horizon, the remaining 354 from the subsoil. The samples were collected on agricultural land in different parts of Norway (Figure 1). The soils have formed on marine deposits, brackish flood sediments, fluvial deposits and glacial till, all common parent material for arable soils in Norway. Textural composition of the samples varied from sand to heavy clay (Figure 2). Loam and clay soils with high sand content are not common in Norway, and were therefore sparsely represented in the dataset. The water content has been measured at saturation (0 hPa), −20, −100, −1000 and −15 000 hPa for most samples, and at −5, −50, −500 and −3000 hPa for some samples. The basic soil properties include organic carbon and/or loss on ignition, dry bulk density and particle size distribution, i.e. percentages of gravel, clay, silt and sand, and in some cases also percentages of coarse, medium and fine sand. Gravel content ranged from 0 to 50%, on average 6%. Dry bulk density ranged between 0.6 and 1.9 g cm^{-3}, with mean values 1.3 g cm^{-3} for topsoils and 1.5 g cm^{-3} for subsoils. We calculated soil organic matter (SOM) as either 1.742 (the Van Bemmelen factor; Nelson & Sommers, 1982) times the measured carbon content or, when only loss on ignition (IGNL) was available, by using a pedotransfer function by Riley (1996):

Figure 1. Map of Norway showing regions from which 437 of the 540 soil samples used in this study have been collected. The locations of the remaining 103 samples are unknown.

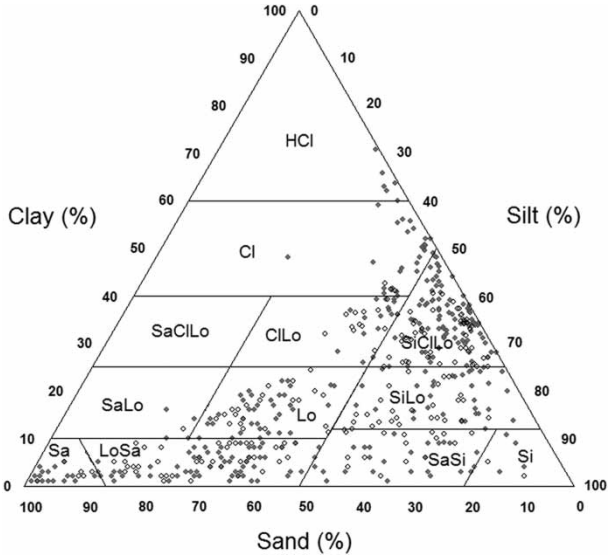

Figure 2. The Norwegian soil texture triangle (Sveistrup and Njøs 1984) with textural composition of soil samples. Abbreviations: H = heavy, Cl = clay, Lo = loam(y), Si = silt(y), Sa = sand(y). Subsoil samples are filled grey circles, topsoil samples open circles.

$$\text{SOM} = 0.74 \times \text{IGNL} - 0.033 \times \text{clay content} - 0.35 \quad \text{for IGNL} < 10 \tag{1}$$

$$\text{SOM} = 0.9 \times \text{IGNL} - 1.2 \quad \text{for IGNL} > 10 \tag{2}$$

SOM then ranged between 0.1% and 17%, with a mean of 4.3% for topsoils and 0.9% for subsoils.

The pedotransfer functions

We used eight sets of PTFs for predicting the soil water content from basic soil physical data; two point PTFs, four continuous functional parameter PTFs and two class functional parameter PTFs. One of the parameter PTFs (Rawls & Brakensiek, 1989) predicts parameters in the Brooks and Corey equation (1964):

$$\theta(h) = \begin{cases} \theta_{(s)}, & \dfrac{h}{h_a} \le 0 \\ \theta_r + (\theta_s - \theta_r) \times \left(\dfrac{h}{h_a}\right)^{-\lambda}, & \dfrac{h}{h_a} > 1 \end{cases} \tag{3}$$

where $\theta(h)$ is the water content at matric potential h, θ_s is the saturated water content, θ_r is the residual water content, h_a is the air entry value or bubbling pressure and λ is the pore-size distribution index. The rest of the PTFs predict parameters in the van Genuchten (1980) equation:

$$\theta(\text{h}) = \theta_\text{r} + (\theta_\text{s} - \theta_\text{r}) \times [1 + (\alpha\text{h})^\text{n}]^{-\text{m}} \tag{4}$$

where α, n and m are shape parameters.

Riley (1996) soil specific PTFs ('Riley SS'). These functions are included in the National Soil Survey Database in Norway. They are point PTFs predicting the water content at matric potentials 0, −20, −100, −1000, −3000 and −15 000 hPa. Different functions are used for soil groups termed Sandy soils, Silty soils, Loamy soils and Clayey soils, based on soil texture. The PTFs were developed for soils from South-east Norway (clay = 0–64%, silt = 36–100%, sand = 0–100%). Required inputs are clay, silt, sand, gravel, dry bulk density and SOM.

Riley (1996) layer specific PTFs ('Riley LS'). Same as in Riley SS, but grouped by topsoil/subsoil instead of soil texture.

Rawls and Brakensiek (1989) PTFs ('Rawls&B'). These are continuous functional parameter PTFs, available, for example, in the simulation model CoupModel (Jansson & Karlberg, 2004), which is often used for simulating water balances in Norway. The PTFs were developed for soils from USA (clay = 5–60%, sand = 5–70%), and predict parameters in the Brooks and Corey equation. Required inputs to the PTFs are clay, sand and porosity. If porosity is not available, it is calculated as 1 – bulk density/2.65 (we used this option), and preferably corrected for entrapped air by an equation including clay, sand, cation exchange capacity of clay and SOM.

Vereecken et al. (1989) PTFs ('Vereecken'). These are continuous functional parameter PTFs predicting parameters in the van Genuchten equation with m restricted to 1. Required inputs are organic carbon (OC), clay, sand and dry bulk density. The PTFs were developed for soils in Belgium (clay = 0–54%, silt = 0–81%, sand = 5.6–98%, OC = 0.01–6.6, bulk density = 1.04–1.23 g cm^{-3}).

Wösten et al. (1999) continuous PTFs ('Wösten'). Continuous functional parameter PTFs predicting parameters in the van Genuchten equation with m restricted to 1–1/n. The θ_r parameter is predicted from soil and layer specific class PTFs (classes: coarse, medium, medium fine, fine, very fine, organic soil). The remaining parameters are predicted using continuous functions. Required inputs are clay, silt, dry bulk density, SOM and layer (topsoil or subsoil). The PTFs were developed for soils in various European countries, primarily in North-western Europe, using data from the HYPRES database.

Wösten et al. (1999) class PTFs ('Wösten CL'). Same as in Wösten, but tabular class PTFs for all van Genuchten parameters instead of continuous PTFs.

Schaap et al. (1998, 2001) continuous PTFs ('Schaap'). Artificial neural network (ANN) based continuous functional parameter PTFs predicting parameters in the van Genuchten equation with m restricted to 1–1/n. Required inputs are clay, silt, sand and dry bulk density. The PTFs were developed for soils in temperate to subtropical climates in North America and Europe (clay = 0–90%, silt = 0–88%, sand = 0–100%). The Rosetta software (Schaap et al., 2001, www.ars.usda.gov/Services/docs.htm?docid=8953), version 1.2, was used to perform the calculations.

Schaap et al. (1998, 2001) class PTFs ('Schaap CL'). Same as in Schaap, but tabular class PTFs instead of continuous PTFs.

As mentioned in the introduction, the main disadvantage with the Riley point PTFs is that they are not easily implemented in a simulation model where SWRC parameters are required as input. A function will then have to be fitted to the predicted water contents, which can be an arduous task if many SWRCs are needed, e.g. in studies of spatial variability. Also, these PTFs do not take into account the interrelation between different points of the SWRC.

The parameter PTFs are particularly useful for modelling purposes when the required input data are available. The parameter PTFs tested here predict parameters in the unimodal van Genuchten and Brooks and Corey functions, and can therefore be inappropriate if the soils under study have multimodal pore size distributions, which is not uncommon for soils with biopores, aggregated loams, morainic soils, unconsolidated sand, solifluction material, etc. (e.g. Othmer et al., 1991; Durner 1994; Mallants et al., 1997; Dexter et al., 2008). We are not aware of PTFs for multimodal functions like that of, for example, Durner (1994), and in any case measured SWRCs contain too few points (typically five or six pairs of water content and matric potential in existing datasets from Norway) to detect multimodality. The individual parameter PTFs have their own strengths and weaknesses: In the Vereecken PTF the parameter m is set to unity, while the closed-form model with m = 1–1/n is often preferred and recommended for simulating flow in the vadoze zone. A recent paper by Weynants et al. (2009) presents a new set of PTFs developed using the same dataset as Vereecken et al. (1989), but with fewer parameters and based on the closed-form expression. Further, Vereecken, along with the continuous Wösten and Schaap PTFs, use bulk density as an input variable, and Rawls&B uses porosity, which can be derived from bulk density. Bulk density is not always readily available, and must then be predicted by a separate PTF, which may introduce additional errors to the SWRC predictions. The Rawls&B PTFs predict parameters in the Brooks and Corey equation. For soils not having a distinct value of the air entry value ($h_a = 1/\alpha$), this function does not offer a satisfactory description of the SWRC in the wet region.

The class parameter PTFs (Wösten CL and Schaap CL) can be useful when input data are scarce, for example, when only textural classes are known, which is often the case if soil maps are the only source of information. One disadvantage of these PTFs is that the same SWRC represents a range of particle size distributions, another that SOM is not included in these PTFs, which is a problem because soils in Norway are highly variable in SOM. Wösten CL provides separate PTFs for topsoils and subsoils, which partly alleviates this problem. The continuous Rawls&B and Schaap PTFs do not include SOM either, but SOM is indirectly represented by bulk density in Schaap and porosity in Rawls&B.

Statistical analyses

For testing the performance of the discrete Riley PTFs, we used the measured data points when comparing measured and predicted water contents, since these PTFs were developed using measured data points. For testing the six functional parameter PTFs, we fitted the van Genuchten equation with restrictions m = 1–1/n and $\theta_r = 1$ volume% to the measured data points using the RETC program (van Genuchten et al., 1991), version 6.02 (www.pc-progress.com/en/Default.aspx?retc-downloads). In this process 60 samples had to be removed from the dataset because they had too few measured data points to obtain a reasonable fit, leaving us with a dataset of 480 samples as opposed to 540 for the Riley PTFs. From the 480 curves fitted to measured data we derived water contents at 15 matric potentials for further comparison with water contents predicted using the PTFs.

We quantified the PTF performance in three ways: (1) For the full dataset, including all available samples with complete matric potentials or matric potential ranges, (2) for four soil groupings with complete matric potential ranges: 'Clay' (clay content $\geq$ 25%), 'Loam' (SaLo + Lo + SiLo from Figure 2), 'Silt' (Si + SaSi from Figure 2) and 'Sand'

(SiSa + Sa from Figure 2) and (3) for specific matric potentials in the case of the Riley point PTFs and specific matric potential ranges in the case of the parameter and class PTFs. The matric potentials for the Riley PTFs corresponded to those that water contents are predicted for by these PTFs, and at the same time for which there were measured water contents for most samples: 0, −20, −100, −1000 and −15 000 hPa. The matric potential ranges for the other PTFs were selected to roughly represent five different areas of the SWRC: (1) gravitational water at and near saturation (0, −5 and −10 hPa), (2) gravitational/capillary water in the moist range (−20, −40 and −60 hPa), (3) capillary water/field capacity range (−100, −200 and −400 hPa), (4) capillary water dry range (−800, −1500 and −2500 hPa) and (5) capillary water approaching wilting point (−4000, −9000 and −15 000 hPa). The range above the wilting point was not considered, as −15 000 hPa was the highest matric potential with available measurements of water content.

Since no single statistic can adequately describe PTF performance, we used several statistics as performance indicators: the modelling efficiency (EF), the Pearson product-moment correlation coefficient (r), relative error (RE), root mean squared error (RMSE) and relative RMSE (RRMSE), given by equations 5 to 9 below:

$$\mathrm{EF} = 1 - \frac{\sum_{i=1}^{n}(\mathrm{P_i} - \mathrm{M_i})^2}{\sum_{i=1}^{n}(\mathrm{M_i} - \overline{\mathrm{M}})^2} \qquad [-\infty, 1] \qquad (5)$$

$$\mathrm{r} = \frac{\sum_{i=1}^{n}(\mathrm{P_i} - \overline{\mathrm{P}})(\mathrm{M_i} - \overline{\mathrm{M}})}{\sqrt{\sum_{i=1}^{n}(\mathrm{P_i} - \overline{\mathrm{P}})^2 \sum_{i=1}^{n}(\mathrm{M_i} - \overline{\mathrm{M}})^2}} \qquad [-1, 1] \qquad (6)$$

$$\mathrm{RE} = \frac{100}{\mathrm{n}} \sum_{i=1}^{n} \frac{\mathrm{P_i} - \mathrm{M_i}}{\mathrm{M_i}} \qquad [-\infty, \infty] \qquad (7)$$

$$\mathrm{RMSE} = \sqrt{\frac{1}{\mathrm{n}} \sum_{i=1}^{n}(\mathrm{P_i} - \mathrm{M_i})^2} \qquad [0, \infty] \qquad (8)$$

$$\mathrm{RRMSE} = 100 \times \frac{\mathrm{RMSE}}{\overline{\mathrm{M}}} \qquad [0, \infty] \qquad (9)$$

$\mathrm{M_i}$ and $\mathrm{P_i}$ are the measured and predicted values respectively, $\overline{\mathrm{M}}$ is the mean of the measured values and $\overline{\mathrm{P}}$ the mean of predicted values. The statistical indicators were evaluated by two approaches, a simple aggregation approach and a more sophisticated integrated approach. The simple approach involved giving rank numbers to the parameters RRMSE, EF, r and RE, and for each PTF the mean rank for the four parameters was calculated. The four parameters were considered to be equally important and not correlated, and thereby given equal weights. The second approach was to combine selected statistical parameters into a fuzzy-based 'integrated index' developed by Donatelli et al. (2004) (see also Fila et al., 2006). The integrated index allows for simultaneous evaluation of different model qualities, and the included statistics are combined to represent three indicator modules: (1) Accuracy, represented by RRMSE and EF – the ability of the model to produce small residuals, (2) Correlation, represented by r – the strength of the linear relationship between predictions and measurements, and (3) Pattern, represented by PI – the absence or presence of systematic patterns in the residuals as a function of the geometric mean particle diameter (d50) and the soil organic carbon content (OC), and also the matric potential (h) if the entire retention curve is considered. The ranges of d50, OC and h are divided into a given number of subranges with the same number of observations within each subrange, and the pattern indices PI are calculated by pair-wise differences between average residuals of each subrange:

$$PI = \max_{a,b=1,\ldots,n;a\neq b}\left|\frac{1}{q_a}\sum_{i=1}^{q_a} R_{ai} - \frac{1}{q_b}\sum_{i=1}^{q_b} R_{bi}\right| \qquad (10)$$

where a and b are two subranges for which differences are calculated, n is the number of subranges, q is number of residuals, and $\mathrm{R_i}$ the residuals in the subranges.

The combination and weighting of all these statistics is based on a fuzzy expert system with decision rules. The indices to be aggregated (RRMSE and EF into the accuracy module, r into the correlation module, PId50, PIOC and PIh into the pattern module, and finally accuracy, correlation and pattern modules into the integrated index) can belong to one of three membership classes: favourable (F), unfavourable (U) or a partial or fuzzy membership between these two thresholds. In the latter case the degree of membership is defined by means of an S-shaped membership function taking any value between 0 and 1, where 0 represents complete non-membership and 1 represents complete membership:

$$s(\chi;\alpha;\gamma)=\begin{cases}0, & \chi\le\alpha\\ 2\left(\dfrac{\chi-\alpha}{\gamma-\alpha}\right)^2, & \alpha\le\chi\le\beta\\ 1-2\left(\dfrac{\chi-\gamma}{\gamma-\alpha}\right)^2, & \beta\le\chi\le\gamma\\ 1, & \chi\ge\gamma\end{cases} \quad (11)$$

where x is the value of the above-mentioned indices, α and γ are the lower and upper bounds (= limits or threshold values – see Table I) respectively, and $\beta = (\alpha+\gamma)/2$. The S-function is flat at values of 0 for $x \le \alpha$ and 1 for $x \ge \gamma$. The complement of this function, 1-S, must also be calculated. The aggregation process involves formulation of fuzzy rules taking the form of 'if ... then ...'statements, exemplified here for the aggregation of RRMSE and EF into the accuracy module:

Rule 1: 'if (RRMSE is F) AND if (EF is F) then (B1 = 0)'

Rule 2: 'if (RRMSE is F) AND if (EF is U) then (B2 = 0.5)'

Rule 3: 'if (RRMSE is U) AND if (EF is F) then (B3 = 0.5)'

Rule 4: 'if (RRMSE is U) AND if (EF is U) then (B4 = 1)'

where B1–B4 are expert weights, i.e. the conclusion of the two premises 'if ... AND if ...' (expert weights for all modules are given in Table I). The expert weight B_i is then multiplied by the 'truth value' (w_i) of a decision rule, which is the minimum among the membership values (m_i) calculated from S and 1–S:

$$w_i = \min(m_1, \ldots, m_n) \qquad n = 1, 2, 3 \quad (12)$$

Further, the sum of the products $B_i w_i$ is divided by the sum of the truth values to obtain the module (or integrated index) value:

$$Module = \frac{\sum_{i=1}^{n} B_i w_i}{\sum_{i=1}^{n} w_i} \quad (13)$$

More details on the integrated index procedure have been presented by Donatelli et al. (2004). We calculated the integrated index using values for expert weights and limits for membership classes as given by Donatelli et al. (2004), see Table I. The pattern indices were calculated by dividing d50, OC and h into five groups.

Results

Performance of the Riley point PTFs

For the full dataset, plots of predicted versus measured water contents for the Riley PTFs are shown in Figure 3. The plots indicate that the PTFs gave fairly good predictions, with a coefficient of determination (R^2) of 0.89 and 0.90 for Riley LS and SS respectively. In terms of modelling efficiency (EF) and correlation coefficient (r), the performance appeared to be quite good and very similar for Riley LS and Riley SS, with EF around 0.90 and r around 0.95 (Table II). The relative error (RE) was positive and approximately 10%, indicating a tendency for

Table I. Limits (F limit and U limit) for membership classes (m1–m3) and expert weights (B) for calculating the integrated index and its modules accuracy, correlation and pattern RC (entire retention curve with different matric potentials) or pattern SW (water contents at specific matric potentials), from Donatelli et al. (2004). The inputs are the indicators RRMSE: relative root mean squared error; EF: modelling efficiency; r = Pearson product-moment correlation coefficient; PIOC: pattern index organic carbon, PId50: pattern index geometric mean particle diameter; and PIh: pattern index matric potential. R1–R8 are decision rules, F and U denote the 'favourable' and 'unfavourable' membership classes respectively.

Indicator	F limit	U limit		R1	R2	R3	R4	R5	R6	R7	R8
RRMSE (%)	≤ 30	≥ 60	m1	F	F	U	U				
EF (-)	≥ 0.5	≤ 0.0	m2	F	U	F	U				
Accuracy			B	0	0.5	0.5	1				
r (-)	≥ 0.9	≤ 0.7	m1	F	U						
Correlation			B	0	1						
PId50 (vol%)	≤ 3	≥ 6	m1	F	F	F	F	U	U	U	U
PIOC (vol%)	≤ 5	≥ 8	m2	F	F	U	U	F	F	U	U
PIh (vol%)	≤ 3	≥ 6	m3	F	U	F	U	F	U	F	U
Pattern RC			B	0	0.4	0.3	0.7	0.3	0.7	0.6	1
PId50 (vol%)	≤ 3	≥ 6	m1	F	F	U	U				
PIOC (vol%)	≤ 5	≥ 8	m2	F	U	F	U				
Pattern SW			B	0	0.5	0.5	1				
Accuracy			m1	F	F	F	F	U	U	U	U
Correlation			m2	F	F	U	U	F	F	U	U
Pattern RC or SW			m3	F	U	F	U	F	U	F	U
Integrated			B	0	0.35	0.15	0.5	0.5	0.85	0.65	1

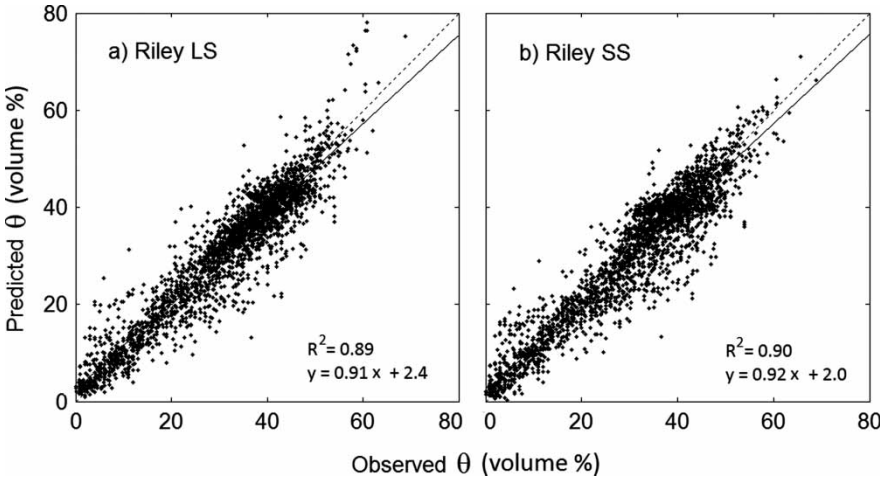

Figure 3. Predicted versus measured volumetric water content (θ) for the layer specific (LS) and soil specific (SS) point pedotransfer functions of Riley (1996). The regression line is solid, the 1:1-line is dotted.

overprediction. The root mean squared error (RMSE) was around 4.5. Correspondingly, the RMSE expressed as a percentage of the measured mean value (RRMSE), was around 15%. The integrated index (Donatelli et al., 2004) offers a means of evaluating PTF performance by different weighting of various statistical indicators and measures of systematic errors. The integrated index was 0 for both PTFs, meaning that the performance was very good (Table II). Pattern indices (PI), which represent the highest absolute difference between mean residuals of five equally sized groups of geometric mean diameter (d50), organic carbon (OC) and matric potential (h), according to equation (10), were favourable or close to it. The mean residuals within five equally sized groups are plotted in Figure 4, and we see that there are no apparent systematic errors.

On average the Riley PTFs overpredicted (positive RE values) water content for all soil groups (Table II). RE was below 3% for Clay and Loam, almost 7% for Silt and around 30% for Sand. RMSE and RRMSE values were lowest for Clay, 3–4 volume% and 10% respectively and highest on Sand, 6.5 volume% and just below 30% respectively. EF and r were high for all soil groups. The PIs were mostly favourable. PIh for Sand was around 5, i.e. close to unfavourable. Accuracy and correlation modules were 0 for both PTFs on all soil groups because RRMSE, EF and r were all favourable. The pattern module was 0.3 for Riley LS and 0.38 for Riley SS because of the relatively high PIh. This resulted in a small value for the integrated index for Sand, and an integrated index of 0 on the other soils.

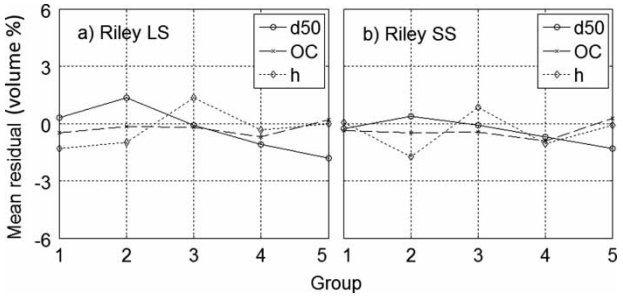

Figure 4. Mean residuals from predictions for the full dataset by the layer specific (LS) and soil specific (SS) point pedotransfer functions of Riley (1996), as a function of five equally sized groups for geometric mean diameter (d50), organic carbon (OC) and matric potential (h).

At saturation and −20 hPa RE was small for both PTFs, and RMSE between 4.6 and 5.6 volume%. RRMSE was 10–14%, EF between 0.37 and 0.48 and r between 0.74 and 0.78. This resulted in low values for the accuracy module, but high values for the correlation module. The pattern module was intermediate because of slight patterns related to particle size, particularly for Riley LS at −20 hPa. The integrated index in this wet range of the retention curve was between 0.16 and 0.34. Performance in the dry range was better; the integrated index was 0 for both PTFs at −100, −1000 and −15 000 hPa. RE (7.6– 32%) and RRMSE values (15–21%) were higher than in the wet range, but RRMSE was still favourable. EF was above 0.7 and thus favourable at these three matric potentials, and r was favourable at −15 000 hPa and nearly favourable at −100 and −1000 hPa. Most of the PIs were also favourable. Riley (1996) validated his own PTFs for specific matric potentials using R^2 as an indicator of PTF performance. He used observations from 124 soil horizons and found that R^2 varied from about 0.5 at saturation to around 0.8 for −100, −1000 and −15 000 hPa. For comparison, the R^2 when validating on our dataset was about 0.6 at saturation, 0.8 at −100 and −1000 hPa and 0.9 at −15 000 hPa (Table II).

Table II. Statistical indicators for PTF performance of the point PTFs Riley LS (layer specific) and Riley SS (soil specific), for the full dataset, for the soil group subset* and for the matric potential subset. For RRMSE, EF, r, and the three pattern indices (PI), bold figures are classified as favourable and underlined figures unfavourable (see Table I). For the integrated index and accuracy, correlation and pattern modules bold figures represent best values.

PTF	RE	RMSE	RRMSE	EF	r	PId50	PIOC	PIh	Accuracy	Correlation	Pattern	Integrated
						Full dataset (n = 2568)						
LS	9.5	4.7	**15**	**0.89**	**0.94**	3.1	**0.94**	**2.7**	**0**	**0**	0.0011	**0**
SS	11	4.5	**15**	**0.9**	**0.95**	**1.7**	**1.2**	**2.6**	**0**	**0**	**0**	**0**
						Clay (n = 1040)						
LS	2.6	3.8	**10**	**0.85**	**0.93**	3.1	**2.4**	**2.8**	**0**	**0**	**0**	**0**
SS	0.49	3.4	**9.4**	**0.88**	**0.94**	**2.3**	**2.1**	**2**	**0**	**0**	**0**	**0**
						Loam (n = 643)						
LS	2.5	3.7	**12**	**0.92**	**0.96**	**2.1**	**2.5**	**2.8**	**0**	**0**	**0**	**0**
SS	1.3	3.9	**13**	**0.91**	**0.96**	**2**	**2.9**	**2**	**0**	**0**	**0**	**0**
						Silt (n = 234)						
LS	6.7	4.7	**15**	**0.92**	**0.96**	**2.7**	**2.8**	3.6	**0**	**0**	0.031	**0**
SS	6.5	4.4	**14**	**0.93**	**0.97**	**2**	**3.1**	3.1	**0**	**0**	**0**	**0**
						Sand (n = 651)						
LS	29	6.6	**29**	**0.83**	**0.93**	**3**	**2.7**	4.9	**0**	**0**	**0.3**	**0.061**
SS	37	6.4	**28**	**0.84**	**0.92**	3.6	**3.2**	5.3	**0**	**0**	0.38	0.1
						θ_s (n = 489)						
LS	−2.7	4.6	**10**	0.48	0.76	4.2	**3.3**	–	**0.0011**	**0.82**	**0.15**	**0.16**
SS	0.67	4.9	**11**	0.42	0.75	5.2	**3.6**	–	0.028	0.89	0.42	0.27
						θ(−20) (n = 495)						
LS	−1.7	5.6	**14**	0.37	0.74	8.3	**3.1**	–	0.066	0.94	0.5	0.34
SS	−3.6	5.2	**13**	0.47	0.78	5.4	**3.3**	–	**0.0045**	**0.67**	**0.46**	**0.26**
						θ(−100) (n = 540)						
LS	16	5.2	**16**	**0.75**	0.88	**2.9**	**1.6**	–	**0**	0.027	**0**	**0**
SS	14	4.8	**15**	**0.79**	0.89	**2.5**	**1.4**	–	**0**	**0.0027**	**0**	**0**
						θ(−1000) (n = 508)						
LS	11	5	**18**	**0.77**	0.89	3.3	**3.4**	–	**0**	0.011	0.0087	**0**
SS	7.6	4.9	**18**	**0.78**	0.89	**1.1**	**3**	–	**0**	**0.0061**	**0**	**0**
						θ(−15 000) (n = 536)						
LS	24	2.6	**21**	**0.92**	**0.96**	**0.93**	**1.1**	–	**0**	**0**	**0**	**0**
SS	32	2.6	**21**	**0.91**	**0.96**	**0.62**	**1.1**	–	**0**	**0**	**0**	**0**

*Clay: clay content ≥ 25%, Loam: clay 10–25% and silt < 50%, or clay 12–25% and silt ≥ 50%, Silt: clay < 12% and silt ≥ 50%, Sand: clay < 10% and silt < 50%.

Performance of the six parameter PTFs

For the full dataset, plots of predicted versus measured water contents for all the continuous PTFs are shown in Figure 5. The plots indicate that the six PTFs gave fairly good predictions, with the coefficient of determination (R^2) mostly above 0.80. The poorest fit is seen for the class PTFs Wösten CL and Schaap CL.

PTF performance statistics for the full dataset are presented in Table III. Mean RE was positive for all PTFs, indicating a tendency for overprediction. RE was highest for Wösten CL (35%), followed by Rawls&B (23%), and lowest for Schaap (4.1%). The accuracy measures EF and r ranged from 0.75 to 0.89 and from 0.89 to 0.95 respectively, the lowest values for the class PTFs and the highest for Wösten and Rawls&B. RMSE varied between 4.4 and 6.8 volume%, lowest for Wösten, and highest for the class PTFs. Correspondingly, RRMSE followed the same ranking, with values between 15 and 24%. By simple aggregation of equally weighted RE, RRMSE, EF and r values, Wösten was ranked as the best PTF, followed by Rawls&B, Vereecken and Schaap, and the class PTFs performing the poorest.

Using the integrated index on the full dataset resulted in a ranking similar to that above. The main

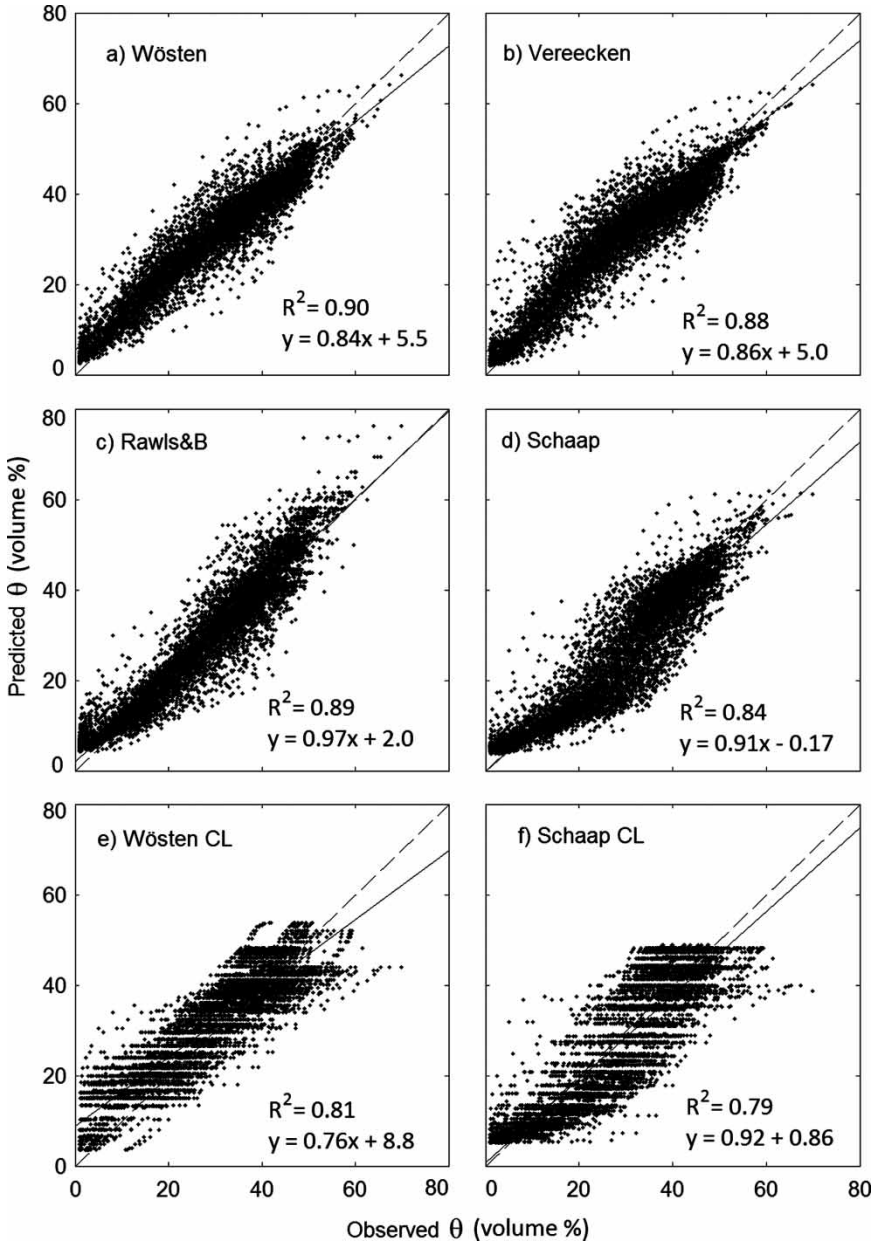

Figure 5. Predicted versus measured volumetric water content (θ) for the parameter pedotransfer functions of Wösten et al. (1999), Vereecken (1989), Rawls and Brakensiek (1989), Schaap and Leij (1998), Schaap et al. (2001). CL denotes class PTFs, the others are continuous PTFs. The regression line is solid, the 1:1-line is dotted.

difference from the previous ranking was that Schaap and Wösten CL changed places, so that Schaap appeared to perform the poorest. The integrated index was zero for Wösten and Rawls&B, indicating very good performance. The poorest value was 0.14 (Schaap) which is also rather good considering that the integrated index has a range between zero and one. For comparison, integrated indices calculated by Donatelli et al. (2004) for the entire retention curve had a similar range of values: 0.0037 to 0.24. The reason for the apparently good performance was that almost all the PTFs we tested had favourable values for RRMSE, EF and r, and consequently accuracy and correlation modules of zero. Thus, the integrated index mainly depended on the value of the pattern module. Pattern indices (PI) are presented in Table III. The mean residuals within each group are plotted in Figure 6. Considering the matric potential ranges, we see from Figure 6a, 6b and 6e that Wösten, Vereecken and Wösten CL on average underpredicted water content close to or at saturation, and overpredicted in the other ranges. Overprediction increased towards the driest range. The PIh values for these PTFs were however close to a favourable limit of 3 volume%. Rawls&B tended to overpredict water content in all matric potential ranges, especially in the wet and moist range (Figure 6c). Schaap generally underpredicted in all ranges, especially in the drier ranges (Figure 6d). Schaap CL overpredicted in the wet and moist ranges and underpredicted in the dry ranges (Figure 6f). Schaap CL had an almost unfavourable pattern index (PIh = 6.0) for Schaap CL, explaining the low ranking of this PTF. PId50 and PIOC were mostly favourable or nearly favourable (Table III). For OC, overprediction seemed to increase with increasing OC for Wösten and Vereecken (Figure 6a and 6b), for Rawls&B and Schaap there was no clear pattern (Figure 6c and 6d), while for the class PTFs mean residuals were higher for low OC and lower for high OC (Figure 6e and 6f). Wösten CL and Schaap CL had the highest PIOC values: 4.9 and 5.6 volume%, respectively. All PTFs tended to overpredict the most (or underpredict the least in case of the Schaap PTFs) for the coarsest soils (d50 group 5 in Figure 6). Systematic errors related to d50 were however not strong, as indicated by the magnitude of PId50. Only Schaap had a nearly unfavourable value for PId50, explaining the higher pattern module value and lower ranking of this PTF.

The PTF performance's dependence on particle size, as indicated by Figure 6, was to some degree also reflected by the mean RE values for individual soil groups (Table III), although these groups are based on classes in the soil textural triangle instead of dividing the dataset into the five equally sized d50-groups ranging from fine to coarse, where each of the five groups may represent several texture classes. For the soil groups the RE values were mostly positive except for Schaap and Schaap CL on Clay and Loam. RE was mostly between $\pm$15% for Clay, Loam and Sand. For Silt it was very high, between 43 and 108%. RMSE varied between 3.6 and 7.8%. It was lowest for Wösten for all soil groups, and also low for Rawls&B and Vereecken, and highest for the class PTFs. The accuracy and correlation measures RRMSE, EF and r were generally favourable for all soils. The most prominent exceptions here were low EF values for the Schaap PTFs on Clay (EF = 0.41 and 0.28 for Schaap and Schaap CL respectively), and somewhat high values for RRMSE for the class PTFs on Sand. Note also that the high RE values on Silt for most PTFs were not reflected in the RRMSE, EF or r statistics, these were all favourable for Silt. Accuracy and correlation modules were close to or equal to zero for all PTFs and soil groups, except for Wösten CL and Schaap CL on Clay. The pattern module was however quite high in several cases, most often due to systematic errors related to the matric potential range, i.e. high PIh values. On Silt, four of the six PTFs had unfavourable values for PIh. PIh was unfavourable for Schaap and Schaap CL on Clay, for Schaap CL on Loam, and for Wösten CL on Sand. Wösten appeared to be the PTF with the least problems with systematic errors. Only on Silt did Wösten come close to an unfavourable value for one of the individual pattern indices. The integrated indices were in the range 0–0.35 on Clay, 0–0.14 on Loam, 0.059–0.11 on Silt and 0.0038–0.30 on Sand. We infer from Table III that Rawls&B, closely followed by Wösten, was the best performing PTF on Clay, while Wösten was the better on Loam and Sand, and Schaap CL the better on Silt. Wösten was ranked second for Silt, the remaining four PTFs had the same integrated index. Schaap CL performed the poorest on Clay, Loam and Sand. The simpler aggregation of statistical indicators gave a slightly different ranking of the PTFs, but the main picture was the same.

PTF performance statistics for the matric potential range subset are presented in Table IV. As we have seen from Figure 6, tendency for over- or underprediction within the ranges varied between the PTFs, but this variation was mostly not reflected by the RE values for each range. RE varied from -3 to 75%, and increased with decreasing degree of saturation. Wösten CL had the highest RE values for four of five matric potential ranges, Rawls&B second highest for these four and highest in the range at and near saturation. Schaap mostly had the lowest relative errors. RMSE varied from 2.9 to 7.3, but there were no apparent differences in RMSE

Table III. Statistical indicators for PTF performance of six continuous parameter PTFs, for the full dataset and for the soil group subset*. For RRMSE, EF, r, and the three pattern indices (PI), bold figures are classified as favourable and underlined figures unfavourable (see Table I). For the integrated index and accuracy, correlation and pattern modules bold figures represent best values.

	Wösten	Vereecken	Rawls&B	Schaap	Wösten CL	Schaap CL
			Full dataset (n = 7200)			
RE	19	15	23	4.1	35	11
RMSE	4.4	4.8	4.8	6.2	6.3	6.8
RRMSE	**15**	**17**	**16**	**21**	**22**	**24**
EF	**0.89**	**0.87**	**0.88**	**0.80**	**0.79**	**0.75**
r	**0.95**	**0.94**	**0.95**	**0.92**	**0.90**	0.89
PId50	3.1	**2.6**	**2.8**	5.8	3.5	**2.6**
PIOC	**1.8**	**3.7**	**1.3**	**2.0**	**4.9**	5.6
PIh	3.1	3.7	**2.3**	4.3	3.8	6.0
Accuracy	**0**	**0**	**0**	**0**	**0**	**0**
Correlation	**0**	**0**	**0**	**0**	**0**	0.0088
Pattern	0.0017	0.045	**0**	0.44	0.096	0.42
Integrated	**0**	0.0014	**0**	0.14	0.0064	0.12
			Clay (n = 2985)			
RE	2.6	5.8	3.3	−15	4.5	−9.5
RMSE	3.6	4.4	3.6	7.0	5.6	7.8
RRMSE	**10**	**13**	**10**	**20**	**16**	**22**
EF	**0.84**	**0.77**	**0.85**	0.41	**0.63**	0.28
r	**0.93**	0.89	**0.93**	**0.91**	0.84	0.84
PId50	**2.7**	3.2	**2.8**	4.0	3.8	4.3
PIOC	**2.7**	5.1	**3.5**	**3.5**	6.4	5.7
PIh	3.7	5.3	**2.1**	9.5	**1.8**	13
Accuracy	**0**	**0**	**0**	0.029	**0**	0.20
Correlation	**0**	0.0025	**0**	**0**	0.17	0.20
Pattern	0.048	0.36	**0**	0.47	0.21	0.57
Integrated	0.0016	0.089	**0**	0.16	0.060	0.35
			Loam (n = 1920)			
RE	11	11	4.2	−8.4	14	−7.1
RMSE	4.7	4.8	5.2	5.1	5.5	5.9
RRMSE	**17**	**17**	**19**	**18**	**20**	**21**
EF	**0.84**	**0.84**	**0.81**	**0.82**	**0.79**	**0.75**
r	**0.93**	**0.93**	**0.94**	**0.93**	**0.91**	**0.90**
PId50	**3.0**	3.5	3.1	4.1	5.0	3.2
PIOC	**2.3**	**3.9**	**2.2**	**1.9**	**4.8**	5.8
PIh	**2.1**	3.6	5.9	5.5	4.1	6.6
Accuracy	**0**	**0**	**0**	**0**	**0**	**0**
Correlation	**0**	**0**	**0**	**0**	**0**	**0**
Pattern	**0**	0.076	0.40	0.45	0.34	0.45
Integrated	**0**	0.0040	0.11	0.14	0.083	0.14
			Silt (n = 705)			
RE	62	43	87	58	108	64
RMSE	4.3	5.1	5.0	6.2	7.6	5.4
RRMSE	**15**	**18**	**18**	**22**	**27**	**19**
EF	**0.93**	**0.90**	**0.90**	**0.85**	**0.77**	**0.88**
r	**0.97**	**0.96**	**0.95**	**0.96**	**0.95**	**0.94**
PId50	**1.0**	**1.5**	**1.1**	**2.1**	**2.6**	3.3
PIOC	**3.2**	**4.5**	**2.2**	**2.9**	5.2	7.5
PIh	5.3	6.3	7.5	6.9	14	**2.8**
Accuracy	**0**	**0**	**0**	**0**	**0**	**0**
Correlation	**0**	**0**	**0**	**0**	**0**	**0**
Pattern	0.35	0.4	0.4	0.4	0.40	**0.29**
Integrated	0.086	0.11	0.11	0.11	0.11	**0.059**
			Sand (n = 1590)			
RE	12	3.8	13	−0.53	57	26
RMSE	5.4	5.6	5.8	5.6	7.7	6.3
RRMSE	**28**	**29**	**30**	**29**	39	33
EF	**0.88**	**0.88**	**0.87**	**0.87**	**0.77**	**0.84**
r	**0.95**	**0.94**	**0.94**	**0.94**	**0.91**	**0.92**
PId50	3.4	5.4	4.5	5.1	4.4	5.8

Table III. (*Continued*).

	Wösten	Vereecken	Rawls&B	Schaap	Wösten CL	Schaap CL
PIOC	**3.9**	**1.7**	**2.8**	**3.2**	**4.4**	6.5
PIh	3.7	3.5	4.7	4.5	9.0	5.0
Accuracy	**0**	**0**	**0**	**0**	0.096	0.0073
Correlation	**0**	**0**	**0**	**0**	**0**	**0**
Pattern	**0.074**	0.30	0.38	0.41	0.53	0.73
Integrated	**0.0038**	0.064	0.10	0.12	0.21	0.30

*Clay: clay content ≥25%, Loam: clay 10–25% and silt <50%, or clay 12–25% and silt ≥50%, Silt: clay <12% and silt ≥50%, Sand: clay <10% and silt <50%.

between matric potential ranges. Thus RRMSE increased with decreasing saturation, like RE. RRMSE values were still favourable (≤ 30%) or close to favourable in most cases. In the driest range RRMSE was between 40 and 50%, i.e. between favourable and unfavourable, for Schaap and the two class PTFs. EF also increased with decreasing saturation, but for EF the higher values are more favourable. Wösten, Vereecken and Rawls&B had the highest EF values (0.70–0.90), in the three drier

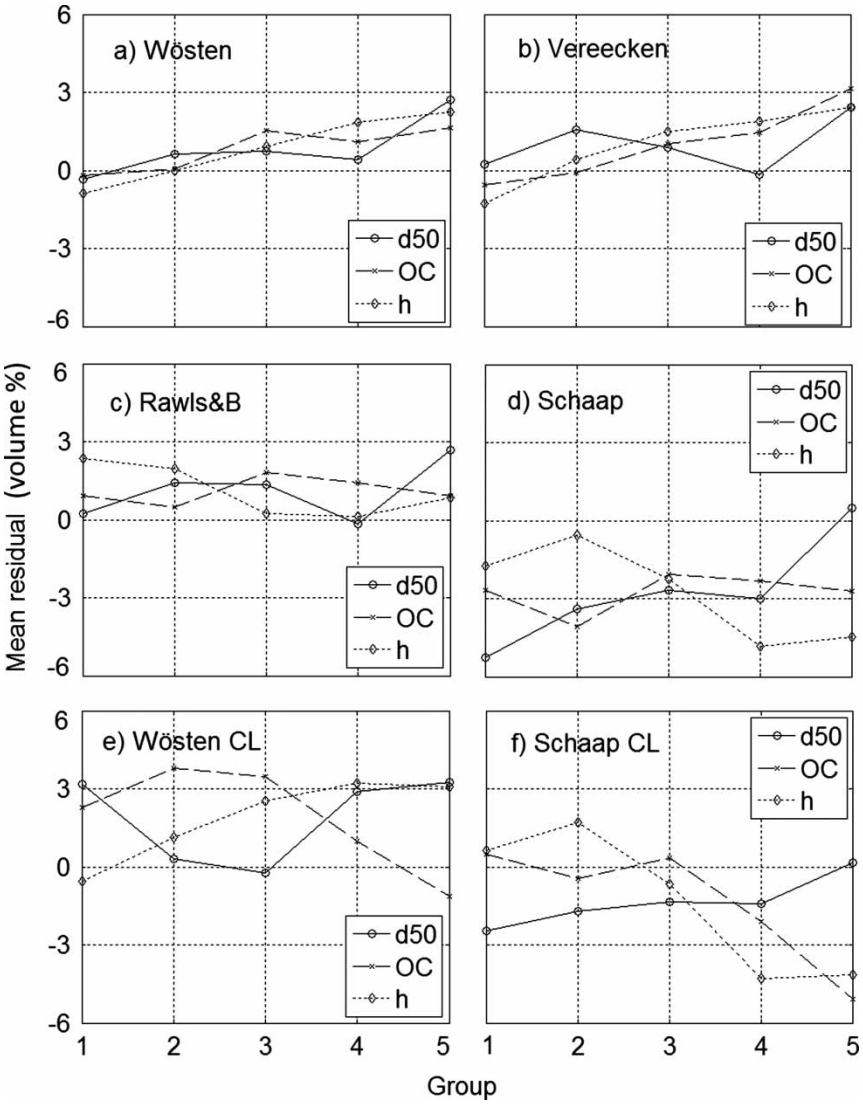

Figure 6. Mean residuals from predictions for the full dataset by the parameter pedotransfer functions of Wösten et al. (1999), Vereecken (1989), Rawls and Brakensiek (1989), Schaap and Leij (1998), Schaap et al. (2001) as a function of five equally sized groups for geometric mean diameter (d50), organic carbon (OC) and matric potential (h). CL denotes class PTFs, the others are continuous PTFs.

Table IV. Statistical indicators for PTF performance of six continuous parameter PTFs, for the matric potential ranges subset (n = 1440 for each range). For RRMSE, EF, r, and the two pattern indices (PI), bold figures are classified as favourable and underlined figures unfavourable (see Table I). For the integrated index and accuracy, correlation and pattern modules bold figures represent best values.

	Wösten	Vereecken	Rawls&B	Schaap	Wösten CL	Schaap CL
			θ_s, $\theta(-5)$, $\theta(-10)$			
RE	−1.2	−2.0	6.3	−3.0	0.7	3.9
RMSE	3.7	3.8	5.4	4.7	6.4	7.0
RRMSE	**9**	**9**	**13**	**11**	**15**	**17**
EF	**0.68**	**0.67**	0.33	0.49	0.05	−0.15
r	0.84	0.84	0.78	0.76	0.37	0.21
PId50	**2.4**	**2.9**	7.4	4.9	7.7	6.9
PIOC	**2.4**	**2.0**	**4.4**	**2.7**	9.5	12
Accuracy	**0**	**0**	0.11	0.00010	0.49	0.5
Correlation	0.19	**0.17**	0.68	0.83	1	1
Pattern	**0**	**0**	0.50	0.37	1	1
Integrated	0.011	**0.0088**	0.31	0.24	0.74	0.75
			$\theta(-20)$, $\theta(-40)$, $\theta(-60)$			
RE	3.6	7.3	8.5	1.4	9.3	8.5
RMSE	5.1	5.6	5.9	5.5	6.6	7.0
RRMSE	**14**	**15**	**16**	**15**	**18**	**19**
EF	**0.65**	**0.59**	**0.55**	**0.60**	0.42	0.36
R	0.81	0.77	0.81	0.79	0.66	0.68
PId50	4.2	6.9	4.1	4.5	7.2	5.0
PIOC	**3.8**	**3.0**	**4.0**	**2.9**	7.9	9.2
Accuracy	**0**	**0**	**0**	**0**	0.025	0.079
Correlation	0.42	0.77	**0.41**	0.57	1	1
Pattern	0.15	0.50	**0.14**	0.25	1	0.88
Integrated	0.084	0.30	**0.076**	0.16	0.50	0.50
			$\theta(-100)$, $\theta(-200)$, $\theta(-400)$			
RE	18	17	20	2.3	34	8.9
RMSE	5.0	5.4	5.3	5.9	6.4	6.0
RRMSE	**17**	**18**	**18**	**20**	**22**	**20**
EF	**0.78**	**0.74**	**0.76**	**0.70**	**0.65**	**0.69**
r	0.89	0.88	0.87	0.86	0.84	0.84
PId50	5.0	3.6	5.8	5.3	7.1	**2.3**
PIOC	**1.7**	**4.3**	**3.5**	**2.2**	5.6	5.6
Accuracy	**0**	**0**	**0**	**0**	**0**	**0**
Correlation	**0.0074**	0.029	0.039	0.075	0.19	0.20
Pattern	0.39	0.040	0.50	0.44	0.54	**0.038**
Integrated	0.10	**0.0022**	0.17	0.14	0.22	0.015
			$\theta(-800)$, $\theta(-1500)$, $\theta(-2500)$			
RE	33	20	35	5.9	57	12
RMSE	4.2	4.6	3.6	7.3	6.1	7.0
RRMSE	**20**	**23**	**18**	36	**30**	34
EF	**0.83**	**0.79**	**0.87**	0.47	**0.63**	**0.51**
r	**0.93**	**0.92**	**0.93**	**0.90**	0.85	0.88
PId50	**2.6**	3.5	3.3	11	6.4	9.2
PIOC	**3.4**	5.1	**3.0**	**3.7**	**2.5**	**4.3**
Accuracy	**0**	**0**	**0**	0.043	**0**	0.021
Correlation	**0**	**0**	**0**	**0**	0.10	0.017
Pattern	**0**	0.030	0.013	0.5	0.5	0.5
Integrated	**0**	0.00061	0.00011	0.18	0.18	0.18
			$\theta(-4000)$, $\theta(-9000)$, $\theta(-15\ 000)$			
RE	41	33	45	14	75	21
RMSE	4.0	4.6	2.9	7.2	6.0	7.1
RRMSE	**27**	31	**19**	48	40	47
EF	**0.81**	**0.75**	**0.90**	0.38	**0.58**	0.41
r	**0.93**	**0.92**	**0.95**	**0.93**	0.83	**0.90**
PId50	**2.1**	3.4	**1.7**	12	6.8	11
PIOC	**4.8**	6.0	**1.7**	**4.6**	**0.9**	**4.8**
Accuracy	**0**	0.00045	**0**	0.41	0.10	0.36
Correlation	**0**	**0**	**0**	**0**	0.23	0.00044
Pattern	**0**	0.16	**0**	0.5	0.5	0.5
Integrated	**0**	0.018	**0**	0.37	0.24	0.34

potential ranges. The class PTFs and Rawls&B had the lowest EF values (-0.15–0.42), in the wet and moist potential ranges. The Schaap PTFs had low EF also in the drier ranges. The correlation measure, r, was mostly above 0.80, but only favourable ($\geq$ 0.90) in the two driest ranges for the four continuous PTFs. r also increased with increasing saturation. The class PTFs had unfavourable r values (0.21–0.68) in the two wetter ranges. From simple aggregation of RE, RRMSE, EF and r it then follows (Table V) that Wösten was the better PTF in the region from saturation to -400 hPa and Rawls&B was the better in the two driest potential ranges. The class PTFs performed poorly in all ranges, Wösten CL the poorest in four out of five cases.

From the above results, the accuracy module of the integrated index ended up with small values in most cases, except for being relatively high for the class PTFs in the wettest range and for the Schaap PTFs in the driest range. The correlation module had high values for all PTFs in the two wetter ranges and low values in the three drier ranges. The pattern module was high in more than half of the cases. The class PTFs and the continuous Schaap PTF had high pattern modules in almost all cases. The other PTFs had relatively high pattern modules in one or two of the potential ranges. High pattern modules generally resulted from high PId50 values. For the class PTFs high PIOC values also contributed to high pattern modules in the wetter ranges. All in all this led to, for the class PTFs, that integrated indices were high (0.5–0.75) in the wet and moist potential ranges and intermediate (0.18–0.34) in the drier ranges, except for a small value (0.015) in the -100 to -400 hPa range for Schaap CL. Integrated indices for the continuous Schaap PTF were intermediate (0.14–0.37) in all ranges. For Wösten, Vereecken and Rawls&B the integrated indices were usually small, $\leq$ 0.1, Vereecken having its lowest performance in the -20 to -60 hPa range and Rawls&B in the saturated range (integrated indices around 0.3 for both). The range for which each and all showed the most similar performance, was in the -100 to -400 hPa range.

Discussion

As we have shown above, summarized in Table V, ranking of the eight PTFs validated in this study depended on how the dataset was subdivided and which statistical indicators were taken into account in the evaluation of performance. Some main features stand out from the analysis:

1. Statistics used and the method of aggregating them indicated slight, but not dramatic differences in ranking of PTFs

Single statistics cannot be recommended as performance indicators, because they can yield quite contradictory results. For example, correlation (degree of linear relationship) can be high, but residuals can still be large. We used two methods for aggregating various statistical indicators. Using an integrated index including weighted statistics and systematic errors produced a slightly different ranking of PTFs than aggregation of equally weighted (or unweighted) basic statistics, but the main picture was quite similar (Table V). There were some incidents where the ranking was clearly different with the two methods. On Loam Wösten shifted from last to third rank with the integrated index, because of fewer problems with systematic errors related to the matric potential than the other PTFs. The same applied to the case where Schaap CL shifted from fifth to first rank for Silt. In the range -20 to -60 hPa Rawls&B shifted from fourth to first rank because this PTF had the lowest pattern module as PId50 and PIOC were low or favourable. The pattern module, and within this the PIh (which is weighted a little higher than PId50 and PIOC), thus determined the ranking when the other statistics were at or close to favourable values. Note here that in our analysis the limits for membership classes and expert weights followed those of Donatelli et al. (2004).

2. The Riley PTFs showed good overall performance

The Riley PTFs performed well in most cases: for the full dataset, the soil group dataset and for matric potentials in the drier range of the SWRC (-100 to $-15\,000$ hPa). Their application was less successful in the wetter range of the SWRC, possibly because bulk density, which is strongly related to soil porosity and thus the saturated water content, is not used as a predictor in the PTFs for θ_s and $\theta(-20)$. From the statistical indicators it appears that the Riley PTFs performed slightly better than the best performing parameter PTFs, as would be expected given that the Riley PTFs were developed using soil samples from similar soils in Norway, and the parameter PTFs were developed using soil samples from other parts of the world. Cornelis et al. (2001), Nemes et al. (2003) and Børgesen and Schaap (2005) have also reported that PTFs that were developed for soils and climatic conditions similar to their own performed best. However, since the performance tests are not directly comparable for the point and parameter PTFs, we will not conclude on it.

Table V. Ranking of PTFs for the full dataset, the soil groups subset* and for the matric potential ranges subset, based on equally weighted basic statistics and on the integrated index. Best PTFs in bold letters.

	Full dataset (n = 7200)
Equal weighting	**Wösten** > Rawls&B > Vereecken > Schaap > Schaap CL > Wösten CL
Integrated index	**Wösten = Rawls&B** > Vereecken > Wösten CL > Schaap CL > Schaap
	Clay (n = 2985)
Equal weighting	**Wösten = Rawls&B** > Vereecken > Wösten CL > Schaap > Schaap CL
Integrated index	**Rawls&B** > Wösten > Wösten CL > Vereecken > Schaap > Schaap CL
	Loam (n = 1920)
Equal weighting	**Wösten = Vereecken** > Rawls&B > Schaap > Schaap CL > Wösten CL
Integrated index	**Wösten** > Vereecken > Wösten CL > Rawls&B > Schaap > Schaap CL
	Silt (n = 705)
Equal weighting	**Wösten** > Vereecken > Rawls&B > Schaap > Schaap CL > Wösten CL
Integrated index	**Schaap CL** > Wösten > Vereecken = Rawls&B = Schaap = Wösten CL
	Sand (n = 1590)
Equal weighting	**Wösten** > Vereecken > Schaap > Rawls&B > Schaap CL > Wösten CL
Integrated index	**Wösten** > Vereecken > Rawls&B > Schaap > Wösten CL > Schaap CL
	θ_s, $\theta(-5)$, $\theta(-10)$ (n = 1440)
Equal weighting	**Wösten** > Vereecken > Schaap > Wösten CL > Rawls&B > Schaap CL
Integrated index	**Vereecken** > Wösten > Schaap > Rawls&B > Wösten CL > Schaap CL
	$\theta(-20)$, $\theta(-40)$, $\theta(-60)$ (n = 1440)
Equal weighting	**Wösten** > Schaap > Vereecken > Rawls&B > Schaap CL > Wösten CL
Integrated index	**Rawls&B** > Wösten > Schaap > Vereecken > Wösten CL = Schaap CL
	$\theta(-100)$, $\theta(-200)$, $\theta(-400)$ (n = 1440)
Equal weighting	**Wösten** > Vereecken > Rawls&B > Schaap > Schaap CL > Wösten CL
Integrated index	**Vereecken** > Schaap CL > Wösten > Schaap > Rawls&B > Wösten CL
	$\theta(-800)$, $\theta(-1500)$, $\theta(-2500)$ (n = 1440)
Equal weighting	**Rawls&B** > Wösten > Vereecken > Schaap = Schaap CL > Wösten CL
Integrated index	**Wösten** > Rawls&B > Vereecken > Schaap = Wösten CL = Schaap CL
	$\theta(-4000)$, $\theta(-9000)$, $\theta(-15\,000)$ (n = 1440)
Equal weighting	**Rawls&B** > Wösten > Vereecken > Schaap > Schaap CL > Wösten CL
Integrated index	**Wösten = Rawls&B** > Vereecken > Wösten CL > Schaap CL > Schaap

*Clay: clay content ≥25%, Loam: clay 10–25% and silt <50%, or clay 12–25% and silt ≥50%, Silt: clay <12% and silt ≥50%, Sand: clay <10% and silt <50%.

The two Riley PTFs, one layer specific, the other soil specific, performed almost equally well, according to the small differences in performance indicators. As these functions provide discrete points, i.e. water contents at specific matric potentials, there is a risk that the PTF predicts a negative change in water content with decreasing matric potential. This problem was more pronounced for Riley LS than for Riley SS. Riley LS predicted $\theta_s < \theta(-20)$ in 89 cases, $\theta(-20) < \theta(-100)$ in 4 cases and $\theta(-100) < \theta(-1000)$ in 19 cases. Riley SS predicted $\theta_s < \theta(-20)$ in 22 cases, and $\theta(-20) < \theta(-100)$ in one case. The problem was generally limited to soils with high clay content, particularly silty clay loam, clay and heavy clay, due to small changes in water content with decreasing matric potential on these soils. The low number of discontinuous predictions with Riley SS indicates that Riley LS is less valid for soils with high clay content, as the majority of samples used for the PTF development were lighter soils, i.e. loam and loamy sand (Riley 1996). Therefore, although the statistical indicators implied little difference in performance between Riley LS and SS, it is recommended that Riley LS is avoided for soils with clay content >25%. It should be taken into account that since the Riley PTFs were developed and validated (by Riley (1996) and in this study) using discrete, measured water contents, possible errors in the measured data in both calibration and validation sets have been neglected. Further, the number of matric potentials (five) for which water contents were compared is rather low, but the PTFs predict water contents at six matric potentials only, and measured data were usually not available at −3000 hPa. The Riley PTFs can be useful for predicting, for example, porosity, field capacity, wilting point and derivatives like plant available water and drainable porosity. For purposes where a more complete SWRC is needed, like model simulations of water flow, these PTFs are of limited usefulness.

3. The regression based continuous parameter PTFs showed the best overall performance, Wösten the best among these

Wösten and Rawls&B were ranked best for the full dataset when considering the integrated index.

Wösten performed well on all soils and in all matric potential ranges, with integrated indices ≤ 0.1. Vereecken and Rawls&B also performed well in most cases. For different soil groups these PTFs had integrated indices around 0.1 or lower. The biggest problem with Vereecken seemed to be the matric potential range between -20 and -60 hPa, with an integrated index around 0.3. A possible explanation for this is that Vereecken uses a restriction of $m = 1$ in the van Genuchten equation, which gives a different slope or curvature of the SWRC in the wet to moist range compared with using $m = 1–1/n$, like we did when fitting van Genuchten to our measured data. In the other ranges Vereecken performed very well. Rawls&B was more problematic near saturation (θ_s to -10 hPa), with an integrated index around 0.3. This can relate to how the calculated value for porosity is adjusted, for example, for entrapped air to obtain θ_s and that SOM is not used as an input in the PTFs. The continuous Schaap PTF, developed by the ANN method, showed poorer performance than its regression based counterparts. ANN PTFs should ideally be trained on a local dataset before application, but this was not possible in the Rosetta software, so this may be one explanation. The lack of SOM as an input may also contribute to poorer performance.

4. The class PTFs often performed poorly because of systematic errors related to particle size and organic matter

On average, looking at the full dataset and the soil group and matric potential subsets, the class PTFs Wösten CL and Schaap CL showed the poorest performance. This relates to the two main disadvantages with these PTFs that has already been mentioned, i.e. that the same SWRC represents a range of particle size distributions and that SOM is not explicitly included in Wösten CL and not included at all in Schaap CL. This explains why systematic errors related to particle size and OC were important in determining the performance. See, for example, the increasing tendency towards underprediction of water content with increasing OC in Figure 6e and 6f, evident from the decrease in mean residuals from groups three to five. Also, the performance of these PTFs was particularly poor in the wet and moist range of the SWRC, an area much influenced by SOM. The performance of Wösten CL appeared to be slightly better than Schaap CL for the full dataset, possibly because Wösten CL provides separate PTFs for topsoils and subsoils. Schaap CL was however ranked best for Silt soils, but this was mainly due to the least problem (among all the PTFs) with systematic errors related to matric potential.

5. PTFs with measured bulk density as input performed the best in the wet and moist SWRC range

Vereecken and Wösten PTFs showed the best performance in the range from saturation to -10 hPa, with integrated indices around 0.01, which implies very good performance, and Schaap and Rawls&B showed intermediate performance. The reason for this ranking is that bulk density is used as input in Vereecken and the continuous Wösten and Schaap PTFs, and we know that the saturated and near-saturated water content strongly depends on bulk density. We used measured bulk density as input, which implies that good predictions of at least the saturated water content should be quite easily obtained with these PTFs. In Rawls&B the porosity is used instead, but when this variable is missing, it is calculated from a simple relationship with bulk density. If measured bulk density had not been available in our dataset, it would have to be predicted by separate PTFs, possibly introducing additional errors and thus reducing the performance in this part of the SWRC. The Riley PTFs showed the approximate same performance (in terms of integrated index) at saturation as the continuous Schaap and Rawls&B PTFs between saturation and -10 hPa, even though bulk density is not used as predictor of saturated water content in the Riley PTFs. SOM is however included as a predictor, and as such appears to be a fairly good alternative because of its influence on bulk density. The poor performance of the class PTFs in this range can partly be explained with bulk density and SOM not being used as input variables.

Acknowledgements

This study was part of the Strategic Institute Programme 'Soil quality and precision agriculture' (project number 143294/I10), funded by the Norwegian Research Council. We thank all who have contributed with data to the database, advice and discussion, technical help on programming and comments to the manuscript: Tore Sveistrup, Trond Knapp Haraldsen, Hugh Riley, Christian Uhlig, Csilla Farkas and Jannes Stolte (all from Bioforsk), Ola Fosheim Grøstad, and two anonymous reviewers.

References

Arya, L. M. & Paris, J. F. (1981). A physicoempirical model to predict the soil moisture characteristic from particle-size distribution and bulk density data. *Soil Science Society of America Journal*, *45*, 1023–1030.

Brooks, R. H. & Corey, A. T. (1964). Hydraulic properties of porous media. *Hydrology Paper No. 3*. Fort Collins: Colorado State University.

Børgesen, C. D. & Schaap, M. G. (2005). Point and parameter pedotransfer functions for water retention predictions for Danish soils. *Geoderma*, *127*, 154–167.

Cornelis, W. M., Ronsyn, J., van Meirvenne, M., & Hartmann, R. (2001). Evaluation of pedotransfer functions for predicting the soil moisture retention curve. *Soil Science Society of America Journal*, *65*, 638–648.

Dexter, A. R., Czyz, E. A., Richard, G., & Reszkowska, A. (2008). A user-friendly water retention function that takes account of the textural and structural pore spaces in soil. *Geoderma*, *143*, 243–253.

Donatelli, M., Wösten, J. H. M., & Belocchi, G. (2004). Methods to evaluate pedotransfer functions. In Ya. Pachepsky & W. J. Rawls (eds.) *Development of pedotransfer functions in soil hydrology. Developments in soil science – Volume 30*, pp. 357–411. Amsterdam: Elsevier.

Durner, W. (1994). Hydraulic conductivity estimation for soils with heterogeneous pore structure. *Water Resources Research*, *30*, 211–223.

Fila, G., Donatelli, M., & Bellocchi, G. (2006). PTFIndicator: An IRENE_DLL-based application to evaluate estimates from pedotransfer functions by integrated indices. *Environmental Modelling & Software*, *21*, 107–110.

Gijsman, A. J., Jagtap, S. S., & Jones, J. W. (2003). Wading through a swamp of complete confusion: how to choose a method for estimating soil water retention parameters for crop models. *European Journal of Agronomy*, *18*, 77–106.

Givi, J., Prasher, S. O., & Patel, R. M. (2004). Evaluation of pedotransfer functions in predicting the soil water contents at field capacity and wilting point. *Agricultural Water Management*, *70*, 83–96.

Gupta, S. C. & Larson, W. E. (1979). Estimating soil water retention characteristics from particle size distribution, organic matter percentage and bulk density. *Water Resources Research*, *15*, 1633–1635.

Jansson, P.-E. & Karlberg, L. (2004). *Coupled heat and mass transfer model for soil-plant-atmosphere systems*. Royal Institute of Technology, Dept. of Civil and Environmental Engineering, Stockholm.

Kern, J. S. (1995). Evaluation of soil water retention models based on basic soil physical properties. *Soil Science Society of America Journal*, *59*, 1134–1141.

Mallants, D., Tseng, P.-H., Toride, N., Timmerman, A., & Feyen, J. (1997). Evaluation of multimodal hydraulic functions in characterizing a heterogeneous field soil. *Journal of Hydrology*, *195*, 172–199.

Minasny, B. & McBratney, A. B. (2002). The Neuro-m method for fitting neural network parametric pedotransfer functions. *Soil Science Society of America Journal*, *66*, 352–361.

Nelson, D. W. & Sommers, L. E. (1982). Total carbon, organic carbon and organic matter. In A. L. Page, R. H. Miller, & D. R. Keeny (eds.), *Methods of Soil Analysis, Part 2 – Chemical and Microbiological Properties*, 2nd edn, 9, Part 2, pp. 539–579. Madison, WI: Agronomy Monograph.

Nemes, A., Schaap, M. G., & Wösten, J. H. M. (2003). Functional evaluation of pedotransfer functions derived from different scales of data collection. *Soil Science Society of America Journal*, *67*, 1093–1102.

Othmer, H., Dierkkrüger, B., & Kutilek, M. (1991). Bimodal porosity and unsaturated hydraulic conductivity. *Soil Science*, *152*, 139–150.

Pachepsky, Ya. A., Timlin, D., & Varallyay, G. (1996). Artificial neural network to estimate soil water retention from easily measurable data. *Soil Science Society of America Journal*, *60*, 727–773.

Rajkai, K., Kabos, S., van Genuchten, M. Th., & Jansson, P.-E. (1996). Estimation of water-retention characteristics from the bulk density and particle-size distribution of Swedish soils. *Soil Science*, *161*, 832–845.

Rawls, W. J. & Brakensiek, D. L. (1982). Estimating soil water retention from soil properties. *Journal of Irrigation and Drainage, Proceedings of the American Society of Civil Engineers*, *108* (IR2), 166–171.

Rawls, W. J. & Brakensiek, D. L. (1989). Estimation of soil water retention and hydraulic properties. In H.J. Morel-Seytoux (ed.) *Unsaturated flow in hydrologic modeling – theory and practice*, pp. 275–300. Boston: Kluwer Academic Publishers.

Riley, H. (1996). Estimation of physical properties of cultivated soils in southeast Norway from readily available soil information. *Norwegian Journal of Agricultural Sciences*, *Supplement No. 25*, 1–51.

Schaap, M. G. & Leij, F. J. (1998). Using neural networks to predict soil water retention and soil hydraulic conductivity. *Soil and Tillage Research*, *47*, 37–42.

Schaap, M. G., Leij, F. J., & van Genuchten, M. Th. (2001). ROSETTA: a computer program for estimating soil hydraulic parameters with hierarchical pedotransfer functions. *Journal of Hydrology*, *251*, 163–176.

Scheinost, A. C., Sinowsky, W., & Auerswald, K. (1997). Regionalization of soil water retention curves in a highly variable soilscape: I. Developing a new pedotransfer function. *Geoderma*, *78*, 129–143.

Sveistrup, T. ,& Njøs, A. (1984). Kornstørrelser i mineraljord, Revidert forslag til klassifisering. *Jord og myr*, *8*, 8–15 (in Norwegian).

Tietje, O. & Tapkenhinrichs, M. (1993). Evaluation of pedotransfer functions. *Soil Science Society of America Journal*, *57*, 1088–1095.

van Genuchten, M. Th. (1980). A closed form equation for predicting the hydraulic conductivity of unsaturated soils." *Soil Science Society of America Journal*, *44*, 892–898.

van Genuchten, M. Th. , Leij, F. J. & Yates, S. R. (1991). *The RETC code for quantifying the hydraulic functions of unsaturated soils, Version 1.0.* EPA Report 600/2-91/065, U.S. Salinity Laboratory, USDA, ARS, Riverside, California, 85 pp.

Vereecken, H., Maes, J., Feyen, J., & Darius, P. (1989). Estimating the soil moisture retention characteristic from texture, bulk density and limited data. *Soil Science*, *148*, 389–403.

Vereecken, H., Diels, J., van Orshoven, J., Feyen, J., & Bouma, J. (1992). Functional evaluation of pedotransfer functions for the estimation of soil hydraulic properties. *Soil Science Society of America Journal*, *56*, 1371–1378.

Wagner, B., Tarnawski, V. R., Wessolek, G., & Plagge, R. (1998). Suitability of models for the estimation of soil hydraulic parameters. *Geoderma*, *86*, 229–239.

Wagner, B., Tarnawski, V. R., & Stöckl, M. (2004). Evaluation of pedotransfer functions predicting hydraulic properties of soils and deeper sediments. *Journal of Plant Nutrition and Soil Science*, *167*, 236–245.

Weynants, M., Vereecken, H., & Javaux, M. (2009). Revisiting Vereecken pedotransfer functions: introducing a closed-form hydraulic model. *Vadose Zone Journal*, *8*, 86–95.

Wösten, J. H. M., Lilly, A., Nemes, A., & Le Bas, C. (1999). Development and use of a database of hydraulic properties of European soils. *Geoderma*, *90*, 169–185.

Paper IV

Kværnø, S.H. & Stolte, J., 2011. Effects of soil physical data sources on discharge and soil loss simulated by the LISEM model. *Submitted to Catena*.

Effects of soil physical data sources on discharge and soil loss simulated by the LISEM model

Sigrun H. Kværnø[1] and Jannes Stolte

Norwegian Institute for Agricultural and Environmental Research, Soil and Environment Division, Fredrik A. Dahls vei 20, N-1432 Ås, Norway

Abstract

The source of input data for soil physical properties may contribute to uncertainty in simulated catchment response. The objective of this study was to quantify the uncertainty in catchment surface runoff and erosion predicted by the physically based model LISEM, as influenced by uncertainty in soil texture and SOM content, and the pedotransfer function derived soil water retention curve, hydraulic conductivity, aggregate stability and cohesion. LISEM was first calibrated using measured data in a sub-catchment, and then run for the whole catchment for a summer storm event with basic input data from two data sources: soil series specific generic data from the national soil survey database, and measured data collected in a grid within the catchment. The measured data were assigned in two ways: mean values per map unit, or stochastic distribution (50 realizations) per map unit. The model was run both for a low risk situation (crop covered surface) and a high risk situation (without crop cover and with reduced aggregate stability and cohesion). The main results were that 1) using non-local database data yielded much higher peak discharge and five to six times higher soil loss than using locally measured data, 2) there was little difference in simulated runoff and soil loss between the two approaches (mean value versus stochastic distribution) to assign locally measured data, 3) differences between the 50 stochastic realizations were insignificant, for both low-risk and high-risk situations, and 4) uncertainty related to input data could result in larger differences between runs with different input data source than between runs with the same input data source but extreme differences in erosion risk. The main conclusion was that inadequate choice of input data source can significantly underestimate or overestimate general soil loss and the effect of measures.

Keywords: variability, uncertainty, surface runoff, erosion, model, soil physical properties

[1] Corresponding author. Tel: +47 406 04 100; fax: +47 63 00 94 10. E-mail address: sigrun.kvaerno@bioforsk.no

1. Introduction

Assessment of environmental risk and possible mitigation strategies relies strongly on the use of simulation models. Modeling of hydrological processes, erosion and nutrient losses is associated with uncertainty. It is considered good practice for risk assessment to quantify uncertainty, because ignoring uncertainty may result in the choice of non-optimal strategies in decision making. There are several sources of uncertainty in the modeling process, including the model conceptualization (i.e. process representation, equations used), the availability, adequacy and quality of input data (meteorological, topographical, soil and crop data), choice of initial and boundary conditions, and parameterization/calibration of the model. The uncertainty related to input data can be composed of: 1) measurement errors, 2) inappropriate sampling procedures, 3) inadequate representation of or failure to account for spatial and temporal variability, 4) erroneous estimates of input values at unsampled locations, 5) aggregation or averaging of values, 6) derivation of input data from maps and remotely sensed data, and 7) prediction of input variables from primary data through use of additional models. By notion variability (heterogeneity, diversity) should be distinguished from uncertainty in that the variability is a property of nature and not reducible through further measurements, while uncertainty (or incertitude) is a property of the risk assessor and in theory reducible. But when variability is not adequately accounted for, it becomes part of the total uncertainty.

Most models dealing with hydrology and nutrient transport require some kind of information about soil physical properties, and in general such models will be highly sensitive to the specification of these parameters (Brown and Heuvelink, 2005). Numerous studies the past couple of decades have documented and quantified spatial and/or temporal variability in soil physical properties. Especially saturated hydraulic conductivity (K_s) has shown to be a highly variable property, varying by several orders of magnitude over short distances (Mallants et al., 1996; Kværnø and Deelstra, 2002; Stolte et al., 2003), and as a calibration parameter it may also be associated with the largest uncertainties (Brown and Heuvelink, 2005). At the same time, K_s is among those parameters to which models are most sensitive (Bonta 1998, Booltink et al. 1998, Davis et al. 1999). Additionally, K_s is very difficult to measure; different measurement techniques and measurement area or volume can yield very different values for K_s (e.g. Banton, 1993; Mohanty et al., 1994). Thus, K_s is associated with high uncertainty in modeling. Also the soil water retention curve (SWRC) has been shown to differ substantially when measured in the field and in the laboratory (Pachepsky et al. 2001).

Despite the vast amount of studies dealing with soil variability, generalization and transferability to other areas is difficult because the extent of variability and its degree of

randomness or spatial and temporal correlation or continuity depends on many factors: which variables we are studying, the natural soil forming factors, anthropogenic influence, and the scale of interest. The practical importance of variability also differs between different studies. Incorporating information about soil variability and increasing the resolution of soil data in simulation models have often shown to improve model predictions (Lathrop et al., 1995; Lilburne and Webb, 2002; Chaplot, 2005). However, some studies have also shown little gain in precision using spatially variable data as compared to mean values or effective parameters (Peck et al. 1977; Lewan and Jansson, 1993). To exemplify: Lindahl et al. (2005) made simulations of outflow and pesticide concentrations on field and catchment scale using both average soil properties (deterministic parameter set) and stochastic assignment of soil properties to account for spatial variability. The stochastic parameter sets successfully predicted the hydrologic response of both field and catchment, while the "average" soil failed to reproduce the small but important summer outflows captured by the stochastic simulation. This also influenced the simulated pesticide leaching. Lundmark and Jansson (2009), on the other hand, concluded that the use of effective parameters for hydraulic properties of three soils was successful in simulating water and chloride dynamics. They noted, however, that this lead to overestimated water and chloride outflow in clay soil, which presented high spatial variability, and of chloride concentration in the sand, which presented high temporal variability. The influence of variability has also shown to differ within single model studies, indicating "threshold behavior". Merz and Plate (1997) simulated catchment runoff, and found that the influence of spatial variability changed with changing storm size. The influence of spatial variability was small for very small and very large events, while the influence was large for medium-sized events. In another study, Vachaud and Chen (2002) illustrated that for areas with high K_s values, there was little loss of information by aggregating input data within a soil class instead of representing the variability, considering the very important gain in terms of input data and time of simulation. Below this threshold, the within soil class variability was important.

At pedon (profile or point) and plot scale soil physical data can be obtained at relatively low cost and effort, while at field and catchment scale data acquisition can be too laborious and costly due to high spatial variability. The most difficult to measure properties, like K_s and SWRC, frequently needs to be derived from other, more easily accessible information by ways of e.g. pedotransfer functions (PTFs). PTFs for SWRC and K_s are abundant in the literature, some popular PTFs being those of Rawls and Brakensiek (1989), Wösten et al. (1999) and Schaap et al. (2001). Statistical evaluation of the uncertainty in

model outputs resulting from using PTFs, sometimes termed a "functional evaluation" of PTFs often show that measured and PTF predicted soil properties result in different model outputs (e.g. Timlin et al. 1996), that poor PTF predictions are inadequate inputs to models (Sobieraj et al. 2001), and that different PTFs result in different model outputs (Gijsman et al. 2003). However, in many cases there are no data available, and there are few or no alternatives to using PTFs. In most areas there will not even be access to the typical inputs to PTFs, like sand, silt, clay and SOM content. The only information available might be geological maps and soil maps. This introduces the additional uncertainties of e.g. map unit delineations, variability within map units, and the problem of assigning values for the necessary input data to the model. Various studies have shown that variability within map units can be considerable (Young et al., 1997; Salehi et al., 2003; Kværnø et al. 2007), and that within-unit variability may be greater than between-unit variability (Lathrop et al., 1995). The significance of map scale, and therefore the level of detail and representation of within map unit variability, has been addressed for example in a recent study by van Dijk et al. (2010), by running two soil erosion models (LISEM and MESALES) for two catchments and two different map scales. In a catchment with relatively homogeneous soil texture the soil map scale had little influence on the simulation results, while in another catchment with larger soil variability the difference between using large scale and smaller scale maps was significant. On the other hand, the use of less detailed class maps can sometimes yield acceptable results because interpolation between sample points and derivation of model data using PTFs tend to result in smoothing, so that the spatial variability in model outputs become less than spatial variability in model inputs (Bechini et al., 2003).

Only a few soil variables can be derived directly from a soil map and the underlying database. For the Norwegian soil maps, produced by the Norwegian Forest and Landscape Institute, this includes texture and organic matter content classes. In Norway soil maps exist only for arable land, which constitutes about 3 % of the total land area. Soil data for other land uses, e.g. for forest, which is an important land use in Norway, are virtually absent all over the country and those data that might exist are not readily accessible. In the soil map for arable land, the map units represent soil series with underlying data for representative or "generic" soil profile data, mostly including horizon names and depths, clay, sand, silt and SOM content. These values are often mean values for profiles of the same type from different locations, from a single profile, or even from a different soil series with similar texture. Where soil samples exist, there are rarely enough samples to reveal spatial correlations, making prediction in unsampled areas difficult. Moreover, spatial correlation parameters

(variogram parameters like sill, range, nugget) will depend on the scale of the sampling scheme (support, spacing and extent), and may not necessarily be representative for the scale of interest in the modeling to be carried out. Using models in Norway indicates relying on the sparse information that exists, making assessment of uncertainty even more important. For many models it will not even be possible to relate this uncertainty to an observed response, because data on e.g. runoff and nutrient concentrations are lacking. But at least uncertainty bounds for the simulated response will be available for use in decision making.

In this paper the main goal is to quantify the uncertainty in surface runoff and erosion predicted by the physically based model LISEM (Limburg Soil Erosion Model (De Roo et al., 1996a, b; Jetten, 2002)), as influenced by uncertainty and variability in soil properties like particle size distribution and SOM content, and the PTF-derived properties SWRC, K, aggregate stability and cohesion. The sub-goals we address are to quantity:

1) differences in simulated surface runoff and soil loss when using locally measured data versus data derived from a soil survey database
2) importance of within map unit variability for simulated surface runoff and soil loss – can a mean value for map units substitute a stochastic approach where information about variability within map units is retained?
3) the effect of input data uncertainty when soil losses are higher, i.e. without crop cover and with reduced aggregate stability and cohesion.

2. Materials and methods

2.1. Site description

This study was carried out in the Skuterud catchment (450 ha), located in the municipalities of Ås and Ski, approximately 30 km south of Oslo, in South-east Norway. The average annual temperature and precipitation in the area (Ås) are 5.3˚C and 785 mm, respectively. The topography of the catchment is undulating. The slopes are the steepest (up to 30 %) in the eastern and western parts, while the central area near the stream is more level. The elevation is 92–150 m above sea level. About 270 ha (60 %) of the catchment area is arable land, 31 % is forest, 2 % forested peatland, and 7 % urban area including roads, houses and gardens (Fig. 1). Coniferous forest (spruce, pine) covers approximately 50 % of the forest area, deciduous forest about 30 % and the rest is mixed coniferous-deciduous (tree maps from Norwegian Forest and Landscape institute). The peat area is dominated by pine. The main crops on arable land are spring and winter sown cereals, sometimes in rotation with oil seed

and potatoes. Grass ley is found on some fields, and a small patch of pasture for cattle is found in the central part of the catchment. Marine deposits, occasionally rich in gravel and stone cover most of the catchment. Coarser marine shore deposits predominate on the fringes of the agricultural land near and in the forested area. The catchment is transected by marginal moraine ridges (‘‘Raet’’) originating from the ice cap melting at the end of the last glaciation. Soil types have only been mapped on arable land in the catchment (Fig. 1).

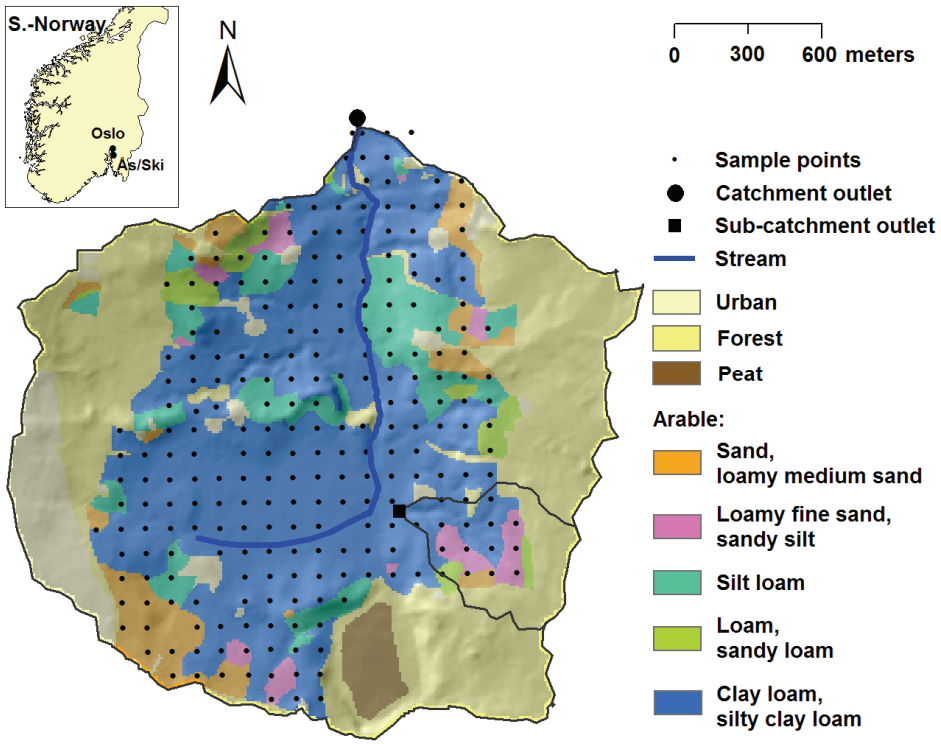

Fig. 1. Land use map and soil map (texture classes only) with hillshade for the Skuterud catchment.

In the soil map reference soil groups are classified according to the World Reference Base for Soil Resources (WRB), and local soil series names are provided. The soil map for Skuterud contains 34 local soil series. The predominating soils in the central and level parts are marine silt loam and silty clay loam soils (WRB Albeluvisols and Stagnosols). The texture of the shore deposits is mainly sand and loamy sand (WRB Arenosols, Umbrisols, Podzols, Cambisols, Gleysols). Lighter clay soils (loam, sandy loam) are found in the transition zones between marine and shore deposits, and on the moraine ridges. The WRB classes with the largest area extent according to the soil map, are Endostagnic Albeluvisols (with textures silt loam and silty clay loam), Luvic Stagnosol (Siltic) (texture silty clay loam) and Endostagnic Cambisol (Dystric) (texture loamy fine sand). Monitoring of discharge and water quality at

the catchment outlet has been carried out since 1993, as part of the Environmental Agricultural Monitoring Programme in Norway, JOVA (Sørbotten, 2011). Suspended sediment, phosphorus and nitrogen are among the water quality variables that are measured. In 2008 monitoring of surface runoff, subsurface drainage discharge, precipitation, and soil water content and temperature was started in a sub-catchment located in the south-eastern part of the catchment (Kramer and Stolte, 2009). This sub-catchment has relatively more sandy soil and forest as compared to the main catchment.

2.2. Model simulations and data handling

2.2.1. Description of the LISEM model

LISEM, The LImburg Soil Erosion Model is a physically based model which simulates hydrology and sediment transport during and immediately after a single rainfall event on a catchment scale. The model was originally developed to test the effect of grass strips and other soil conservation measures on soil loss. LISEM is a spatially distributed model, completely incorporated in a raster geographical information system (PCRaster (Wesseling et al., 1995)). The basic processes incorporated in the model are rainfall, interception, surface storage in micro-depressions, infiltration, vertical movement of water in the soil, overland flow, channel flow, detachment by rainfall and throughfall, transport capacity and detachment by overland flow. Also included is the influence of compaction (e.g. by tractor wheelings), small paved roads and surface sealing, losses of P, NO_3-N and NH_4-N in solution and suspension, and gully formation.

LISEM uses rainfall intensities (alternatively snowmelt intensity) per time interval as the only driving variable. Data from multiple rain gauges can be used for creating spatially distributed rainfall. The rainfall is added to the current water height in each grid cell, taking slope angle into consideration. Interception by vegetation is simulated by regarding the canopy as a simple storage.

Infiltration can be calculated by different sub-models depending on the data availability, objective of the simulation and modeller's level of experience. We used the SWATRE sub-model in our simulations: Infiltration and soil water flow in the soil profile are simulated by solving Richard's equation, which combines Darcy's law and the continuity equation:

$$\partial\theta/\partial t = (\partial[K(h)\times(\partial h/\partial z + 1)])/\partial z \qquad (1)$$

where θ = volumetric soil water content ($m^3\ m^{-3}$), K = hydraulic conductivity ($m\ s^{-1}$), h = matric potential (m), t = time (s), and z = gravitational potential or height above reference level. Values for θ and K at different h are given in tabular form for each horizon in individual soil profiles linked to a soil profile type map.

Amount of suspended sediment is modeled as erosion minus deposition, where erosion is the sum of splash detachment by rain drops (Ds) and flow detachment by runoff (Df). Splash detachment, Ds ($g\ s^{-1}$), is the sum of all splash under and beside plants and splash on ponded and dry areas, and is calculated as:

$$Ds = (2.82/As \times Ke \times exp(-1.48 \times h) + 2.96) \times P \times A \quad (2)$$

where As = aggregate stability (median number of drops to decrease the aggregate by 50 %), Ke = rainfall kinetic energy, including direct throughfall and drainage from leaves ($J\ m^{-2}$), h = the depth of the surface water layer (mm), P = amount of rainfall and throughfall (mm), and A = the surface area over which the splash takes place (m^2). The ability of flowing water to erode is assumed independent of the amount of material it carries and is only a function of the energy expended by the flow. Soil detachment by flow, Df ($kg\ s^{-1}$), and deposition during flow, Dp ($kg\ s^{-1}$), can both be expressed as:

$$D = Y \times (T_c - C) \times V_s \times w \times dx \quad (3)$$

where D = Df or Dp, Y = efficiency factor (-), T_c = transport capacity of the flow ($kg\ m^{-3}$), C = sediment concentration in flow ($kg\ m^{-3}$), V_s = settling velocity of the particles ($m\ s^{-1}$), w = width of flow (m), dx = grid cell size. The efficiency factor Y is 1 when deposition takes place (at $C > T_c$), otherwise it is a function of critical shear velocity (u_c) and the minimum critical shear velocity (u_{min}, $cm\ s^{-1}$), or expressed by the soil cohesion (Coh, kPa):

$$Y = u_{min}/u_c = 1 / (0.89 + 0.56 \times Coh) \quad (4)$$

Both cohesion of soil and plant roots can be accounted for, and are given as maps. Transport capacity of overland flow, T_c ($kg\ m^{-3}$), is a function of stream power (flow velocity × energy slope), critical stream power ($0.4\ cm\ s^{-1}$), material density ($2650\ kg\ m^{-3}$) and coefficients related to the median texture (d50). The net sediment in suspension is transported

between cells with the kinematic wave. Erosion and deposition in channels are treated in the same way as in rills on land.

2.2.2. Model setup, input data and parameters

LISEM is a distributed model that works with square grid cells. We used a grid cell size of 10 × 10 m in our simulations. The model was calibrated for the sub-catchment for a storm event on August 13, 2010. This event was not large enough to produce surface runoff for the whole Skuterud catchment, so a larger storm event on August 19, 2008, was chosen for the simulations for Skuterud. The time step used for the simulations was 30 seconds. The total simulation period was 1000 minutes.

Measured precipitation data were used as driving variable to the model (1 minute resolution). The precipitation data for calibration on the sub-catchment scale were monitored at the same location as runoff from the sub-catchment. The precipitation data used in the simulations for the Skuterud catchment were from a monitoring station operated by the Norwegian Water Resources and Energy Directorate and located in the urban area of the catchment (1 minute resolution). In addition to precipitation time series, the LISEM model requires input in the form of soil hydraulic tables (text files) with hydraulic conductivity and soil water retention as a function of matric potential, and maps with other parameter values. These maps include general catchment maps, land use and vegetation maps, soil surface maps, erosion maps, profile maps, and channel maps. We prepared all these maps using a digital elevation model (DEM), land use map, soil map and stream map (see Fig. 1). The DEM for the Skuterud catchment was made from a topographical map in ArcMap version 9.3. Digital land use and soil maps were available from the Norwegian Forest and Landscape Institute, and a channel map was taken from the topographical map of the area. The soil map covers approximately 94 % of the arable land, while no soil map exists for the other land use types. A geological map was used to determine the superficial deposits in the missing areas, and based on this we assumed the soil series in forest and urban area and in the shore deposit area on arable land to correspond to AJe3, and the soil series in the marine deposit area on arable land to correspond to ERk8. The vegetation maps were derived from the land use map, i.e. with different parameter values for the four land use types forest, urban area, peatland and arable land. The DEM was used to create maps for slope gradients and drainage direction. The soil map combined with the land use map was used to create the profile map, i.e. the map with unique soil profile IDs. This map is linked to a text file containing information about soil profile layer depths and which ID corresponds to which soil hydraulic table. The soil surface

and erosion maps were made by assigning values either to the profile map ID or the land use ID.

In our study, the main focus was on soil physical properties on arable land, i.e. the soil water retention and hydraulic conductivity, and cohesion and aggregate stability. These properties were calculated from textural composition and SOM using pedotransfer functions, as explained in section 2.2.3. For topsoils on arable land the assignment of values for textural composition and SOM followed four approaches:

1. Deterministic approach with generic soil data ("Generic run"): Texture and SOM were derived for soil map units using generic (representative) soil profile data provided by Å. Nyborg (pers. comm.) at the Norwegian Forest and Landscape Institute. A map unit may be a consociation, which consists of one dominating taxon, or it may be a complex, consisting of two or three taxons. We aggregated the soil map by representing complexes by the first taxon (= the dominating taxon) of the map signature. This resulted in a total of 33 main soil series within the catchment boundaries. The generic profiles are currently used as basis for thematic maps developed by the Norwegian forest and landscape institute, like the erosion risk map. The texture and SOM values of these profiles may be a mean value from several profiles, or they may even come from a different soil series with the same texture (Nyborg, pers. comm.).

2. Deterministic approach with measured data, mean values ("Mean run"): Texture and SOM were derived from a set of measured data from the Skuterud catchment. The dataset contained 247 topsoil (0 – 20 cm depth) samples collected in a regular grid with 100 m spacing, located within the area of arable land (Kværnø et al. 2007). On these samples contents of SOM, clay, silt, fine sand, medium sand, coarse sand and gravel had been determined. Data were clustered to appropriate mapped texture classes to facilitate areas with no measured data, with the data from Skuterud to represent the range of and variability in texture variables and SOM within similar map units. We chose to aggregate map units with the same texture class (the map signature contains a code for texture class corresponding to the Norwegian textural triangle by Njøs and Sveistrup (1984)) into "texture map units", as differences in clay, silt and sand content between map units with the same texture class appear to be insignificant in this catchment (Kværnø et al. 2007). The sampled texture data were then linked to the five texture map units they had been collected from. SOM was uncorrelated with the texture variables, and it was therefore assumed that the whole dataset of 247 samples was representative for all texture map units. For each texture map unit a mean value for gravel,

sand fractions, sand, silt and clay content was calculated, and the same mean value for SOM was used for all texture map units. A single run was made with these mean values.

3. Stochastic approach with measured data ("Stochastic runs"): Texture and SOM were derived from the same dataset as in approach 2, and linked to texture map units in the same way. We generated 50 realizations with different values for texture variables and SOM for each grid cell within the texture map units. For most map units there were too few observations to derive probability distributions of the relevant variables, we therefore made a random sampling with replacement directly from the measured data. Since clay, silt and sand must sum up to 100 %, and are clearly inter-correlated, whole sets of clay, silt, fine sand, medium sand, coarse sand and gravel were sampled simultaneously, i.e. all variables for a specific grid cell from the same measured sample point. SOM values were sampled randomly from the probability distribution of SOM from the whole dataset. SOM was positively skewed, and a square root transformation was used to approximate to normality. For computational efficiency we had to put a limitation to the number of combinations of SOM and texture variables. This was done by dividing SOM into 24 classes with an increment of 0.5 and substituting each sampled SOM value by the midpoint of the class the SOM value belonged to.

4. Combined stochastic-deterministic approach based on both measured and generic data ("Combined runs"): Hydraulic properties were assigned as in approach 3, based on measured texture and SOM data (the same 50 realizations as in approach 3), while aggregate stability and cohesion were identical to approach 1, i.e. based on generic soil profile data. This to get an indication of the relative importance of uncertainty in hydrograph and uncertainty in aggregate stability and cohesion.

Approaches 1, 2 and 3 were first run for a state representing summer, i.e. with plant cover, and afterwards for a state representing a "worst case" with bare soil surface and reduced aggregate stability and cohesion, as would be expected after a winter season. In the "worst case" simulations aggregate stability and cohesion were reduced by 25 %, based on the findings of Kværnø and Øygarden (2006), who studied effects of freezing and thawing on aggregate stability. They found that for a clay loam soil in the Skuterud catchment aggregate stability was reduced by approximately 25 % after six cycles of repeated freezing and thawing, as compared to unfrozen soil. Unpublished data from a study conducted by the same

authors showed an equal decrease in cohesion (shear strength) on the same soil after six freeze-thaw cycles.

Due to lack of measured data the topsoil properties in forest, peat land and urban area were kept constant in all simulations. The subsoil (25 – 100 cm depth) properties were also kept constant and limited to a sandy subsoil for the shore deposits and a clay subsoil for the marine deposits, as a study by Stolte et al. (1996) has shown that variability in physical properties of the subsoil is of little importance when using single rain events. The soil series AJe3 and ERk8, for which soil profiles have been excavated in the Skuterud catchment, were chosen to represent shore deposits subsoil and forest and urban topsoil, and marine deposits subsoil, respectively. The whole subsoil was represented by a mean value for textural composition and SOM content, calculated from the horizons with available data. There was no information available for the organic soil in the peat land.

2.2.3. Derivation of hydraulic and physical soil properties from texture variables and SOM

As mentioned, we derived the physical properties of interest from the basic texture and SOM data by using pedotransfer functions:

For the mineral soils we predicted the soil water retention curve (θ(h)) and hydraulic conductivity (K(h)) from the continuous functional parameter PTFs of Wösten et al. (1999), while the class PTFs of Wösten et al. (1999) were used for the peat land. The parameters θ_s (saturated water content), θ_r (residual water content), α, n, m (= 1 – 1/n), l (pore connectivity and tortuosity factor) and K_s (saturated hydraulic conductivity) in the Mualem-van Genuchten equations (equations 5 and 6) are predicted.

$$\theta(h) = \theta_r + (\theta_s - \theta_r)/[1 + (\alpha|h|)^n]^m \quad (5)$$

$$K(h) = K_s \times (1 - (\alpha|h|)^{nm} \times [1 + (\alpha|h|)^n]^{-m})^2/[1 + (\alpha|h|)^n]^{ml} \quad (6)$$

The θ_r parameter is given by soil and layer specific class PTFs (classes: coarse, medium, medium fine, fine, very fine, organic soil), and takes on a value of either 0.01 or 0.025. Required inputs are clay, silt, dry bulk density, SOM and layer (topsoil or subsoil). The PTFs were developed for soils in various European countries, primarily in North-western Europe, using data from the HYPRES database (Wösten et al. 1999). The PTFs for the SWRC have been evaluated by Kværnø and Haugen (2011). The Wösten PTFs were found to represent the SWRC of soils in Norway satisfactorily, and was also ranked best when compared to other

PTFs. The PTFs for K_s have not been validated for soils in Norway since there are too limited data to validate against in Norway.

Bulk density (ρ_b), an input variable to the Wösten PTFs, was predicted using the PTFs of Riley (1996):

$$\rho_b = 1.522 - 0.065 \times SOM + 0.0064 \times gr + 0.0026 \times d - 0.0015 \times si + 0.0022 \times cl \quad \text{for } SOM < 6\ \% \qquad (7)$$

$$\rho_b = (1 - (52.5 + 0.99 \times SOM - 0.0071 \times SOM^2)/100) \times (2.65 - 0.019 \times SOM + 0.0035 \times cl) \quad \text{for } SOM \geq 6\ \% \qquad (8)$$

where gr = gravel, d = depth (cm), si = silt and cl = clay. This PTF was chosen after conducting an evaluation of selected PTFs for bulk density: Riley (1996), Leonaviciute (2000), Manrique and Jones (1991), Kätterer et al. (2006) and Rawls & Brakensiek (1989). The validation material was 186 topsoil samples from the dataset used by Kværnø and Haugen (2011) for evaluating PTFs for the SWRC. The PTFs were ranked according to a combination of five equally weighted statistical indicators: the coefficient of determination (R^2), modeling efficiency (EF), relative root mean squared error (RRMSE), mean absolute error (MAE), and relative error (RE). The Riley PTF (indicator values: $R^2 = 0.50$, EF = 0.47, RRMSE = 11 %, RE = 0.64, and MAE = 0.10), developed for soils in Norway, was ranked best for all indicators, and therefore used in our study.

Shear strength (τ), representing the cohesion parameter in the LISEM model, was measured by a vane shear test in 22 of the sample points in the 100 m spaced grid, to cover the soil texture classes found in the soil map covering the catchment. We used a four blade vane, 2 cm in diameter and 4 cm long. 10 replications were made in each of the 22 locations. From these data we developed a local PTF for shear strength by multiple linear regression with all available basic soil properties: coarse sand (cs), medium sand (ms), fine sand (fs), silt (si), clay (cl), gravel (gr) and SOM. To avoid the problem of colinearity, a principal components analysis on correlations was carried out prior to the regression. The first two principal components (PCs) were used as regressors, as they together explained 85 % of the variation. This resulted in the following equation for τ:

$$\tau = exp(2.96 - 0.0021 \times cs - 0.0025 \times ms - 0.0034 \times fs + 0.0029 \times si + 0.0062 \times cl - 0.0030 \times gr + 0.037 \times SOM) \qquad (9)$$

with $R^2 = 0.37$ and RMSE = 0.27. For PC1 $p < 0.0001$, and for PC2 $p = 0.0004$. An unrealistic relationship between shear strength and SOM was obtained by including three samples with the highest SOM content (SOM > 6 %), and these samples were in the end left out of the analysis to avoid this. However, the equation was still used for the whole range of SOM.

Aggregate stability (AS) was predicted using a PTF developed by Grønsten (2008), based on a dataset from Norway:

$$AS = 91.6 + 3.5 \times SOM - 1.06 \times (fs + si) \quad (10)$$

This PTF was developed for soil that was not tilled, and was therefore the most appropriate of Grønsten's four PTFs since our simulations would be run for a period before harvest of the cereal. The PTF applies to the aggregate fraction 2-6 mm, and the method of aggregate stability measurement was a rainfall simulator (Marti 1984). In this method, aggregate stability can range between 0 and 100 %, which refers to how much soil is left on a sieve after being subjected to artificial rainfall. The aggregate stability required by LISEM is based on another measurement method, so the values from equation (10) had to be converted to correspond to this. Since the maximum possible value for aggregate stability in LISEM is 200, we simply doubled the predicted aggregate stability. Calibration of the model suggested that this approach was fair enough.

2.2.4. Model calibration and final parameterization

LISEM was calibrated using measured surface runoff from the sub-catchment, during an event in August 2010. The area mapped as clay soil was represented by the ERk8 soil type, and the area mapped as sand soil was represented by AJe3. A 30 sec time step was used for the simulations with a total simulation period of 1000 minutes. The spatial resolution was 10 × 10 meters. Vegetation parameters were chosen according to assumptions made for forest dominated by coniferous trees, and for mature cereal. Manning's n for channel was set to 0.01. K_s for the clay soil was multiplied with a factor 4.51 to match the measured hydrograph (Fig. 2). This can be explained by the fact that the PTF for K_s is based on data using the Mualem-van Genuchten equation, which does not take macropore flow into account.

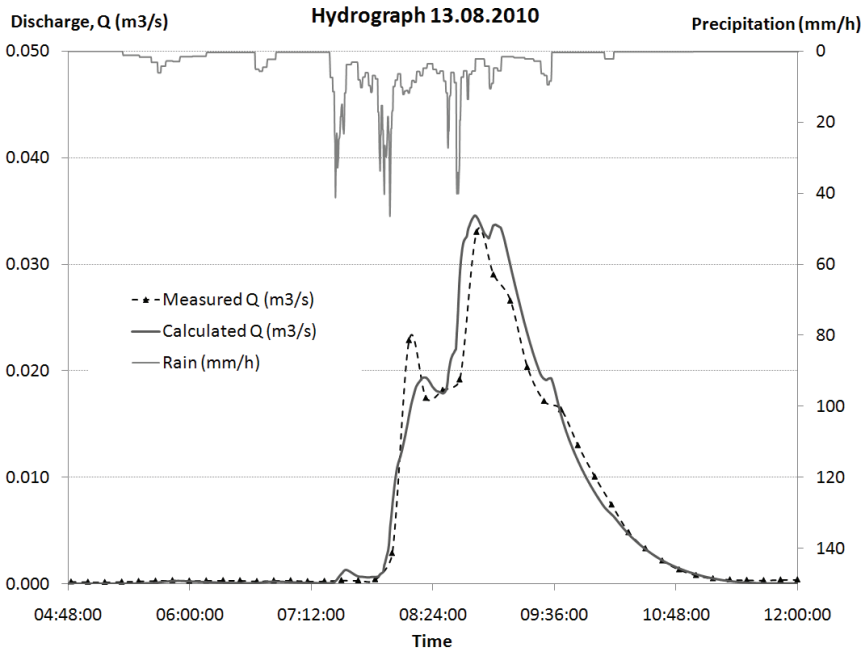

Fig. 2. Observed rainfall and measured and calculated surface discharge in the sub-catchment during the August 13 event 2010.

Table 1. LISEM parameter values used in this study.

Parameter	Stream	Urban	Forest	Peat	Arable
Channel cohesion (chancoh)	15000	-	-	-	-
Channel Manning's n (chanman)	0.04	-	-	-	-
Channel width (chanwidt)	1	-	-	-	-
Slope of channel sides (chanside)	45	-	-	-	-
K_s [1]	-	81.6	81.6	8.0	Variable
Porosity	-	0.444	0.444	0.766	Variable
Depth topsoil	-	25	25	25	25
Initial matric potential (inithead)	-	-300	-300	-300	-300
Random roughness (rr)	-	0.8	3.2	3.2	0.88
Manning's n (n)		2.4	1.2	1.2	0.6
Fraction of soil covered by vegetation (per) [2]	-	0.9	0.9	0.9	1/0
Vegetation height (ch) [2]	-	0.2	7	7	0.7/0
Leaf area index (lai) [2]	-	1.5	6	4	2.5/0
d50 value of the soil (d50)	-	50	50	50	50
Cohesion of bare soil (coh)	-	20	20	158	Variable
Additional cohesion by roots (cohadd)	-	5	10	0.01	1
Aggregate stability (aggr)	-	66	66	190	Variable

[1] Equal to PTF predicted K_s on sand soils, and 4.51 × PTF predicted K_s for clay soil map units, based on calibration.

[2] On arable land these parameters were set to 0 for the "worst case" winter condition simulations.

The Albeluvisols (e.g. the widespread ERk8) in particular can be highly macroporous, so a higher value for K_s can be expected. After calibration the simulated surface runoff matched the measured surface runoff very well (Fig. 2). The parameters for the sub-catchment were assumed to be applicable for the total Skuterud catchment, with the exception of Manning's n for the channel (stream), which finally was set to 0.04 to obtain a realistic runoff peak timing as compared to the measured total discharge (surface runoff + drainage + baseflow) from the catchment. The initial pressure head was set to -5 kPa for the calibration period, based on local measured soil moisture content. During the August 2008 event the soil was drier prior to the event, and a value of -30 kPa was chosen based on soil moisture data from a meteorological station approximately 2 km from the catchment. The calculated soil loss was compared and adapted to measured soil loss by altering the channel cohesion. Measurement was done by sampling the surface water and analyzing the sediment concentration. Calculated soil loss during the high peak of discharge was 0.5 mg/l, in line with the measured value of 0.6 mg/l during that period. The parameters used in the simulations for the Skuterud catchment are presented in Table 1.

3. Results and discussion

3.1. Surface runoff

Fig. 3 shows the simulated surface runoff for the Generic run, the Mean run and for the 50 Stochastic runs, for the summer condition (crop covered soil) simulations. The hydrographs for the Combined runs were not different from the Stochastic runs, so these are not shown or discussed further. The winter scenario is discussed in section 3.4. The main dynamics of the simulated hydrographs (focusing on the summer condition) can be summarized as follows:

Rising limb: For all runs, surface runoff started after 10 minutes, and gradually increased, reaching a small local maximum at approximately 80 minutes. This water may come from the peat land, which has the lowest K_s, but also from arable land with low K_s values. As more rain fell and reached a maximum intensity of 60 mm/h at 224 minutes, runoff increased rapidly. The increase was more rapid for the generic run than for the mean run and stochastic runs. A small drop in runoff occurred during a short period without rain, but runoff increased more rapidly again when rainfall continued. At this point, also the mean run departed from the stochastic run, producing more surface runoff, but less surface runoff than for the generic run. The difference between the 50 stochastic runs was negligible.

Peak discharge: The peak discharge simulated by the different approaches, for both summer and winter conditions, is shown in Fig. 4. Results for the winter condition will be discussed in section 3.3. The main peaks under summer conditions were 1566 l s^{-1} for the Generic run, 1193 l s^{-1} for the Mean run and 1163 l s^{-1} for both the Stochastic and Combined runs. As seen from Fig. 3, the main peak of the summer condition Generic run coincided with the second incident of 60 mm/h rainfall intensity. The time to peak was 344 minutes for runoff, and 338 minutes for the rainfall, i.e. a lag time of 6 minutes. A distinct second runoff peak (1315 l/s) occurred at 458 minutes. There was no rainfall in this period, indicating that this peak came from an area that has a longer lag time from peak rainfall to peak runoff, alternatively as a result of a shift in dominating runoff process (e.g. sheet flow versus channeled flow). On arable land the surface storage capacity was probably reached at different times on different soil, depending on K_s and the SWRC. Additionally, surface storage capacity depends on slope and surface roughness. The dynamics of the Mean run appears different from the generic run in this period. For the Mean run there were two almost equally large peaks (1188 and 1193 l/s) at 420 and 474 minutes respectively, i.e. later than the peak runoff for the Generic run. For the Stochastic runs, the first distinct peak was the largest, and occurred at 414 minutes on average for the 50 runs. The last peak was less prominent than for the Generic and Mean runs. The differences between the 50 Stochastic runs was negligible; the difference between minimum and maximum peak discharge was 19 l s^{-1}, and the the coefficients of variation (CV = standard deviation × 100 %/ mean) for peak discharge and peak time were less than 1 %.

Recession limb: Runoff recession was very similar for the Generic and Mean runs and all the Stochastic runs. There was still some rainfall in the recession period, but apparently not enough water to fill up the storage capacity. The Generic run deviated a little from the Mean and Stochastic runs, with higher runoff in this period.

From the above results, it appears that there is a large difference in the amount of surface runoff simulated using the Generic run compared to the Mean run and Stochastic runs, and also that the runoff dynamics in the period around peak discharge differ between the different approaches. One of the main reasons can be differences in average K_s values between the approaches, as K_s is a parameter for which the LISEM model has shown to be highly sensitive (De Roo et al. 1996b; Stolte et al., 2003). Less surface runoff simulated by the Mean run and Stochastic runs corresponds with higher area-weighted mean K_s (86 and 92 cm d^{-1}, respectively) on arable land in these runs than in the Generic run (59 cm d^{-1}). The air filled porosity at the initial time step of the simulations (difference between θ_s and $\theta(-30)$, the

initial matric potential) may also contribute to the differences in simulated surface runoff, as it determines the total water storage capacity of the soil and thus influences saturation excess overland flow. These differences are small when area weighted means for arable land are considered: 0.14 m^3 m^{-3} for the Generic run and 0.15 m^3 m^{-3} for the Mean run. The results also indicate that there is little gain in terms of reduced uncertainty or increased precision from stochastic assignment of input data to map units in the form of numerous realizations, over the use of a mean value for each map unit, as long as the input data source is the same. This is in agreement with the finding of Vachaud and Chen (2002), who simulated water balance elements and nitrate leaching, and found that for high K_s values (>10 cm d^{-1}) there was little loss of information by aggregating input data within a soil class instead of representing the variability, considering the very important gain in terms of input data and time of simulation. Below a threshold for K_s, the within soil class variability was important. Lindahl et al. (2005) also found that retaining information about variability was important in simulations of outflow and pesticide concentrations, i.e. that the use of average soil properties failed to reproduce the small but important summer outflows captured by the stochastic simulation, while hydrologic response was better predicted using a stochastic assignment of soil properties to account for spatial variability. Merz and Plate (1997), found that the influence of spatial variability on simulated runoff changed with changing storm size. We have only simulated one summer event in this study, events of varying size and in various seasons should also be investigated.

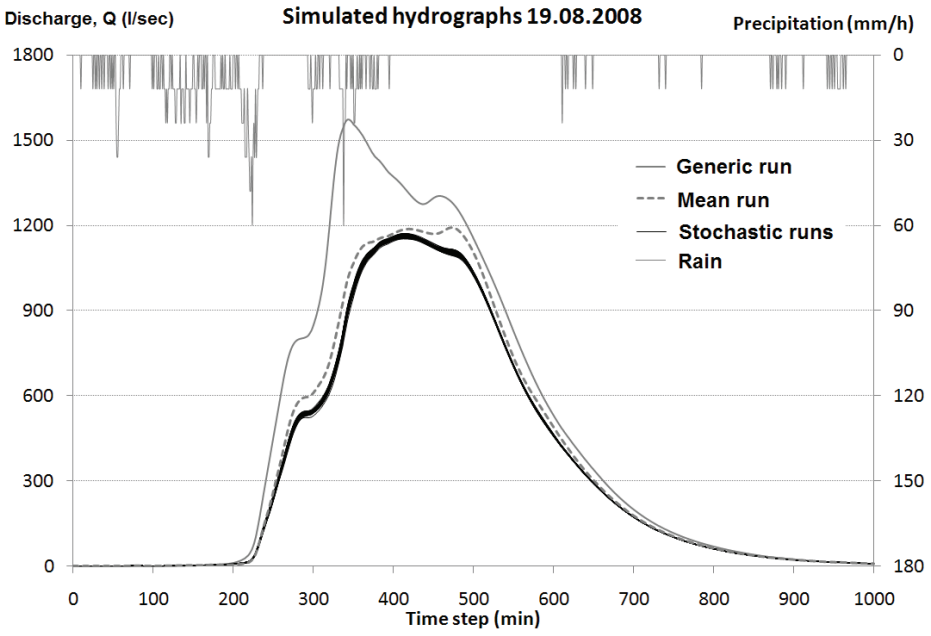

Fig. 3. Simulated surface runoff for the Generic run, Mean run and 50 Stochastic runs, together with rainfall intensity.

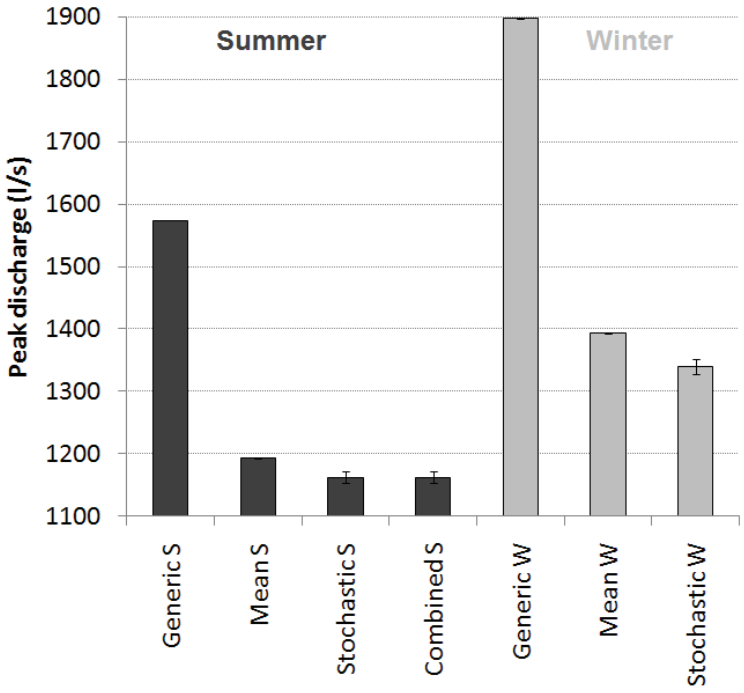

Fig. 4. Simulated peak discharge for the different input data approaches, summer conditions and "worst case" winter conditions. The bars shown for the Stochastic and Combined approach represent the mean of the 50 realizations, while the whiskers represent minimum and maximum values.

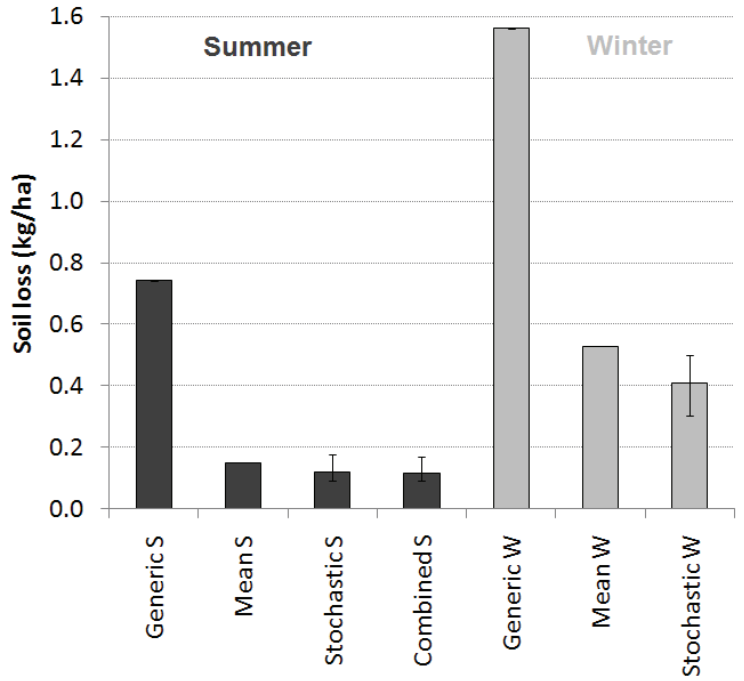

Fig. 5. Simulated soil loss for the different input data approaches, summer conditions and "worst case" winter conditions. The bars shown for the Stochastic and Combined approach represent the mean of the 50 realizations, while the whiskers represent minimum and maximum values.

3.2. Soil loss

The simulated soil loss from the land area (erosion in the main channel not included) is presented for all approaches under summer and winter conditions, in Fig. 5. Results for the winter condition runs are discussed in section 3.4. For summer conditions, soil loss was similar for the Mean run and Stochastic runs: 0.15 and 0.12 kg ha^{-1} respectively. The soil loss simulated in the Generic run was 0.74 kg ha^{-1}, i.e. five times higher than the Mean run and on average 6.2 times higher than the Stochastic runs. The large differences indicate that the choice of input data source is very important. The differences in area weighted mean aggregate stability (70 and 78 (-) for the Generic and Mean runs respectively) and cohesion (28 and 27 kPa for the Generic and Mean runs respectively) between the approaches were small, and suggests that the main reason for more soil loss simulated by the Generic run was that considerably more surface runoff was simulated by this approach (see section 3.1.). The soil loss simulated by the Combined approach, for which the input data were based on measured data for the hydraulic properties and generic data for the aggregate stability and cohesion, was almost the same as for the Stochastic approach (Fig. 5), confirming that the hydraulic properties and consequently the hydrograph was more important in explaining differences between approaches than the aggregate stability and cohesion. Variability between the 50 Stochastic runs was small, with a CV of 12 % for soil loss. The CV for the 50 Combined runs was also 12 %.

3.3. Spatial patterns of simulated runoff and erosion

The influence of soil properties on runoff generating areas in the Generic and Mean runs can be investigated in more detail using runoff maps produced by the model. Fig. 6 shows, for different time steps, the difference between simulated surface runoff of the Generic run and the mean run, as a percentage of the surface runoff for the Generic run: Fig. 6A shows the earliest phase of the rising limb (*186 minutes*), with a large positive difference between the two runs in most of the arable area. In the Mean run only small patches of arable land contributed to surface runoff at this time, while in the Generic run most of the clay map units had started to generate runoff because values for K_s and air filled porosity were lower than in the mean run (Fig. 7A and B). The sand map units, although having lower topsoil K_s values than most of the clay soil map units, did not generate surface runoff at this stage. There are three main explanations for this: Firstly, the K_s in the sand map unit subsoil is higher (77 cm/d) than for the clay map unit subsoil (23 cm/d), allowing for faster redistribution of infiltrating water in the sand map units. Secondly, unsaturated hydraulic conductivity of the

clay is lower than on sand, so unsaturated flow is slower. Thirdly, the air filled porosity available for infiltrating water is higher on the sand map units (area weighted: 0.23 for Generic run, 0.21 for Mean run) compared to the clay map units (area weighted: 0.13 for generic run, 0.14 for mean run). Model output values for soil matric potential for given pixels also show that the topsoil of sand map units reached saturation later than the clay map units.

At *198 minutes* (Fig. 6B), after a considerable rain amount, the sandy soils were still not generating runoff in any of the runs. In the Mean run, an increased area of the silty clay loam map unit started to generate runoff as well, making differences between the Generic and Mean runs smaller. In the Mean run the loam and silt loam map units were not generating runoff at this time, while in the Generic run they did, due to a lower K_s value. The differences between the runs were larger in the valley depressions, i.e. more surface water had collected in the depressions in the Generic run. There were also small patches where the Mean run generated more runoff than the generic run. At *224 minutes* (Fig. 6C), coinciding with a prolonged period of high rainfall intensities, including one minute of 60 mm/h, the differences between the runs became smaller for most of the clay soil areas. In the Mean run the loam, silt loam and sand map units, and even a small area with forest, had started to contribute as well. The Mean run simulated more runoff on loamy medium sand map units than the Generic run because K_s of these units mostly were lower in the Mean run than in the Generic run. One of the silt loam map units in the steepest part of the catchment generated more runoff in the Mean run than in the Generic run at this time step, even if K_s actually was higher in the mean run than in the generic run (211 and 68 cm/d respectively, see also Fig. 7A). At further inspection of additional runoff maps (not shown), it appears that the difference between the runs shift between negative and positive more frequently in this steep area than in the more level areas, a result of more rapid response to rainfall and higher flow velocity in the steep parts. At *338 minutes* (Fig. 6D), coinciding with the second event of 60 mm/h and shortly before the peak runoff of the generic run, differences were increasing relative to at 224 minutes in some areas, while decreasing in others. In some areas the differences were shifting from positive to negative, e.g. for the loamy fine sand map units. At 398 minutes (Fig. 6E), the Mean run simulated more runoff than the Generic run in most of the area, except on loam and loamy medium sand map units, and in the depressions. At *474 minutes* (Fig. 6F), in a period without rainfall and coinciding with the largest peak of the Mean run and the early phase of recession of the Generic run, many parts of the catchment were no longer contributing to runoff. It appears that runoff was now mostly concentrated flow. The Generic

run produced more runoff from the silt loam, loam and loamy medium sand units, and less runoff from the silty clay loam and loamy fine sand units.

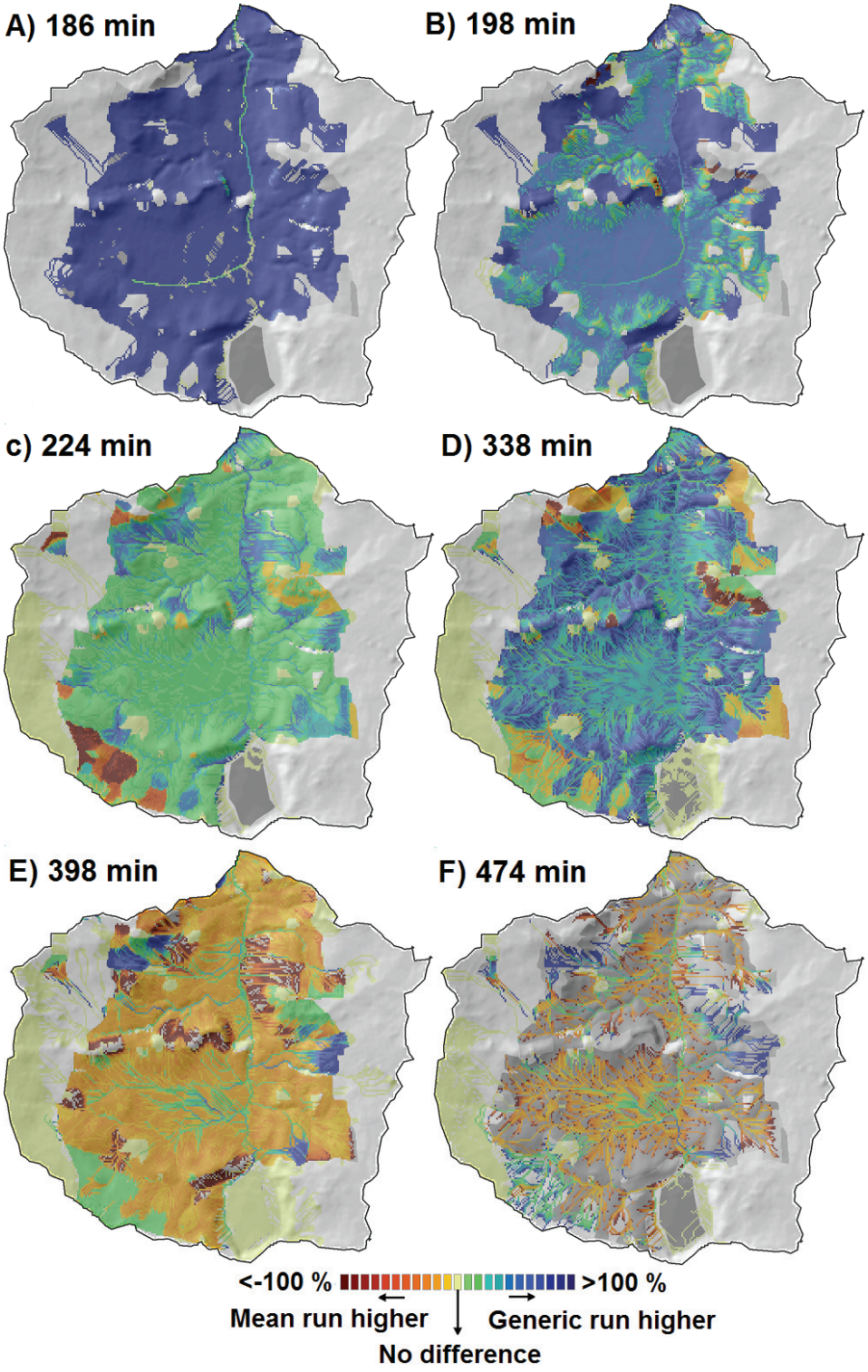

Fig. 6. Spatial distribution of relative difference in simulated surface runoff between the generic run and mean run, at different time steps: Difference = ($runoff_{generic}$ – $runoff_{mean}$) × 100 %/$runoff_{generic}$). With hillshade, and texture map units (darker grey) in background. Grey areas do not generate runoff in any of the runs.

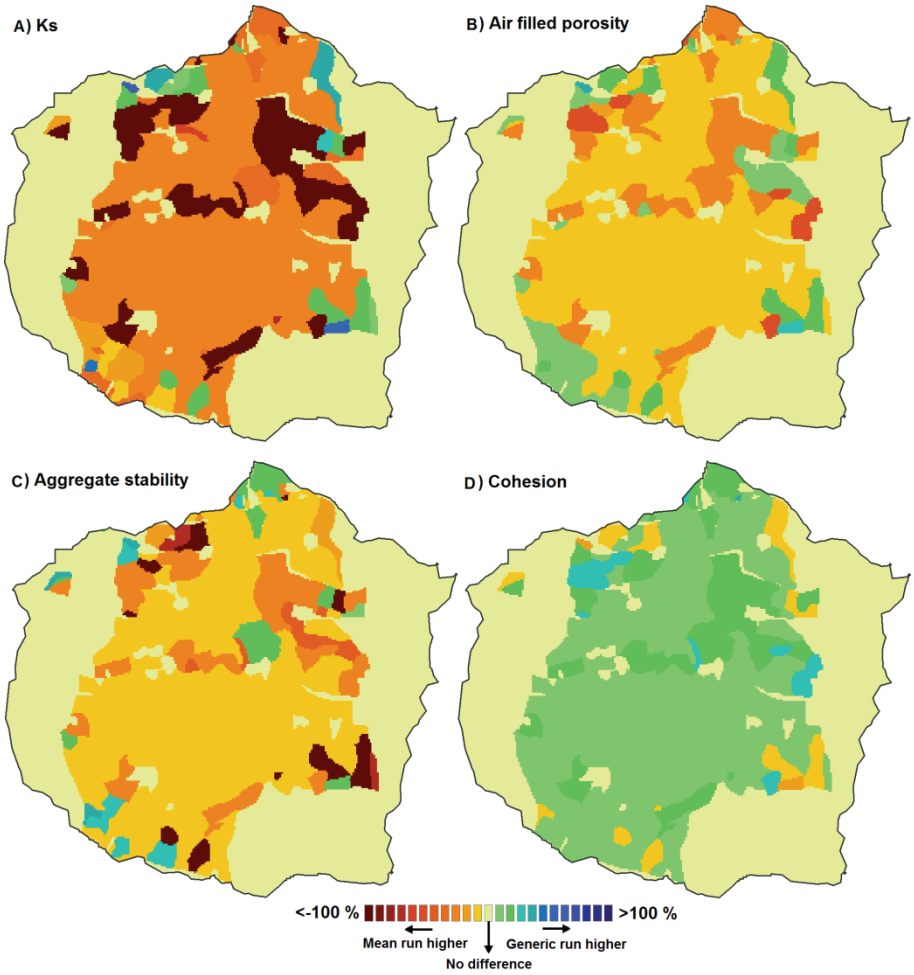

Fig. 7. Spatial distribution of relative difference in soil physical properties between the generic run and mean run: Difference = ($property_{generic}$ – $property_{mean}$) × 100 %/$property_{generic}$).

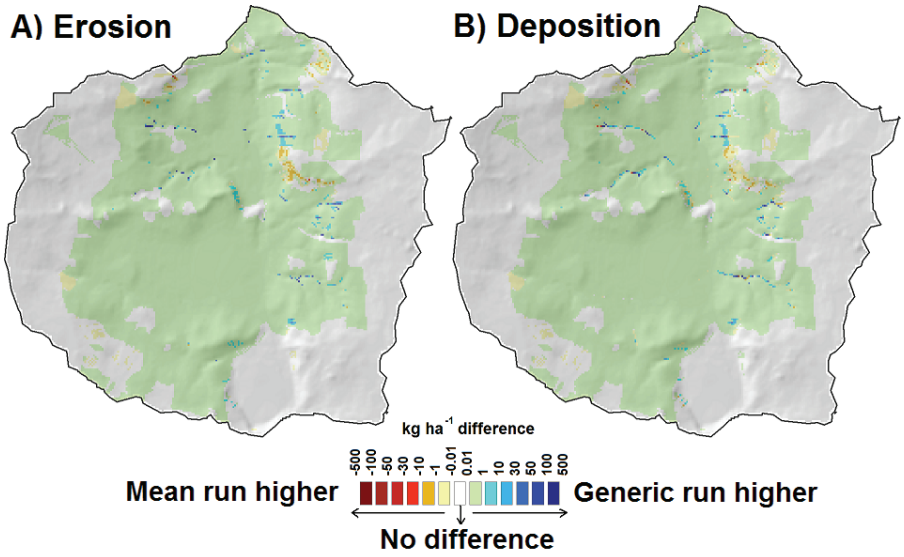

Fig. 8. Spatial distribution of kg ha^{-1} difference in simulated erosion and deposition (absolute value) between the generic run and mean run. With hillshade.

Fig. 8 shows maps for the relative difference in simulated erosion (Fig. 8A) and deposition (Fig. 8B) in the catchment. For most of the arable land area the Generic run simulated more erosion and more deposition than the Mean run. Exceptions were some of the loamy medium sand map units and one of the silt loam map units. The latter corresponds to the highly dynamic steep silt loam area with higher surface runoff for the Mean run, despite higher K_s. In this particular area the cohesion, important for flow detachment, was higher in the Generic run than in the Mean run (Fig. 7D), possibly contributing to higher soil losses here. Aggregate stability, important for splash erosion, was lower in the Generic run than in the Mean run (Fig. 7C), but this variable may be less influential than cohesion because the soil is crop covered and splash erosion accounts for a smaller part of the soil loss. Differences in this steep silt loam area were mostly in the range of 0 – 20 %.

A few studies have shown that the LISEM model, as well as other erosion models, does not simulate spatial erosion patterns adequately (Takken et al., 1999; Hessel et al., 2003, Jetten et al., 2003). Presently this cannot be verified for the Skuterud catchment, as there is little information available on spatial erosion patterns there.

3.4. "Worst case" winter condition runs as compared to summer condition runs

For the winter condition runs the peak discharge was higher than for the summer condition runs because of less interception due to lack of a crop. The simulated peak discharge under winter conditions was 1898 l s^{-1} for the Generic run, 1393 l s^{-1} for the Mean run and 1339 l s^{-1} for the Stochastic runs (Fig. 4). The relative difference between the summer and winter condition was approximately the same for all approaches (winter peak discharge 1.2 times the summer peak discharge), but the absolute difference was large: 323, 200 and 177 l s^{-1} for the Generic, Mean and Stochastic runs, respectively. The simulated peak time was some minutes earlier for the winter condition runs than for the summer condition runs, i.e. 14 minutes earlier for the Generic and Mean runs, and 7 minutes earlier for the Stochastic runs. As for the summer condition runs, the difference between the 50 Stochastic runs was negligible, with a difference of 23 l s^{-1} between minimum and maximum peak discharge, and a CV of less than 1 % for both peak discharge.

The simulated soil loss was considerably higher for the winter condition runs than for the summer condition runs (Fig. 5). The simulated soil loss was 0.53 kg ha^{-1} for the Mean run, 0.41 kg ha^{-1} for the Stochastic runs and 1.6 kg ha^{-1} for the Generic run. The CV for the Stochastic runs was 8.1 %, indicating that the variability between runs was slightly lower than for the summer condition runs (CV = 12 %, section 3.2.). On the other hand, absolute

differences between minimum and maximum values were considerably higher for the winter condition: 0.20 kg ha^{-1} as compared to 0.08 kg ha^{-1} for the summer condition.

The absolute and relative differences between approaches and summer/winter conditions are presented in Table 2 to illustrate that the uncertainty related to input data source (approach) can be larger than the difference in soil loss for extremes with respect to erosion risk (summer/winter condition).

The ratio of soil loss under summer conditions to soil loss under winter conditions was approximately 0.5 for the Generic run, and approximately 0.3 for the Mean and Stochastic runs. Lundekvam (2007) has reported that the ratio of soil loss at spring tillage to soil loss at autumn tillage was 0.2 for a clay soil plot study in South-eastern Norway, over a 7-year period. This ratio corresponds quite well to the figure for the Mean and Stochastic runs, giving an indication of the models' potential to simulate effects of tillage practices as a measure against soil erosion. Given the calculated ratios above, and also that the absolute differences between summer and winter conditions varied greatly for different approaches (0.82, 0.38 and 0.29 kg ha^{-1} for Generic, Mean and Stochastic runs respectively), it is clear that the simulated effect of potential measures will depend on the chosen input data source. This is important for example considering the fact that such ratios are used to represent the cover and management factor (C-factor) in the widely used Universal Soil Loss Equation (USLE).

These findings suggest that inadequate choice of input data sources can significantly underestimate or overestimate general soil loss and the effect of measures.

Table 2. Absolute (largest-smallest) and relative (smallest/largest) difference in simulated soil loss, between approaches and between summer and winter condition. S = summer condition runs, W = winter condition runs, G = Generic runs, M = Mean runs, S = Stochastic runs.

	S G - M	S G - S	S M - S	W G - M	W G - S	W M - S	W-S G - G	W-S M - M	W-S S - S
Absolute	0.59	0.62	0.030	1.0	1.2	0.12	0.82	0.38	0.29
Relative	0.20	0.16	0.80	0.34	0.26	0.77	0.48	0.28	0.29

4. Conclusions

In this study we have simulated a storm event driven surface runoff and erosion in a catchment with emphasis on the effect of uncertainty in input data for soil physical properties. The main conclusions of this study are:

- The input data source is important for the amount and timing of surface runoff and for soil loss. Input data derived from the national soil survey database resulted in a peak discharge that was almost 400 l/s higher than the peak discharge simulated using locally measured data, time to peak was 130 minutes earlier and the soil loss was five times higher. In most circumstances measured data will not be available, and the only option is to use the soil survey database. It is therefore important to take uncertainty into account. The value of K_s, derived from the basic input data using a pedotransfer function, was especially important in explaining the differences, as LISEM is highly sensitive to this parameter. The predicted K_s will strongly depend on the basic soil properties as long as PTFs are used, emphasizing the importance of having access to adequate basic data and PTFs.
- The two approaches of assigning locally measured input data, i.e. using a mean value on one hand and a stochastic distribution on the other hand, did not result in large differences in simulated runoff and soil loss. The variability in model output for the realizations in the stochastic approach was negligible, especially for simulated surface runoff. The possibly small gain in precision by using the stochastic approach instead of the mean value approach cannot justify the extra effort made in input data generation, model runs and processing of results for multiple realizations. This needs to be verified also for other situations (surface cover, event size, season).
- Running the model for both a low risk situation (crop covered surface) and a high risk situation (bare soil with freeze-thaw induced changes in aggregate stability and cohesion) showed that the variability in model output for the stochastic approach was similar in both cases, i.e., the uncertainty did not appear to depend on the erosion risk. Comparison of absolute and relative differences between the two risk situations and the three input data approaches showed that the uncertainty related to input data could result in larger differences between runs with different input data source than between runs with the same input data source but extreme differences in erosion risk. Effects of removing the crop cover and decreasing the structural stability varied between the input data approaches.
- Inadequate choice of input data sources can significantly underestimate or overestimate surface discharge, soil loss and consequently the effect of measures to reduce soil erosion.

Acknowledgements

This study was funded by the Norwegian Research Council, NORKLIMA programme, project number 200678/S30 (ExFlood project). We thank Robert Barneveld for assistance with field work, to Torfinn Torp (Bioforsk) for discussions regarding stochastic assignment of input data, and to Åge Nyborg (Norwegian Institute for Forest and Landscape Research) for providing generic soil profile data.

References

Banton, O., 1993. Field- and Laboratory-Determined Hydraulic Conductivities Considering Anisotropy and Core Surface Area. Soil Sci. Soc. Am. J. 57, 10-15.

Bechini, L., Bocchi, S., Maggiore, T., 2003. Spatial interpolation of soil hydraulic properties for irrigation planning. A simulation study in northern Italy. Eur. J. Agron. 19, 1-14.

Bonta, J.V., 1998. Spatial variability of runoff and soil properties on small wa-tersheds in similar soil-map units. Trans. ASAE 41, 575-585.

Booltink, H.W.G.J, J. Bouma, P. Droogers, 1998. Use of Fractals to Describe Soil Structure. In: Selim, H.M., Ma, L. (Eds.). Physical Non-equilibrium in Soils. Modelling and Application. Ann Arbor Press, Chelsea (MI), 157-221.

Brown, J.D., Heuvelink, G.B.M., 2005. Assessing Uncertainty Propagation Through Physically based Models of Soil Water Flow and solute Transport. In: Anderson, M.G. (Ed.). Encyclopedia of Hydrological Sciences, John Wiley and Sons, Ltd., pp 1181-1195.

Chaplot, V., 2005. Impact of DEM mesh size and soil map scale on SWAT runoff, sediment and NO3-N loads predictions. J. Hydrol. 312, 207–222.

Davis, S.H., Vertessy, R.A., Silberstein, R.P., 1999. The sensitivity of a catchment model to soil hydraulic properties obtained by using different measurement techniques. Hydrol. Processes 13, 677-688.

De Roo, A.P.J., Wesseling, C.G., Ritsema, C.J., 1996a. LISEM: a single-event physically based hydrological and soil erosion model for drainage basins. I: Theory, Input and Output. Hydrol. Processes 10, 1107-1117.

De Roo, A.P.J., Offermans, R.J.E., Cremers, N.H.D.T., 1996b. LISEM: a single-event physically-based hydrological and soil erosion model for drainage basins: II. Sensitivity analysis, validation and application. Hydrol. Process. 10, 1119– 1126.

Gijsman, A.J., Jagtap, S.S., Jones, J.W., 2003. Wading through a swamp of complete confusion: how to choose a method for estimating soil water retention parameters for crop models. Eur. J. Agron. 18, 77-106.

Grønsten, H.A., 2008. Prediction of soil aggregate stability and water induced erosion on agricultural soils in Southeast Norway. PhD Thesis 2008:54. Department of Plant and Environmental Sciences, Norwegian University of Life Sciences, Ås. ISBN: 978-82-575-0856-2.

Hessel, R., Jetten, V., Baoyuan, L., Yan, Z., Stolte, J., 2003. Calibration of the LISEM model for a small Loess Plateau catchment. Catena 54, 235-254.

Jetten, V., 2002. LISEM user manual, version 2.x. Draft version January 2002. Utrecht Centre for Environment and Landscape Dynamics, Utrecht University, 48 pp.

Jetten, V., Govers, G., Hessel, R., 2003. Erosion models: quality of spatial predictions. Hydrol. Processes 17, 887-900.

Kätterer, T., Andrén, O., Jansson, P.-E., 2006. Pedotransfer functions for estimating plant available water and bulk density in Swedish agricultural soils. Acta Agric. Scand. Sect B 56, 263-276.

Kramer, G.J., Stolte, J., 2009. Cold-Season Hydrologic Modeling in the Skuterud Catchment. An Energy Balance Snowmelt Model Coupled with a GIS-based Hydrology Model. Bioforsk Report 4(126), 46 pp. ISBN: 978-82-17-00548.

Kværnø, S.H., Deelstra, J., 2002. Spatial variability in hydraulic conductivity and soil water content of a silty clay loam in the Skuterud catchment. Jordforsk report 62/02, 30 pp. ISBN: 82-7467-433-2.

Kværnø, S.H., Haugen, L.E., 2011. Performance of pedotransfer functions in predicting soil water characteristics of soils in Norway. Acta Agric. Scand. Sect B 61, 264-280.

Kværnø, S.H., Øygarden, L., 2006. The influence of freeze–thaw cycles and soil moisture on aggregate stability of three soils in Norway. Catena 67, 175-182.

Kværnø, S.H., Haugen, L.E., Børresen, T., 2007. Variability in topsoil texture and carbon content within soil map units and its implications in predicting soil water content for optimum workability. Soil Tillage Res. 95, 332-347.

Lathrop Jr., R.G., Aber, J.D., Bognar, J.A., 1995. Spatial variability of digital soil maps and its impact on regional ecosystem modeling. Ecol. Model. 82, 1–10.

Leonaviciute, N., 2000. Predicting soil bulk and particle densities by pedotransfer functions from existing soil data in Lithuania. Geoandgrafijos metrastis 33, 317–330.

Lewan, L., Jansson, P.-E., 1993. Implications of spatial variability of soil physical properties for simulation of evaporation at the field scale. Water Resour. Res. 32, 2067-2074.

Lilburne, L.R., Webb, T.H., 2002. Effect of soil variability, within and between soil taxonomic units, on simulated nitrate leaching under arable farming. New Zealand. Aust. J. Soil Res. 40, 1187–1199.

Lindahl, A.M.L., Kreuger, J., Stenström, J., Gärdenes, A.I., Alavi, G., Roulier, S., Jarvis, N.J., 2005. Stochastic Modeling of Diffuse Pesticide Losses from a Small Agricultural Catchment. J. Environ. Qual. 34, 1174-1185.

Lundekvam, H.E., 2007. Plot studies and modelling of hydrology and erosion in southeast Norway. Catena 71, 200-209.

Lundmark, A., Jansson, P.-E., 2009. Generic soil descriptions for modelling water and chloride dynamics in the unsaturated zone based on Swedish soils. Geoderma 150, 85-95.

Mallants, D., B.P. Mohanty, D. Jaques, J. Feyen, 1996. Spatial variability of soil hydraulic properties in a multi-layered soil profile. Soil Sci. 161, 167-181.

Manrique, L.A., Jones, C.A., 1991. Bulk density of soils in relation to soil physical and chemical properties. Soil Sci. Soc. Am. J. 55, 476-481.

Marti, M., 1984. Kontinuierlicher Getreidebau ohne Pflug im Südosten Norwegens-Wirkung auf Ertrag, physikalische und chemische Bodenparameter (in German). Department of Soil Fertility and Management. Agricultural University of Norway, ISBN: 82-576-3502-2, 155 pp.

Merz, B., Plate, E.J., 1997. An analysis of the effects of spatial variability of soil and soil moisture on runoff. Water Resour. Res. 33, 2909-2922.

Mohanty, B.P., Kanwar, R.S., Everts, C.J., 1994. Comparison of Saturated Hydraulic Conductivity Measurement Methods for a Glacial-Till Soil. Soil Sci. Soc. Am. J. 58, 672-677.

Peck, A.J., Luxmoore, R.J., Stoltzy, J.L., 1977. Effects of Spatial Variability of Soil Hydraulic Properties in Water Budget Modeling. Water Resour. Res. 13, 348-354.

Pachepsky, Y., Rawls, W.J., Gimenez, D., 2001. Comparison of soil water retention at field and laboratory scales. Soil Sci. Soc. Am. J. 65, 460–462.

Rawls, W.J., Brakensiek, D.L., 1989. Estimation of soil water retention and hydraulic properties. In H.J. Morel-Seytoux (Ed.), Unsaturated Flow in Hydrologic Modeling - Theory and Practice. Kluwer Academic Publishers, Boston. pp. 275-300.

Riley, H., 1996. Estimation of physical properties of cultivated soils in southeast Norway from readily available soil information. Norw. J. Agric. Sci., Supplement No. 25, 1-51.

Salehi, M.H., Eghbal, M.K., Khademi, H., 2003. Comparison of soil variability in a detailed and a reconnaissance soil map in central Iran. Geoderma 111, 45–56.

Schaap, M.G., Leij, F.J., van Genuchten, M.Th., 2001. ROSETTA: a computer program for estimating soil hydraulic parameters with hierarchical pedotransfer functions. J. Hydrol., 251, 163-176.

Sorbieraj, J.A., Elsenbeer, H., Vertessy, R.A., 2001. Pedotransfer functions for estimating saturated hydraulic conductivity: implications for modeling storm flow generation. J. Hydrol. 251, 202-220.

Stolte, J., Ritsema, C.J., Veerman, G.J., Hamminga, W., 1996. Establishing temporally and spatially variable soil hydraulic data for runoff simulation in a soil erosion study in the loess region of the Netherlands. Hydrol. Processes 10, 1027-1034.

Stolte, J., van Venrooij, B., Zhang, G., Trouwborst, K.O., Liu, G., Ritsema, C.J., Hessel, R., 2003. Land-use induced spatial heterogeneity of soil hydraulic properties on the Loess Plateau in China. Catena 54, 59-75.

Sveistrup, T., Njøs, A., 1984. Kornstørrelser i mineraljord, Revidert forslag til klassifisering. Jord og myr 8, 8–15 (in Norwegian).

Sørbotten, L.-E. (Ed.), 2011. Jord- og vannovervåking i landbruket (JOVA). Feltrapporter fra programmet i 2009. Bioforsk rapport 6(38), 54 pp (In Norwegian). ISBN: 978-82-17-00768-5.

Takken, I., Beuselinck, L., Nachtergaele, J., Govers, G., Poesen, J., Degraer, G., 1999. Spatial evaluation of a physically-based distributed erosion model (LISEM). Catena 37, 431-447.

Timlin, D.J., Pachepsky, Ya.A., Acock, B., Whisler, F., 1996. Indirect estimation of soil hydraulic properties to predict soybean yield using GLYCIM. Agric. Syst. 52, 331-353.

Vachaud, G., Chen, T., 2002. Sensitivity of computed values of water balance and nitrate leaching to within soil class variability of transport parameters. J. Hydrol. 264, 87-100.

Van Dijk, P., Sauter, J., Hofstetter, E., 2010. Soil maps as data input for soil erosion models: errors related to map scales. Geophysical Research Abstracts vol. 12, EGU10-8409, EGU General Assembly 2010.

Wesseling, C.G., Karssenberg, D., Van Deursen, W.P.A., Burrough, P.A., 1995. Integrating dynamic environmental models in GIS: the development of a dynamic modelling language, Trans. GIS, 1, 40-48.

Wösten, J.H.M., Lilly, A., Nemes, A., Le Bas, C., 1999. Development and use of a database of hydraulic properties of European soils. Geoderma, 90, 169-185.

Young, F.J., Hammer, R.D.,Williams, F., 1997. Estimation of map unit composition from transect data. Soil Sci. Soc. Am. J. 61, 854–861.